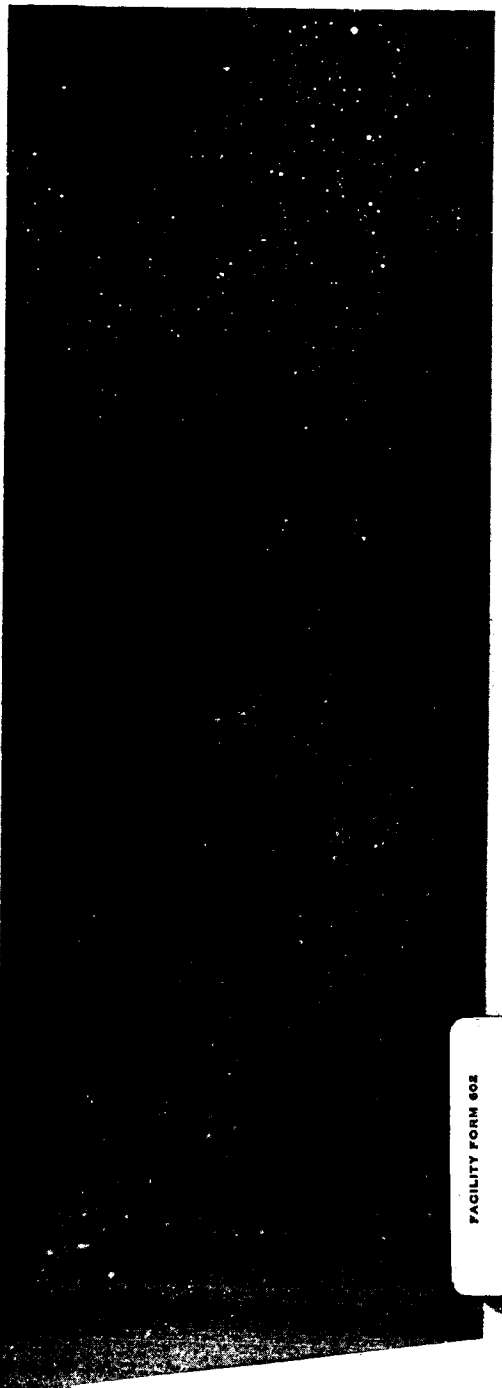
SCOTT

ER-4955



SOLAR RANKINE SYSTEM PERFORMANCE AND STATUS SUMMARY

FACILITY FORM 602

N 65-20791 (ACCESSION NUMBER)

(THRU)

141 (PAGES)

1 (CODE)

CR-57765 (NASA CR OR TMX OR AD NUMBER)

03 (CATEGORY)

GPO PRICE $ _____

OTS PRICE(S) $ _____

Hard copy (HC) $4.00

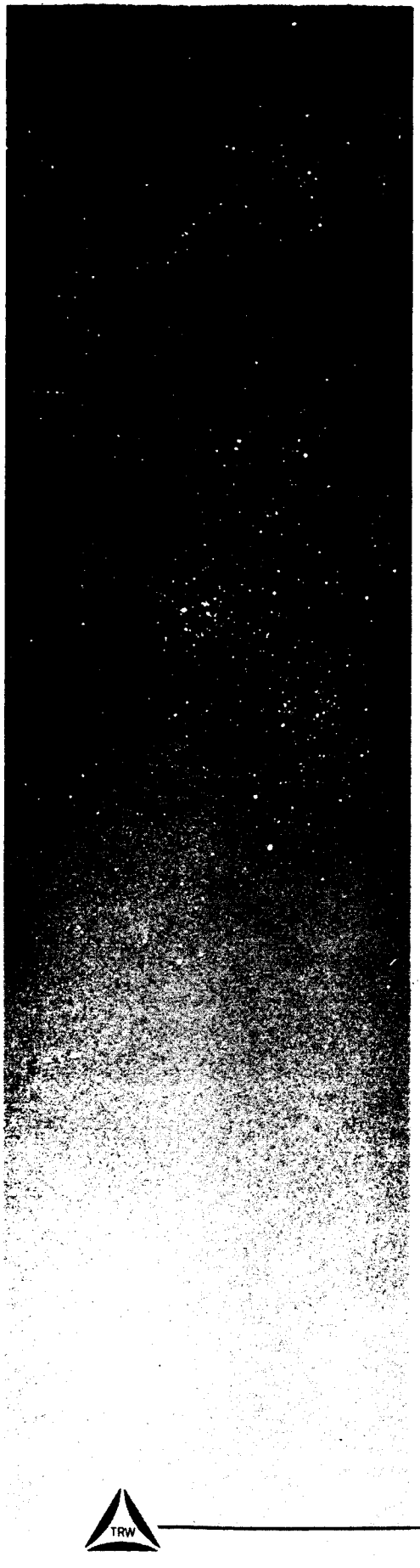
Microfiche (MF) $1.00

JULY 24, 1962

TAPCO a division of Thompson Ramo Wooldridge Inc.

N65/20791

ER-4955



SOLAR RANKINE SYSTEM PERFORMANCE AND STATUS SUMMARY

JULY 24, 1962

TAPCO a division of
Thompson Ramo Wooldridge Inc.

ER-4955

SOLAR RANKINE SYSTEM
PERFORMANCE AND STATUS SUMMARY

Prepared by:

Rankine Power Systems Department Staff

July 19, 1962 0840

cc

TABLE OF CONTENTS

		Page
I.	INTRODUCTION	1
II.	CONCLUSIONS	1
III.	REVIEW OF DEVELOPMENT PROGRESS - CURRENT OBJECTIVES	2
	Sunflower Turbo-Alternator Development	2
	SNAP I and SPUD Results	12
	Mercury Compatibility	22
	Hydrogen Containment	39
	Sunflower Solar Collector Status	53
	Sunflower Boiler and Condenser Status	58
IV.	REVIEW OF SYSTEM AND COMPONENT IMPROVEMENT AREAS	69
	Alternators	69
	Additional System Factors	79
V.	RESULTANT SYSTEM EXAMPLES	88
VI.	CONCEPT RELIABILITY ASSESSMENT	95
VII.	ADVANCED SYSTEMS	101
VIII.	COMPETITIVE COMPARISONS	114
	Electronic Power Conversion and Control	114
	System Comparisons	120

INTRODUCTION

There are a number of space power system concepts competing for a range of general and specific mission requirements. Selection of specific systems for development and application requires consideration of missions, dates, reliability requirements, technological status, cost of development, range of applicability and a host of interrelated questions.

This report is intended to illuminate some of these areas, particularly as they relate to solar Rankine systems.

The solar Rankine system offers unique advantages of simplicity and performance. This conclusion is strengthened by recent data and analyses, relating both to the mercury Rankine concept and competing concepts. Items of particular note are:

a) The results of our continuing successful turbo-alternator test.

b) Status of other major components of the Sunflower system.

c) The growth potential of the Sunflower design, especially as made possible by alternator developments.

d) General areas of immediate and potential improvements in performance and concept details.

CONCLUSIONS:

Stated in broad terms, the conclusion of this report are:

1. There are no remaining areas of uncertainty regarding the feasibility of solar mercury Rankine systems. This specifically includes mercury compatibility, hydrogen containment, endurance capability and reliability achievability.

2. The performance of the Sunflower system as currently defined can be significantly improved by:

   Time and dollars
   Review of detailed specifications
   Increasing output power.

REVIEW OF DEVELOPMENT PROGRESS - CURRENT OBJECTIVES

Sunflower Turbo-Alternator Development

This section deals with the developmental progress to date on the turbo-alternator (designated CSU for Combined Shaft Unit) and covers the following topics:

1. Brief discussion of test results and analysis of the first Sunflower CSU (CSU I-1).
2. CSU redesign based on test results and analyses.
3. A brief resume of CSU I-3 testing over the first 1000 hours.
4. An overall performance evaluation of CSU I-3.

CSU I-1 Test Results and Analysis

The CSU I-1 assembly was completed and the unit placed on test November 22, 1961. The test was very short in duration (about 1½ hours) but also very illuminating relative to the first design. On first start the unit accelerated to 25,000 rpm quite freely, but subsequently appeared to be erratic in both speed and power suggesting liquid drag on the shaft. This condtion prevailed throughout the test. The speed was ultimately increased to 40,000 rpm, but alarming variations in power combined with apparent increases in bearing clearances (from flow pressure data) suggested an impending failure. Therefore, the CSU was shut down to allow examination of data and hardware. Post test bearing calibrations verified that bearing wear had taken place and the CSU was therefore removed from the test rig for disassembly and inspection.

Inspection revealed extensive wear on the alternator journal and thrust bearings and light wear on the turbine journal. Examination of the bearing drain lines showed severe flow restrictions at several of the butt welds.

Data and performance analysis conclusions were as follows:

- Bearing wear resulted from (1) excessive shaft loads and (2) reduced load capacity of the bearings.
  1. Excessive shaft loads were caused by:
     a) The presence of liquid Hg around the shaft due to restricted drain lines plus possibility of condensation in the alternator rotor gap.
     b) A large magnetic rotating load due to rotor magnetic imbalance.
     c) A pressurized turbine bearing drain collector (causing excessive thrust) due to vaporization of lube drain fluid which was restricted from draining.
  2. Reduced load capacity:
     a) The alternator journal bearing showed evidence during test

of either thermal increases in clearance or lube bypass between the housing and bushing prior to the wear indications. Both situations would have weakened the bearing capacity.

b) The thrust bearing wear pattern indicated misalignment which resulted from an eccentric loading from its retaining device, thereby reducing its capacity.

CSU Redesign

The CSU redesign was aimed at control of package thermal distributions to maintain proper bearing clearances and alignments and to prevent condensation in vapor spaces around the rotor. Redesign was also directed to reduce the magnetic unbalance by improved quality control, elimination of flow passage restrictions and better mechanical support of the bearings.

A thermal stress computer analysis was conducted on the bearings and supports. The results were used to specify the assembly fits and clearances required to insure proper and safe operating fits and clearances. Thermal analysis of the alternator was conducted to predict coolant temperatures required for proper rotor gap conditions. These analyses and the results of the first test were used to redesign the next available unit (CSU I-3). Each step of the redesign was a logical attack on specific problems evidenced from the first test but within the framework of the original concept and hardware. A layout of the original concept is shown as Figure 1 . The changes involved are listed below:

1. The turbine inlet was converted to a 360° collector scroll to afford better thermal and mechanical symmetry relative to the turbine bearing alignment.

2. Revisions were made in the alternator bearing support housing to provide better thermal separation from the alternator housing and better thermal and mechanical symmetry relative to journal bearing alignment. Bearing feed and drain bosses were slit away from flanges and a supramica washer inserted between flanges for thermal separation.

3. The thrust bearing retainer axial loading was reduced and made symmetrical by modification of associated static seals.

4. The alternator journal bearing bushing fit was increased slightly to provide a better lube seal and the cold bearing diametral clearance was reduced from .0018 in. to .00105 in. in accordance with computer thermal analysis. The target for operating clearance was .0014 - .0015 inches.

5. An evacuated heat shield was placed around the alternator bearing support housing to help control bearing clearance and sealing of the lube supply, and to prevent accumulation of condensate in the alternator rotor cavity.

6. The thrust bearing lube supply annulus was placed in the housing rather than the bearing O.D. to provide a better lube seal.

7. Axial thermal take-up provisions of the shaft were provided by incorporating belleville springs under the turbine lock nut, and the thrust spacer material was changed. These modifications were made to improve shaft integrity and balance.

8. Quality control on magnetic rotor imbalance resulted in a shaft imbalance of 2-4 lbs. for CSU I-3 compared to 16.5 lbs. for CSU I-1.

9. The turbine journal sleeve support lands were eliminated and the sleeve was placed in full contact with the shaft to improve mechanical support and thermal influences on clearance.

10. The turbine journal bushing fit was increased slightly in the support, and cold bearing clearance was reduced from .0018 in. to .00135 in. in accordance with computer thermal analysis. The target clearance was .0011 in. to .0016 in. so that the assembly clearance was a compromise depending on whether or not seal vapor entered the drain cavity.

11. Turbine seal and heat shield diametral clearances were reduced along with bearing clearances to improve turbine performance and reduce temperature effects on the turbine bearing.

12. X-ray quality control was applied to all tubing welds to avoid weld penetrations into the flow passages.

13. The cavity between alternator stator and housing was sealed at one end with a belleville washer and at the other with a close clearance fit which decreases during operation from thermal expansion. Sealing this gap provides three functions:

    a) keeps liquid Hg out of the rotor cavity and vapor Hg out of the stator gap,

    b) affords symmetrical heat transfer of alternator loss heat to the coolant,

    c) affords better circumferential temperature distribution and consequently better bearing alignments.

14. A second alternator garter spring support was added to eliminate resonant vibrations which could effect the alternator bearing or possibly crack the glass bore seal.

15. The alternator housing and bearing support flanges were electron beam welded rather than Heliarc to preclude weld distortions and stresses and afford better bearing alignment.

The list of changes sounds extensive, but in reality consists of attention to details based on a better knowledge of the unit from results of its first test. The basic concept is unchanged, no new castings were involved and, in fact, nearly every change was applied to semi-finished hardware existing from the previous design.

CSU I-3 Test Results

The CSU I-3 unit was built to the original design concept, but with the revisions just noted. The completed assembly had only two significant print deviations.

1. The journal bearing bushings were located radially out of position. This deviation was considered inconsequential.

2. The second stage labyrinth seal clearance was .001 inch large radially, because dimensions were completed prior to final redesign.

Although turbine nozzle details were completed to print, a cold gas nozzle test revealed that the first stage nozzle throat area was 5% small and the third stage nozzle throat area 17% large. These deviations were accepted for economical and schedule reasons as well as for verification of the nozzle gas tests prior to modifying print dimensions. CSU I-3 was installed in the test rig and placed on test May 23, 1962. Before the start the check off went very well except that the drains were again restricted as indicated by additional instrumentation which was installed after the CSU I-1 test. It was then determined that a head control valve in the test rig drain manifold line was providing the restriction. In all probability this was the major reason for having to shut down CSU I-1. The valve was cut out, the checkoff completed and the unit was started. A graphical summary of pertinent operational parameters is shown in Figure 2. The start was extremely smooth. Power and speed during the start were exceptionally easy to control and there were no indications of liquid drag in the unit. The start procedure was terminated at 20,000 rpm and speed was put on automatic control where it is possible to see even very minute variations in consumed power from the turbine. Such variations would show up on the control load current trace on the oscillograph, but were completely absent as contrasted to the CSU I-1 test. Dwell at 20,000 rpm was 2½ hours during which time bearing, turbine, and alternator performance was observed and found to be excellent.

From 20,000 rpm the unit speed was increased in 5000 rpm increments to 40,000 rpm, the design speed, within about eight hours. During this time, the bearings, pump, turbine and alternator continued to perform quite predictably and well within expected ranges of operation. After about one hour operation at 40,000 rpm, the speed was reduced to 35,000 rpm and the first 500 hour run initiated. The speed was reduced because current analyses at the time of start had indicated possible excessive rotor retaining sleeve temperature at design speed in terms of creep strength. However, subsequent analyses have failed to verify the situation and, therefore, after 500 hours running the speed was again increased to 40,000 rpm where it is at the time of this writing 1400 hours from start.

One of the most gratifying aspects of this test is the characteristics of the bearings. They have not only exhibited extremely steady performance, but also have verified the thermal stress computer analysis which now provides greater flexibility in bearing application. In the case of the turbine bearing, the clearance closed from the assembly value of .00135 in. to .0011 in. which is desireable since it suggests that seal vapor is not entering the bearing drain cavity. Also, this bearing is operating very close to optimum clearance for the flow pressure characteristics available from the power conversion system and at this condition has shown rock steady performance. The alternator bearing performance, on the other hand, has been confused with lube heater problems in the test rig where a supple-

mentary heater had to be added in the vicinity of the flowmeter. Note from the time plot that the alternator bearing clearance settled out at .0015 clearance (compared to anticipated of .0014 to .0015 in.) after stable operation was started at 35,000 rpm. It is suspected that this bearing may yet be .0015 in. although flow pressure relationships indicate .0017 in. The significant factor, however, is the very steady performance of this bearing since it stopped its apparent clearance growth.

The thrust bearing performance is somewhat more difficult to evaluate since its pressure flow characteristic changes with both clearance and thrust load. However, its trend is in the direction expected, and performance has actually progressed into the predicted range, see Figure 3, and became stable at about 700 hours or shortly after the last series of power increases. The thrust bearing clearance has been evaluated during the run and appears .0002 inches larger than at assembly which is also the change predicted from differential thermal expansion.

The CSU pump initially demonstrated performance in excess of its design specification, delivering a useful flow of 41 ppm at 510 psia with a suction head of 5.5 psia. This compares with its design specification of 35 ppm, 450 psia and 4.75 psia suction head. A pump calibration was made during the run and initially appeared to demonstrate the flat head vs. flow characteristics typical of subcomponent testing. However, during the calibration effort a foreign particle (perhaps a metal chip) apparently lodged in the jet boost nozzle and offset the calibration to the more familiar sloping performance curve of an unboosted centrifugal pump. Since that time, however, the modified pump performance has not deteriorated or changed over a period in excess of 900 hours at 40,000 rpm or a total running time in excess of 1400 hours.

The alternator was magnetized during assembly to produce 110 volts per phase during test and actually produced 108 to 109 volts at 40,000 rpm. The alternator has short circuit and spike current change protection in the form of series capacitors in the output line. Short circuits or spike changes can demagnetize an unprotected rotor causing loss of power and even overspeed damage. The capacitors have already demonstrated their function on several occasions. In one instance, a wattmeter coil shorted, placing a short on the CSU alternator, but only demagnetized the unit about 5 volts. Because the protection was there it was possible to wire in a second wattmeter and cut out the first one with a loss of only an additional 1 volt - a procedure which would result in disaster with an unprotected alternator. In a third instance during a manual electrical check, a short was inadvertently placed on the alternator with a subsequent loss of about .5 volts indicating virtual short circuit stability at about 102 volts for a total loss of about 6-7 volts. Relative power during all of these situations remained unchanged since current increases compensated the voltage losses.

It should not be overlooked that the first breadboard speed control has been employed to control the load of the CSU and this component has also performed without deterioration for the duration of the test.

CSU I-3-1 Performance Evaluation

A performance evaluation of CSU I-3 is shown on Figure 4. Note the design operating conditions. A statistical average of reduced data at design inlet and exhaust conditions and speed shows a measured power of 2925 watts being delivered.

from the alternator. This is less than the design value of 3500 watts, but is accounted for as follows:

The alternator power at constant speed may be defined by the following equation:

$$\frac{P_a}{\eta_a} = W(H_1 - H_2)\,\eta_t - P_c$$

Where P_a = alternator output power

W = Hg vapor weight flow

$H_1 - H_2$ = isentropic enthalpy drop

η_t = turbine efficiency

P_c = bearing, pump and seal power

η_a = alternator efficiency = .87

The effect of a 5% undersized first stage nozzle (noted earlier) is to reduce vapor flow to the turbine at design nozzle pressure, or W = 13.0 ppm, instead of design of 13.7 ppm. The measured output power may be considered proportional to flow since η_a and P_c will stay constant and η_t may be assumed constant for the small flow change. Therefore, correcting for the first stage influence

$$P_a = 2925 \times \frac{13.7}{13.0} = 3082 \text{ watts}$$

Furthermore, the effect of 17% excess nozzle throat area in the third stage results in a turbine efficiency loss equivalent to 200 watts shaft power at 13.7 ppm. At 87% alternator efficiency this amounts to 200 x .87 = 174 watts alternator output. Adding the third stage correction:

$$P_a = 3082 + 174 = 3256 \text{ watts.}$$

The remaining difference of (3500 - 3256) = 244 watts is assignable to any one or more of the following listed items and remains to be determined from further testing and analysis.

a) Turbine output power
b) Bearing power
c) Seal power
d) Pump power
e) Alternator efficiency
f) Instrumentation errors.

SUNFLOWER I — MERCURY RANKINE CYCLE

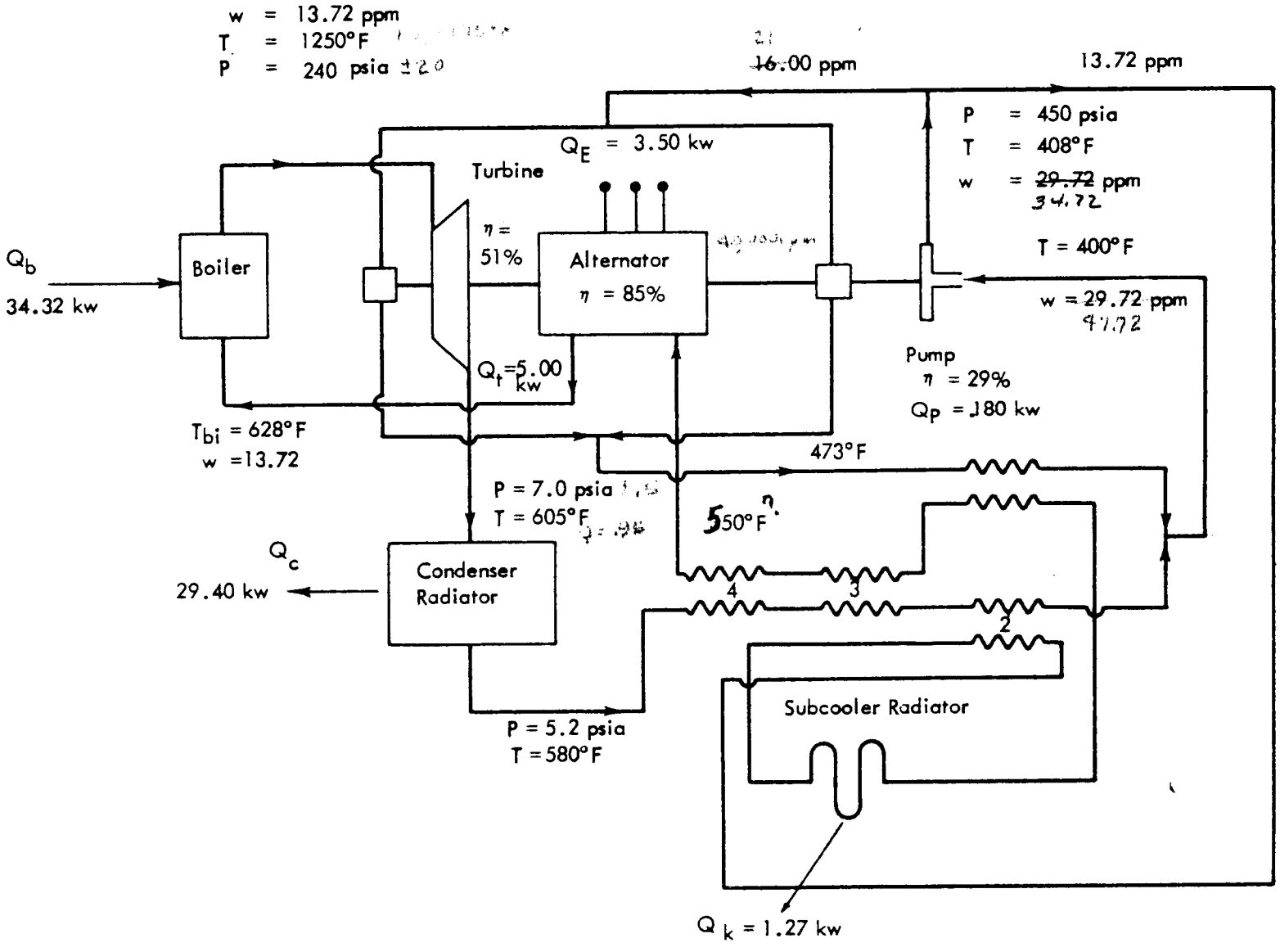


FIGURE 1

ISOMATIC VIEW - ENVELOPMENT AND ACCEPTANCE TEST CELLS

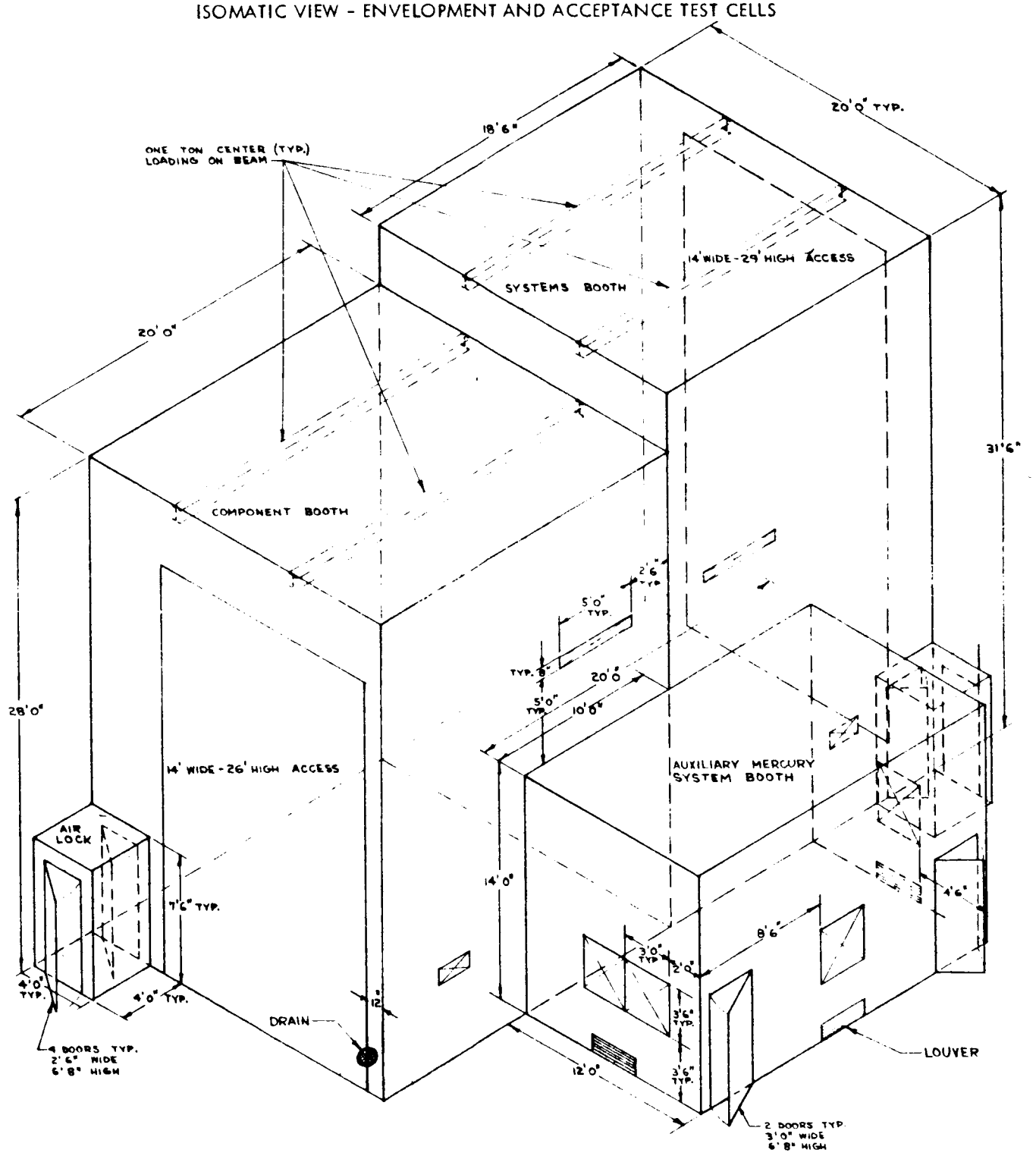


FIGURE 5

COMBINED SHAFT UNIT LAYOUT

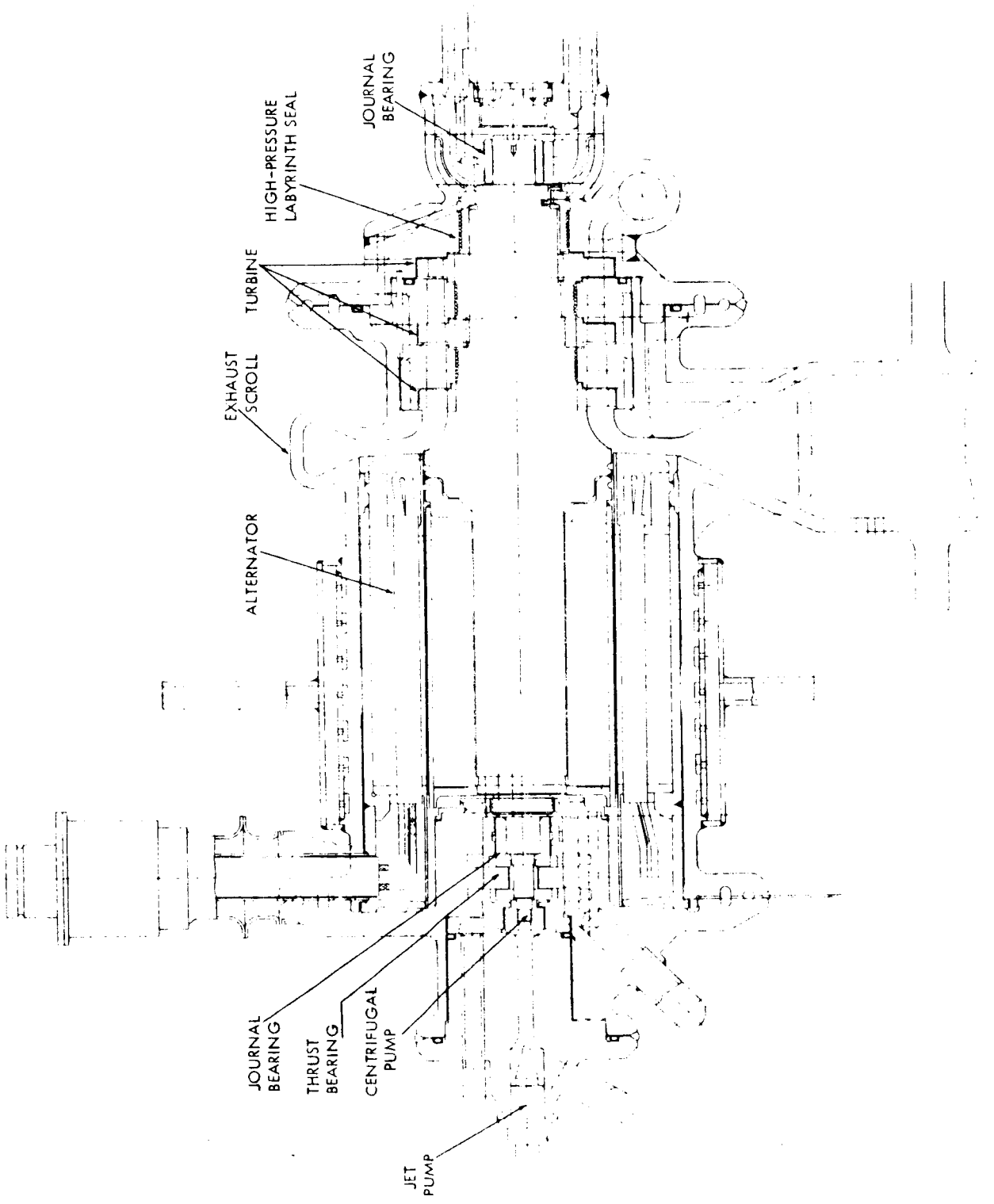


FIGURE 17

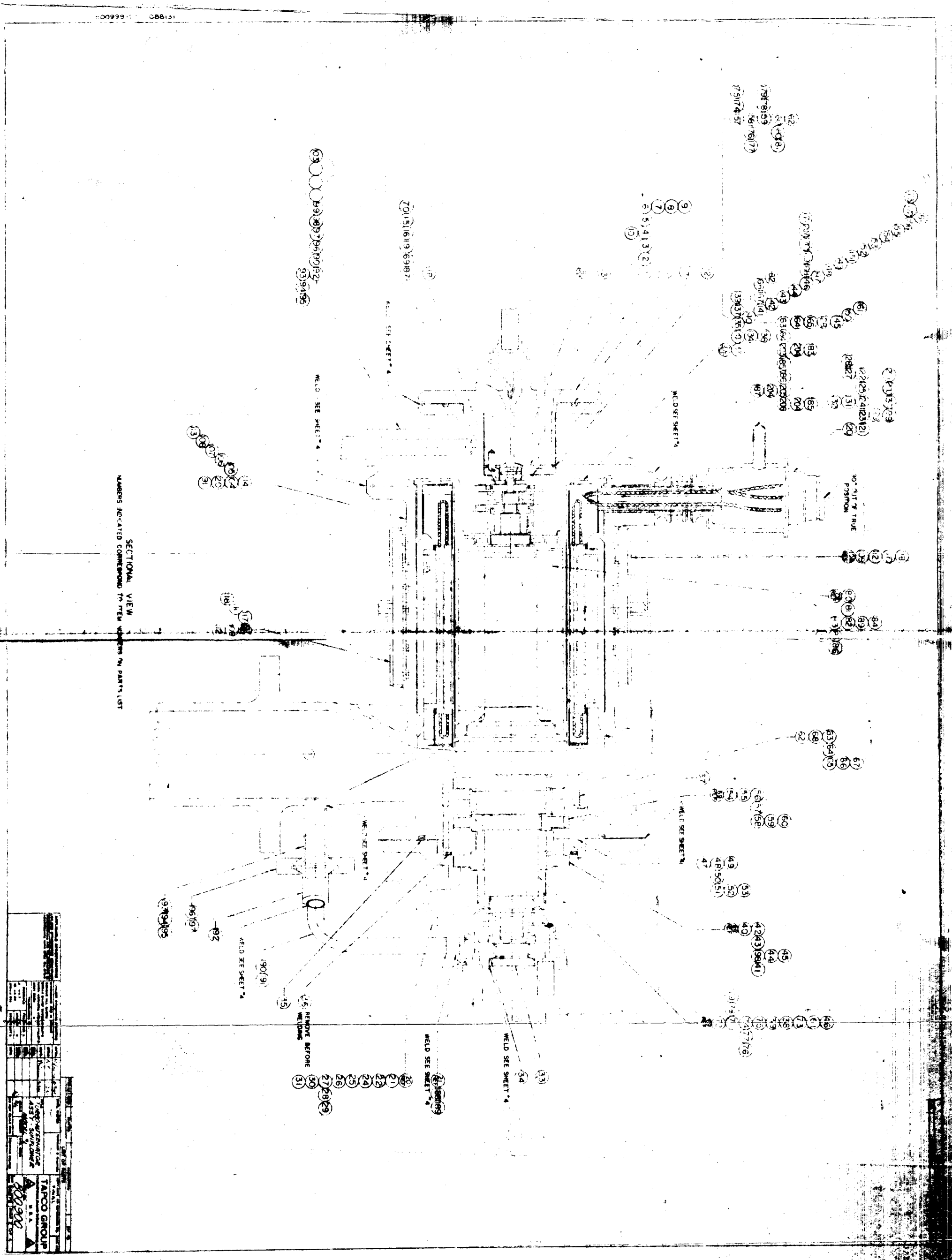

SECTIONAL VIEW
NUMBERS INDICATED CORRESPOND TO ITEM NUMBERS ON PARTS LIST
WELD SEE SHEET "4
REMOVE BEFORE WELDING
TAPCO GROUP

Figure 1

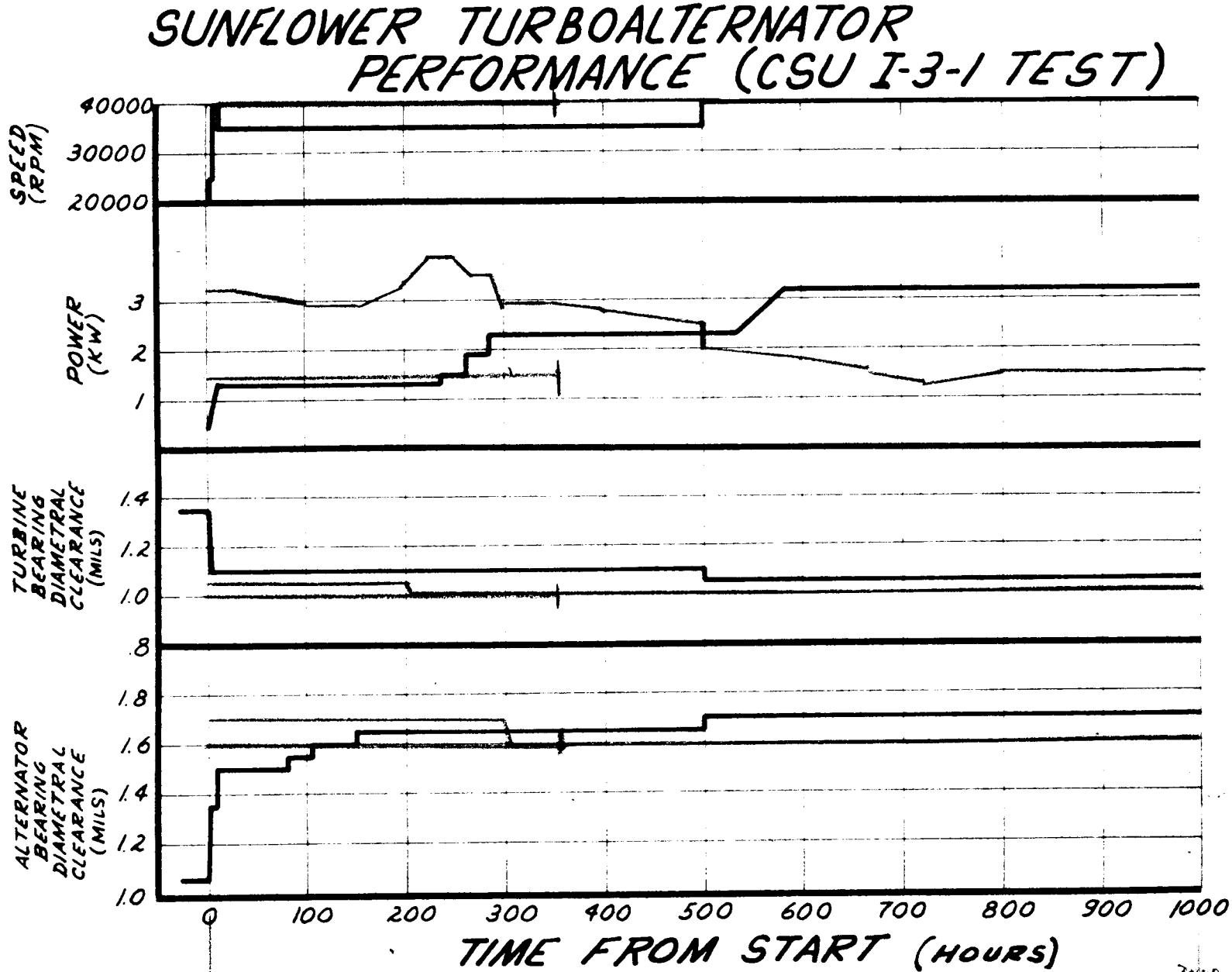

SUNFLOWER TURBOALTERNATOR
PERFORMANCE (CSU I-3-1 TEST)
SPEED (RPM)
40000
30000
20000
POWER (KW)
3
2
1
TURBINE BEARING DIAMETRAL CLEARANCE (MILS)
1.4
1.2
1.0
.8
ALTERNATOR BEARING DIAMETRAL CLEARANCE (MILS)
1.8
1.6
1.4
1.2
1.0
0
100
200
300
400
500
600
700
800
900
1000
TIME FROM START (HOURS)

FIGURE 2

CSU I-3 THRUST BEARING FLOW-PRESSURE RELATIONSHIP

400 °F INLET TEMP., ANY SPEED

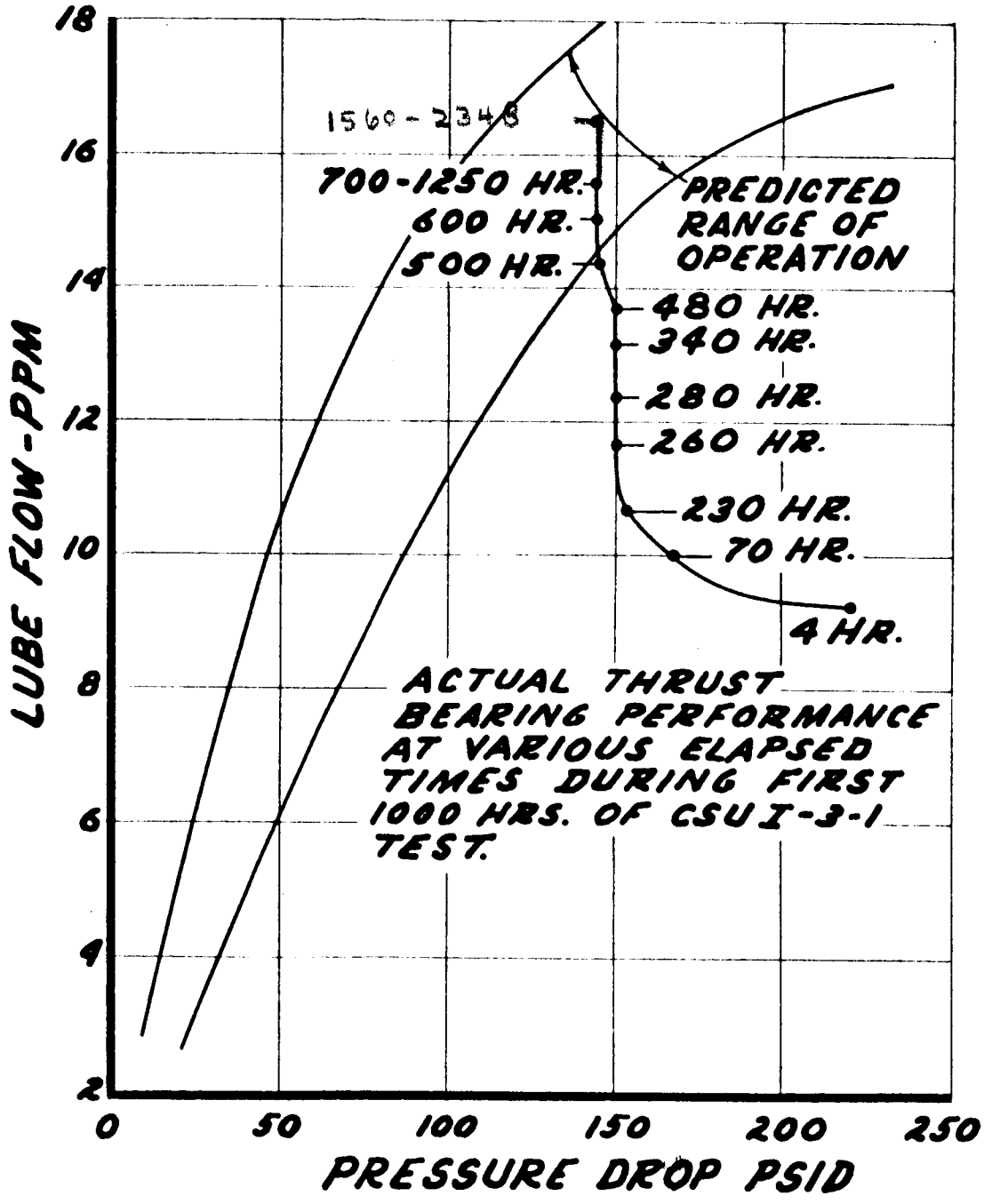


FIGURE 3

SUNFLOWER TURBOALTERNATOR PERFORMANCE

PARAMETER		OPERATING CONDITIONS DESIGN POINT	TEST DATA
SPEED	(RPM)	40000	40000
TURB. INLET PRESSURE	(PSIA)	240	240
TURB. INLET TEMPERATURE	(°F)	1250	1250
TURB. EXH. PRESSURE	(PSIA)	7.0	7.0
TURBINE FLOW RATE	(PPM)	13.7	13.0
ALTERNATOR OUTPUT	(WATTS)	3500	2925

FLOW CORRECTION (1ST STAGE NOZZLE)

$$2925 \times \frac{13.7}{13.0} = \quad 3082 \text{ WATTS}$$

TURBINE SHAFT POWER CORRECTION (3rd STAGE NOZZLE)

200 x .87 = 174

ESTIMATED CORRECTION POWER 3256

UNACCOUNTABLE (3500-3256) = 244 WATTS

SOURCES OF UNACCOUNTABLE POWER 244 WATTS

- TURBINE SHAFT POWER
- BEARING POWER
- SEAL POWER
- PUMP POWER
- ALTERNATOR EFFICIENCY
- INSTRUMENT ERRORS

FIGURE 4

SNAP 1 and SPUD Results

The SNAP 1 and SPUD programs have provided substantial experimental evidence of the applicability of the mercury Rankine cycle to the solar space power system requirement. Major highlights of accomplishments under these programs include the following: 1) component concepts were established, 2) component and system performance capabilities were demonstrated, 3) an endurance run of 2500 hours was successfully completed, and 4) a complete hermetically sealed and automatically controlled mercury Rankine system was arranged for ballistic flight and was launched in an Atlas scientific passenger pod.

In addition to these results, zero gravity tests under the OFFBACE program have provided preliminary indications of the capability of the mercury Rankine system for stable heat transfer and hydronamics during operation in space.

The purpose of the present discussion is to present a summary of these results and to show how they support the SUNFLOWER program. A further purpose is also to show how the the turboalternator unit, developed under the SNAP 1 and SPUD programs, can be profitably applied for application to the low power range of solar space power systems.

The SNAP 1 program, and related activities, have been under way at TRW since early in 1956. This program originally established several major facts which provide the basis of mercury Rankine power system technology. These are as follows:

1) Mercury can be successfully used as a bearing lubricant - eliminating system contamination, due to the presence of other lubricants, and also eliminating rubbing seals.

2) Sufficiently high efficiencies can be obtained on small impulse turbines to make the performance of the Rankine system attractive - the SNAP 1 turbine achieved an efficiency of 46% at its design point, and an efficiency of 48% at its optimum speed.

3) The mercury boiler feed pumps can operate at high efficiency at the small flow required and, in combination with a jet inducer, can operate at the low net positive suction head required.

4) The alternator can achieve the required efficiency and can operate in a mercury vapor environment.

5) The boiler and condenser can achieve the required heat transfer coefficients and can be designed to provide stable flow under normal gravity or zero gravity conditions.

6) The turboalternators may be stably and accurately controlled - by use of a frequency sensing device operating in conjunction with a parasitic load and a variable boiler flow regulator.

7) Materials can be found which are not subject to serious mercury corrosion and mass transfer.

In addition to these factors, the SNAP 1 system was shown to be capable of producing an overall thermal to electrical conversion efficiency of 10% at only a 500 watt power level. The turboalternator unit, as designed under the SNAP 1 program and as further developed under the Air Force SPUD program is shown in Figure 5. It will be noted that this unit employs the mercury lubricated hydrosphere bearings. These bearings have shown themselves to be capable of very accurate shaft positioning and stable high speed operation. They have also shown good load-carrying capability, and low power consumption since an extra thrust bearing is not required.

2500 Hour Test

A further demonstration provided, by combined support of the AEC SNAP 1 and the Air Force SPUD programs, was the capability of the mercury Rankine system for long endurance operation. The SPUD turboalternator unit, previously shown, was operated for a period of 2509 hours, with the test being discontinued by a planned shutdown initiated at the request of the Air Force. The power conversion system which was used in this test, included a space type boiler, operated at temperatures of over 1500°F and delivering superheated vapor to the turbine at the design temperature of 1300°F. The system also included a multiple tube condenser and subcooler, a boiler flow regulator, and other auxiliaries required for a space power conversion system. During the entire operating period, the alternator delivered its rated power, of approximately 300 watts, to a load bank. This test was continuous, on a 24 hour per day basis, except for two brief shutdowns that occurred, due to test rig operating problems and not due to any failure of the power conversion system. This test was accomplished as a limited funding, endurance feasibility, demonstration and was therefore, conducted with available hardware, which had been previously extensively operated in performance and preliminary endurance testing. The system was constructed of readily available materials (primarily 316 series and precipitation hardening stainless steel) and, therefore, did not incorporate the advanced material compatibility research results, which are later described. Even with these limitations, however, the endurance demonstration was readily and successfully accomplished so that a substantial amount of funding, allocated by the Air Force for the test, was still available to begin work on a ballistic zero gravity test which is later described.

A summary of system and component performance and inspection results obtained from this endurance test will now be given.

Turbine

Turbine performance was excellent throughout the test with no efficiency deterioration being noted. Upon disassembly, the turbine was found to be in good condition with only microscopic erosion detectable on the third stage rotor blades and a deposit of approximately .001 inch in the first stage nozzle throat.

Alternator

No notable change occurred in the mechanical integrity or electrical performance of the alternator. This result was obtained in spite of the fact that the

alternator bore seal was somewhat defective at the beginning of the test, allowing air to leak into the system. The alternator showed applicability of the basic principles and materials for operation in mercury vapor for over one year. Improved bore seals, subsequently developed, have superior compatibility and also eliminate air leakage.

Bearings

The bearing condition was as good at the end of the test as it had been at the beginning, with neither appreciable wear or contamination being indicated. A very slight deposit evidently occurred during the first 1000 hours, but during the last 1500 hours no appreciable change occurred in bearing pressures or flow rates. The bearing operation was stable and dependable throughout the entire test.

Pump

A declining pump outlet pressure was noted early in the test. During the last 1000 hours of operation, however, the pump outlet pressure only decreased from 250 to approximately 230 psia. The pump was slightly eroded at the end of the test and a contamination deposit was evident, which was evidently responsible for the output pressure decline. This reduction in pump performance was concluded, however, to be due to excessive air entrainment in the mercury, resulting from leakage through the alternator bore seal.

Boiler

The boiler coils were found to be in very good condition at the end of the test with only slight distortion due to the fact that the superheater section had been operated during the test at a temperature of almost 1600°F. The maximum boiler corrosion noted was localized pitting at the boiling interface to a depth of .002 to .006 inches. This pitting at the interface was attributed to agitation of the liquid interface and would suggest the importance of constructing the boiler preheater section of a material which is more resistant to corrosion and erosion than 316 stainless. It is also thought that the majority of this pitting occurred during the early life of the boiler, particularly during the 48 hour mercury preconditioning exposure to which the system was subjected.

Condenser Subcooler

The condenser and subcooler were suprisingly free from corrosion and contamination. These surfaces were as shiny and clean at the end of the test as they were at the start. Maximum corrosion depth detected was .001 inches.

Filters, Ejector Pump and Boiler Flow Regulator

Performance of all of these components was good. No substantial erosion or deposits were noted. The only performance deficiencies noted were as follow:

1) The filters experienced high pressure drop which is thought to be a wetting phenomenon.

2) The ejector pump performance was somewhat erratic, due to excessive air entrainment.

System Corrosion and Mass Transfer

The only appreciable corrosion noted was the .006 inches pitting at the boiler liquid interface. Only several grams of contaminant were removed from the system, primarily from the subcooler and from the pump impellor.

In general, this endurance test showed that the mercury Rankine system is capable of long endurance operation, even if it is constructed from readily available materials. The operating life, of nearly four months, demonstrated, was substantially in excess of 60 day life originally specified for SNAP 1 and, in fact, indicated that a one year operating period should be readily attainable, with a hermetically sealed system.

Ballistic Program

Following successful completion of this endurance run, the Air Force sponsored the SPUD Ballistic program. This program was intended to show applicability of Rankine power system technology to use in space by designing, fabricating, and testing a complete hermetically sealed, automatically controlled, power system for launching in a pod attached to the Atlas missile. A further major purpose of this experiment was to obtain data on operation of this system for 20 to 30 minutes in zero gravity, during the ballistic free fall period of the Atlas flight.

Before describing this experiment and its results, however, it is worthwhile to mention the more limited zero gravity results which were obtained under the OFFBACE program sponsored by the AEC and conducted by TRW. The OFFBACE experiments were conducted in the Air Force C 131B and the KC 135 zero gravity flight laboratories. They included tests on condenser operation with a non-circulating loop and with a complete loop. The complete loop included a space type mercury boiler, an orifice simulating a turbine nozzle, a multiple tube condenser, and a motor driven, jet primed, centrifugal pump. These tests showed that the heat transfer and fluid dynamics of the Rankine cycle are not substantially effected during operation for periods up to 31 seconds, in zero gravity. The boiler, condenser, and pump for these OFFBACE experiments were all essentially the same as the components which had been designed for use in the SNAP 1 and SPUD systems.

The SPUD power system was, therefore, redesigned for installation in an Atlas scientific passenger pod, as shown in Figure 6. In this system, the SPUD turboalternator was designed to circulate mercury through the space type boiler, with the mercury vapor then driving the turbine and discharging into a tapered, multiple tube, condenser radiator, which was incorporated into the surface of the pod. This system was hermetically sealed and was automatically controlled by a frequency sensing, parasitic load, control which worked in conjunction with an adjustable flow boiler flow regulator. The thermal energy for operation of the boiler during a 30 minute flight period was supplied by a storage battery.

Extensive pressure, temperature, flow rate, speed and power instrumentation was provided with the output from the transducers transmitted via a 6 channel, commutated, telemetry set.

During the development and test program, which preceeded the launch of this system, numerous important features were shown concerning the operational feasibility of the mercury Rankine system. These results are partially summarized as follows:

1) Stable, dependable operation was achieved on the complete power system at rated output.

2) Excellent performance was achieved on the centrifugal pump. Full rated output pressure was achieved at pump inlet pressures of only 1 psia, and no output pressure deterioration was noted in over 80 hours of accumulated operating time. This result confirms that the pump contamination and erosion noted during the endurance test was, indeed, primarily due to air entrainment and will not occur with a hermetically sealed system.

3) Reliable and dependable multiple start and stop operation of the system was demonstrated.

4) Operating capability of the combined rotating unit at vibration levels of 5 g's were demonstrated and the structural integrity of the complete system was demonstrated at vibration levels of 3.5 g's.

5) The automatic control system showed capability of maintaining a constant frequency within ± 2 cps at the rated frequency of 2000 cps. The adjustable boiler flow regulator was shown to be capable of controlling turboalternator power output over a broad range.

6) The power system was shown to be capable of meeting Mil Spec radio noise limits.

This power system was delivered to Cape Canaveral on schedule and successfully passed its preflight qualification test with less difficulty than was experienced by numerous "standard" components such as programmers, telemetry sets, and relays. The system was, therefore, installed on the Atlas 6F missile and was successfully started and launched on December 20, 1961, as shown in Figure 7.

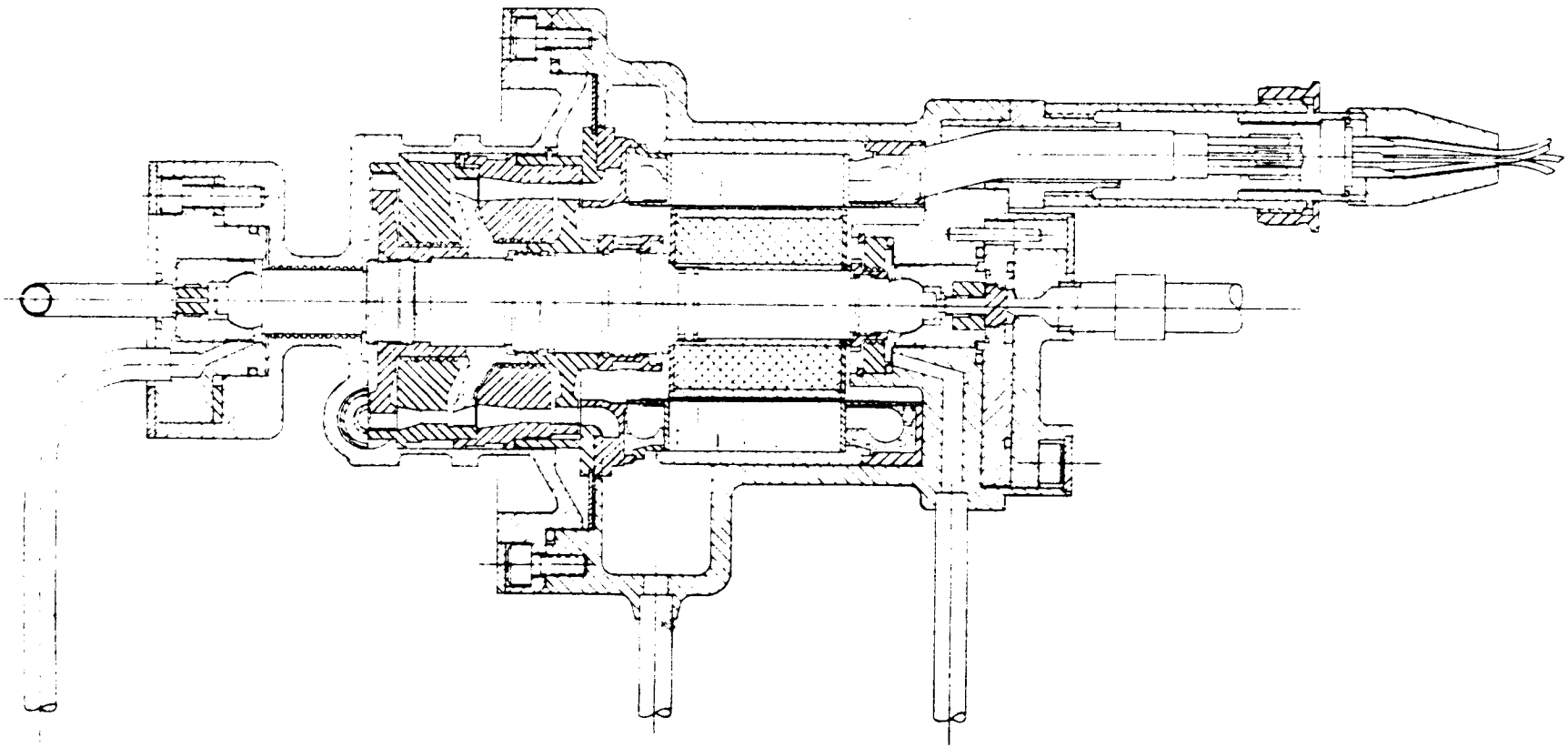
The startup and stabilization sequence of the power system was accomplished with no delay, whatsoever, in the Atlas countdown sequence. The system was in a "Go" condition at launch with the only deficiency noted being a high pressure drop across a bearing inlet filter. This high pressure drop (thought to be attributable to a wetting phenomenon) resulted in a very low supply pressure to the hydrosphere bearings.

During the early launch period, the telemetered data indicated that the power system maintained constant frequency within less than 1% of the rated frequency and all other components operated exactly as anticipated. This smooth operation

was maintained in spite of a vibration, measured at over 10 g's, which began 30 seconds after liftoff and persisted until nearly 2 minutes after liftoff, at which time the Atlas attitude control system failed due to malfunction of a hydraulic system. During this period, the Atlas experienced violent attitude oscillations and it went completely out of control at the time of staging. During this period, the turboalternator appears to have undergone a severe speed oscillation. At about 4 minutes after liftoff, when the last readable telemetry signal was received, however, it appears to have been still rotating.

In spite of the fact that no zero gravity data was obtained, this test resulted in a very impressive demonstration of the operational capabilities of the mercury Rankine system during ground operation and during an extremely severe launch environment. The only system performance deficiency noted was the high filter pressure drop which developed. It should be noted that this deficiency can be readily corrected by utilizing a different type of filter which has been tested under the SNAP 2 and SUNFLOWER programs.

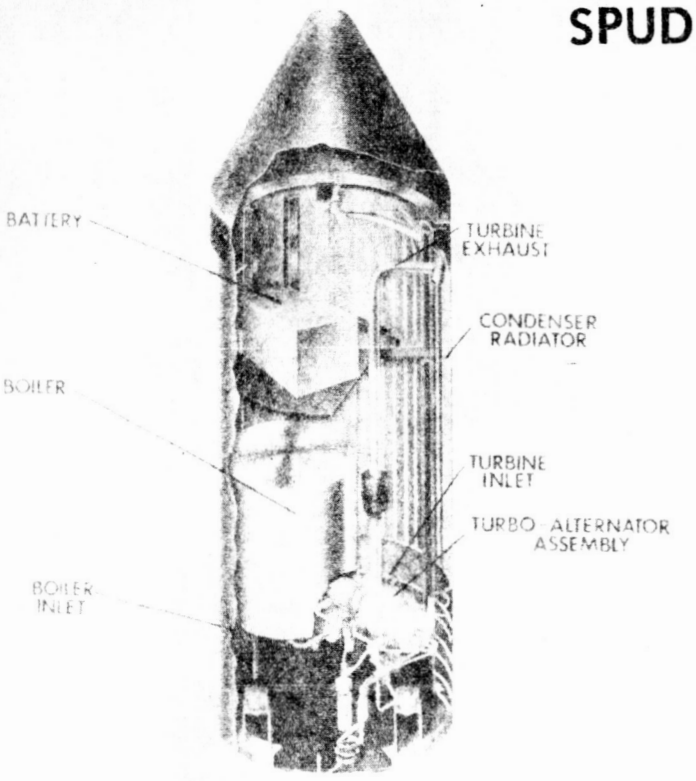
In conclusion, it may be stated that the SNAP 1 and SPUD programs have provided a substantially conclusive demonstration of the performance, endurance, and environmental capabilities of the mercury Rankine power systems. An additional ballistic flight of the SPUD unit is now being negotiated which will provide a second opportunity for obtaining long duration zero gravity operating data. The OFFBACE experiments have already shown capability for zero gravity operation for limited duration. In addition to providing this general guidance, the SPUD power system provides an excellent potential for an operational solar power system in the low power range. Over $7,000,000 have been expended in the development of this equipment and, due to its high efficiency, this conversion unit has excellent performance in the 1500 watt to 3 kilowatt power range. The 3 kilowatt power output capability can readily be provided by substituting an advanced TRW brushless alternator for the permanent magnet alternator as shown in Figure 8. The 3 kilowatt alternator can be installed with the same bearing span as present SPUD units and provides a stiffer, lighter weight, rotor assembly. Performance of both a 1500 watt and a 3 kilowatt conversion unit in a SUNFLOWER type, solar space power system, is discussed later in this report.



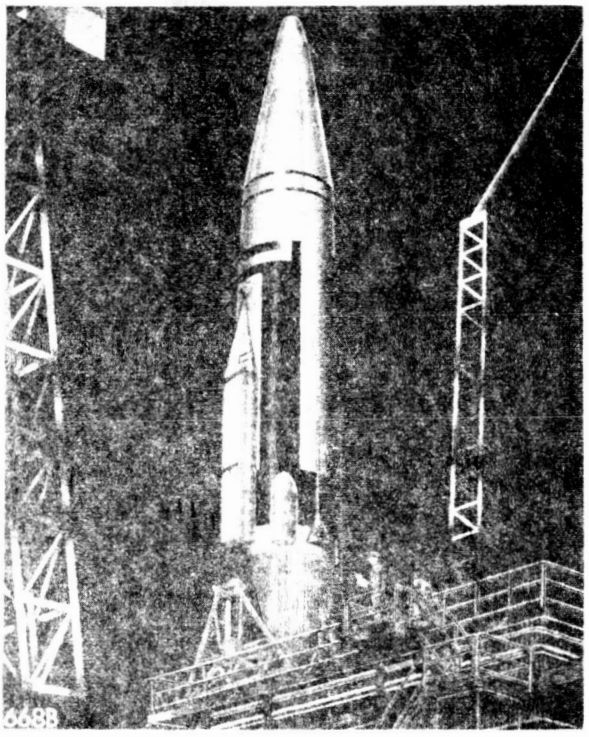
SPUD COMBINED ROTATING UNIT

FIGURE 5

SPUD BALLISTIC PROGRAM



SPACE POWER SYSTEM
TEST PACKAGE

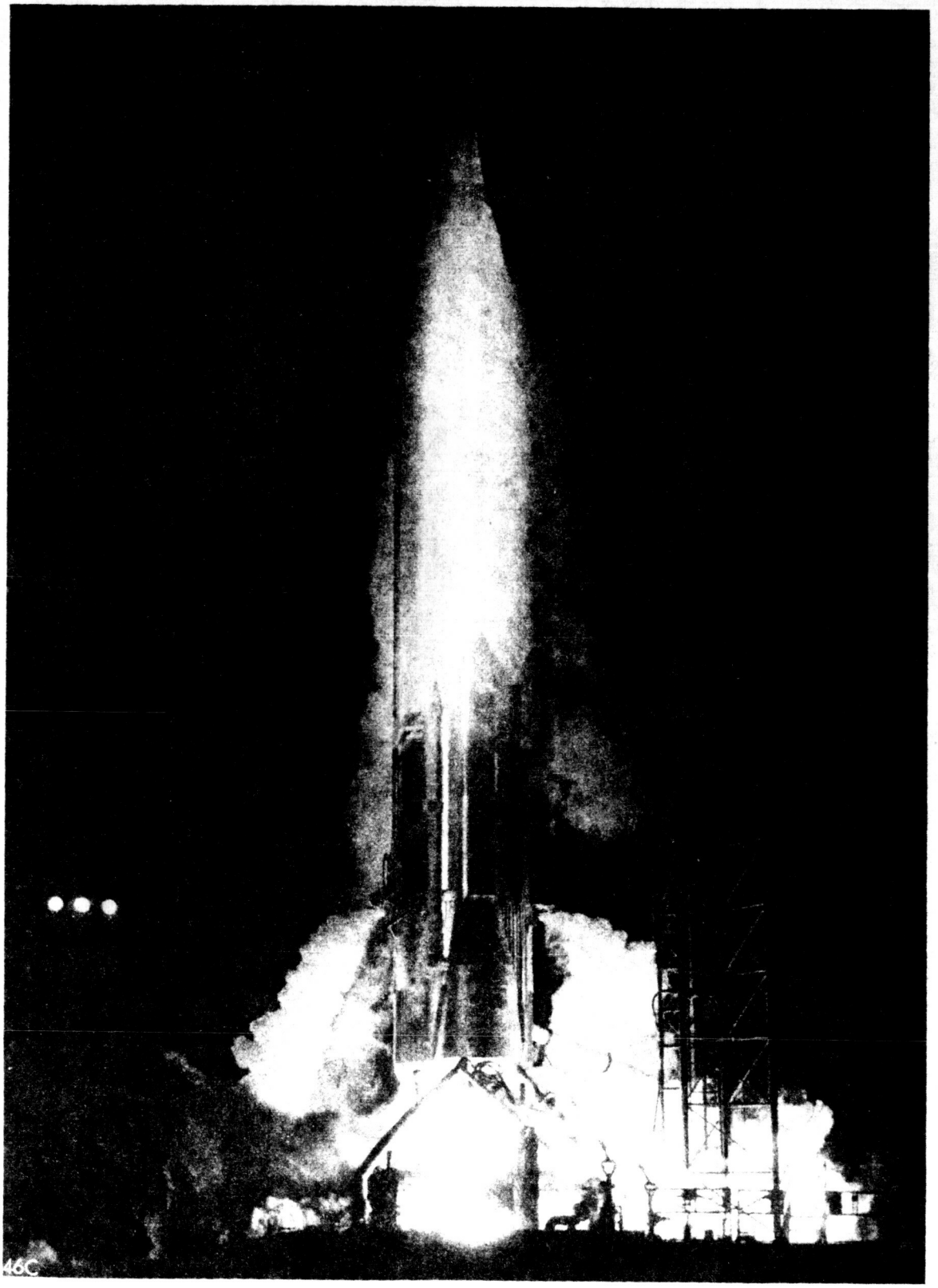


SPUD TEST POD MOUNTED
ON ATLAS MISSILE



SPUD TURBO ALTERNATOR HARDWARE
MOUNTED IN TEST CAPSULE

FIGURE 6



FIRING OF ATLAS MISSILE WITH SPUD EXPERIMENT

FIGURE 7

3 KW MODIFICATION

of

SPUD COMBINED ROTATING UNIT

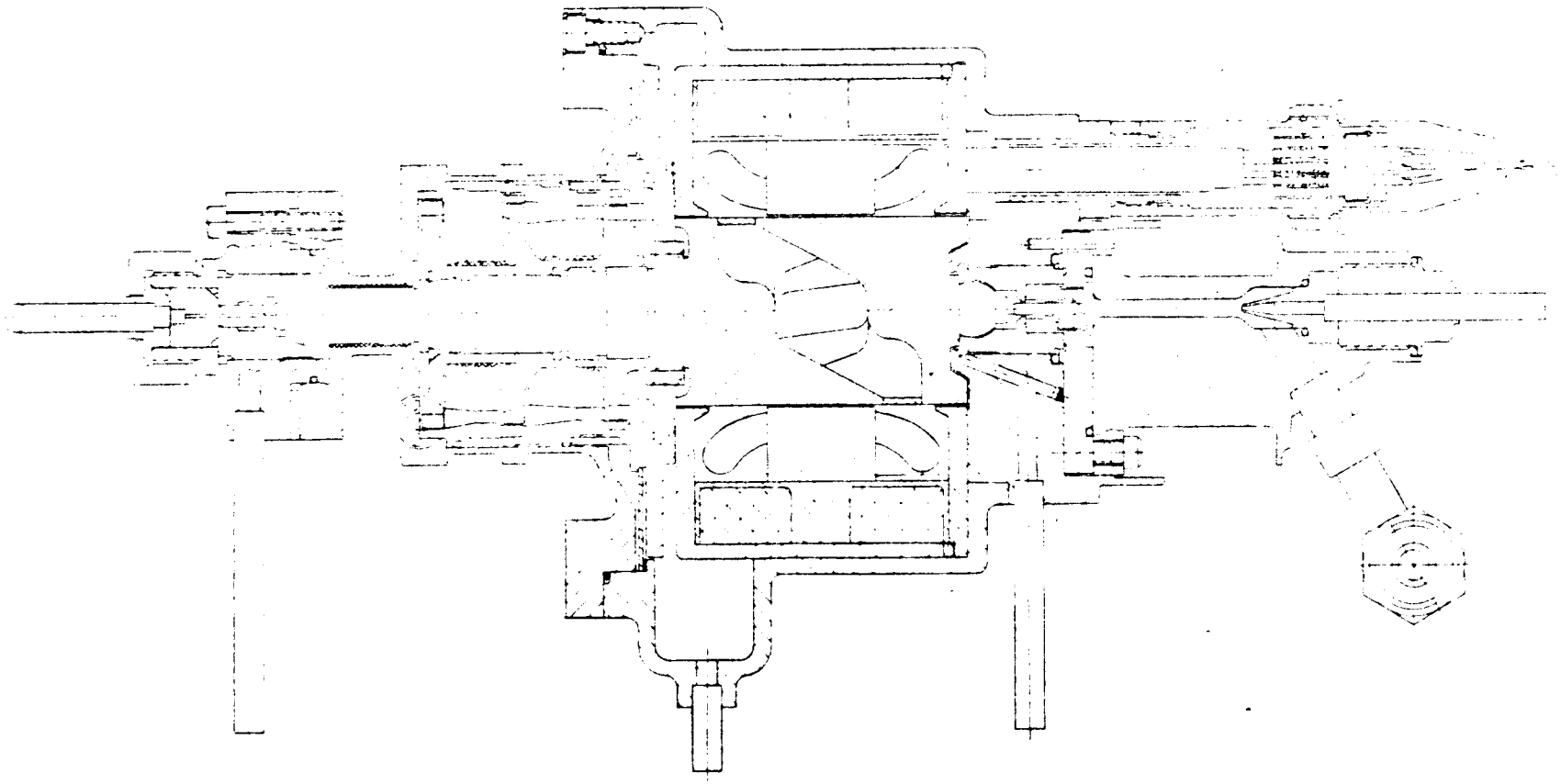


Figure 8

Mercury Compatibility

Materials Test Data

The mercury corrosion effort at Thompson Ramo Wooldridge is supported by SNAP 2. This program is being conducted for Atomics International who holds the prime AEC contract.

Mercury corrosion is a consequence of the fact that most metals have at least a slight solubility in mercury. The solubility increases exponentially with temperature. Thermal gradient mass transfer occurs in any power conversion system since temperature gradients exist. In other words, dissolution takes place in the higher temperature sections and fouling usually results in lower temperature regions. Fouling is caused by precipitation or deposition of mass transported corrosion products which may occur in orifices, nozzles and other critical areas. Erosion may also result from corrosion product transfer. Thus two undesirable effects are taking place: (1) wall penetration and (2) mass transport of corrosion products. The latter is thought to be most detrimental to system life.

Some of the essentials studied were: material resistance to corrosion, time-temperature parameters, and corrosion product removal. Comparison of corrosion results obtained were made with other investigations and found to be favorable.

The testing methods employed include the bent reflux tube (BRT), Figure 9. The tube is fabricated from Pyrex or Vycor (for testing over 1000°F) shaped as an inverted "L" with a dam at the bend. A sample abraided through 2/0 metallographic paper is placed in the condenser. The tube, samples and mercury are evacuated to less than 1mm of Hg and sealed. The tube is then placed partially into a holder in a furnace which is heated only at the bottom. Consequently, a thermal gradient exists which results in distillation of mercury from the boiler and condensation in the condenser. The specimen which is immersed in a pool of liquid is thus exposed to fresh mercury continuously since the pool of mercury fills and empties periodically, returning some of the mercury and corrosion products back into the boiler. Flow rate is about 1/2 lb. of Hg per hour. Advantages are that both weight loss and penetration information may be obtained, additives, time-temperature effects, stress and bimetallic effects may be studied. Disadvantages are that mass transfer and temperature gradient effects are not amenable to study. Therefore, in order to study effects of mass transfer and thermal gradients the loop tests, Figure 10, are used. They are also used to corroborate screening test results. These results are important because the test loop system more closely approaches the characteristics of the power conversion system. Loop tests have generally corroborated BRT material classifications. Loops are fabricated from 1/2" O.D. tubing 76 in. high x 14-1/2" wide. Flow rate is on the order of 10 lb. of Hg per hour. Circulation is of the natural two-phase type.

Bent reflux tube results are evaluated on the basis of equivalent penetration derived from weight loss data. This gives an indication of the amount of potential corrosion products generated by the material. Measured penetrations also influence classifications if these are excessive.

Loop tests are evaluated on the basis of penetration and amount of corrosion products generated.

Over 100 materials have been screened at 900°F and classified as to corrosion resistance. General material behavior based on composition is shown in Figure 11.

Each group corresponds to our classification system -- I through V. Equivalent penetrations for each group are:

Class:	I	II	III	IV	V
Mils/year:	0.1	0.1 to 2.5	2.5 to 25	25 to 50	50

All materials which develop a corrosion layer show diffusion or parabolic controlled weight losses and penetrations. For example, the diffusion controlled weight loss for Haynes 25 at 900°F is shown in Figure 12. The dissolution rate is also plotted and may be seen to be a maximum initially. This rate drops off with time to a rate which is almost constant after about 90 days. The same behavior may be seen for penetration in Figure 13. This protection offered by development of a corrosion layer suggests that a system may be pre-corroded and refilled with clean mercury to remove the inchoate corrosion products.

If this corrosion layer is vacuum annealed and exposed to air, an improvement in corrosion resistance is experienced. For example, a five day pre-corrosion treatment at 900°F reduced Type 347 weight losses by a factor of about 3. The same beneficial effects were noted for Haynes 25.

Some select materials were tested as a function of time and temperature from 600 to 1200°F for times from 30 to 90 days (some as long as 120 days) in the BRT. Assuming diffusion controlled corrosion the parabolic rate constants were plotted. The tentative Arrhenius plots are shown in Figure 14. The lines indicate average values and the bars - maximum values. The curves show that the 300 series would generate the most corrosion products at 1100°F - about 480 mg/in^2 in one year. Haynes 25 would generate about 33 mg/in^2; the 1010 and 410 group about 19 mg; Cb + 6.8% Ti about 1.2 mg; tungsten about 0.74 mg and columbium about 0.24 mg. Tantalum would be the most resistant and would probably not generate any corrosion products at this temperature.

Incidentally, comparisons of weight loss data from these curves have been made with the data published in the Liquid Metals Handbook. For example, for the 300 series at 1200°F a value of 26 mg cm^{-2} mo^{-1} was calculated as compared to the published value of 32 mg cm^{-2}mo^{-1}. For Sicromo 5S values of 0.45 mg cm^{-2}mo^{-1} at 900°F and 4.5 mg cm^{-2}mo^{-1} at 1200°F were calculated as compared to the published values of 0.3 and 4 mg cm^{-2}mo^{-1}, respectively. For 1010 our values were low by a factor of 15.

Data obtained by the groups studying mercury corrosion is usually reported as penetration. It should be pointed that another important factor closely associated with the amount of corrosion product is the intensity of the attack as measured by weight loss. Our work results in data giving both penetration and weight loss and thus an indication of attack intensity.

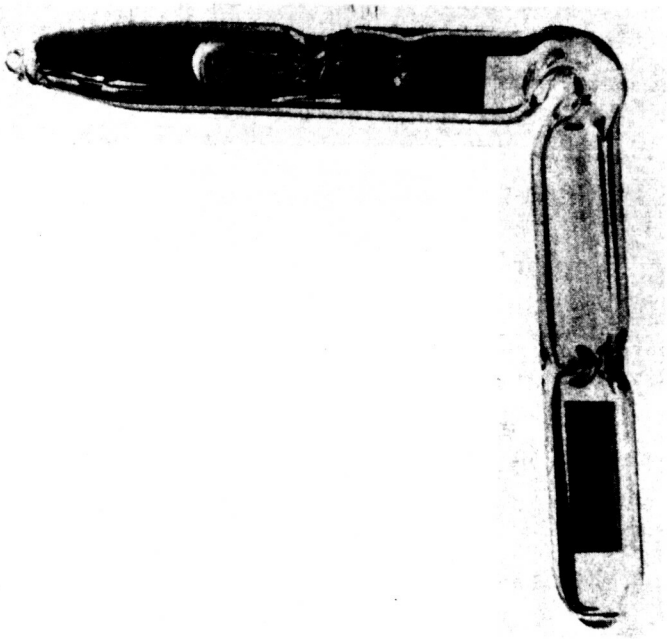
A summary of penetrations obtained for Haynes 25 from BRT and loop tests and from other investifations are shown in Figure 15. Loop penetrations are about 3-fold greater that BRT penetrations in the lower temperature regions; however, at higher temperatures the penetrations overlap. The NASA data fits in quite well with Thompson Ramo Wooldridge penetration data and indicates an average of about 9 mils of penetration in one year of operation for Haynes 25. Brookhaven loop data agreed with our BRT results. The Brookhaven loop contained a titanium source in the subcooler. In the next Figure 16, are shown penetration rates obtained from

this and other investigations for a variety of materials. Diffusion controlled corrosion was assumed in calculating the rate constants. Agreement, in general, is not bad considering the different test conditions. Of interest is the penetration observed on Type 410 loops which were in the Haynes 25 loop range. The amount of leached elements removed from both the Haynes 25 and the Type 410 loops were about 7 grams each at a boiling temperature of 1000°F for a 5000 hour test period. Considering both the high temperature properties and resistance to attack, Haynes 25 appears to be the preferred conventional material of construction at these temperatures especially if corrosion products can be partially removed.

Since it is feared that mass transport and accumulation of corrosion products might tend to accumulate in critical areas, a Haynes 25 loop containing a corrosion product separator was tested. The test was conducted for 1000 hours at a boiling and condensing temperature of 1100°F. A schematic of the separator is shown in Figure 17. The unit was made of three compartments which contained: (1) columbium turnings, (2) magnets, and (3) iron wool. The mercury entered the columbium separator at 730°F, the magnets at 615°F, the iron wool at 560°F and exited at 540°F. The location of the separator is shown in Figure 18. The separator removed 85% of the corroded metal leached from the container walls as shown in Figure 19. The total leached metal weight was 3.2 grams.

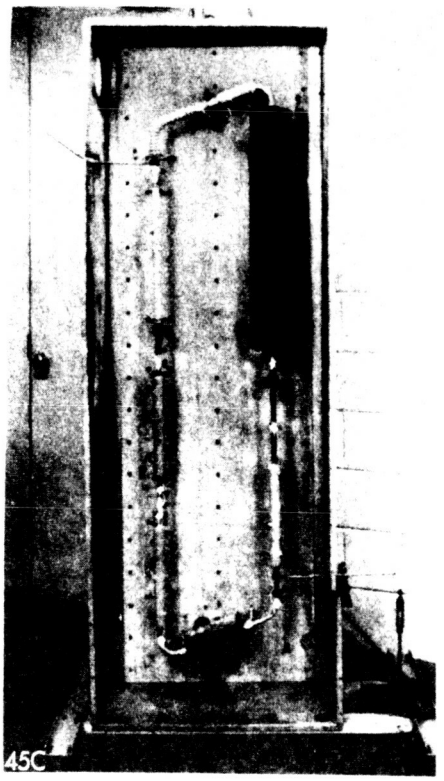
The test demonstrated that it is possible to remove some of the corrosion products and thus further improve the longevity of a power conversion system.

In summary, materials were screened and classified as to corrosion resistance at 900°F with the BRT test. Time-temperature parameters were determined for some materials. A corrosion product removal test was considered to be successful. Comparisons of Thompson Ramo Wooldridge corrosion data with other investigations appeared to be favorable.



GLASS TUBE FOR MERCURY CORROSION TEST

FIGURE 9



CORROSION TEST LOOP

FIGURE 10

RELATIVE CORROSION OF SOME MATERIALS IN MERCURY AT 900°F.

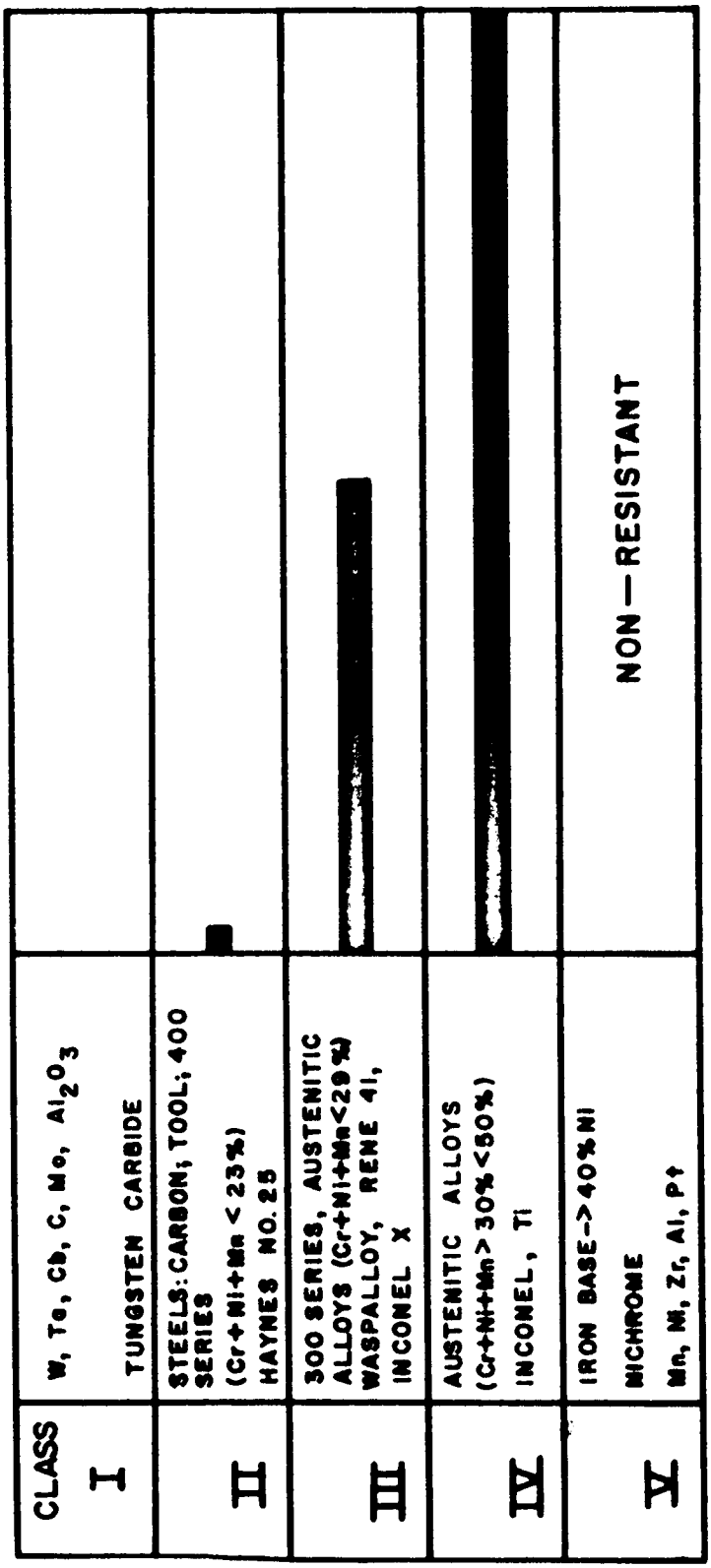


FIGURE 11

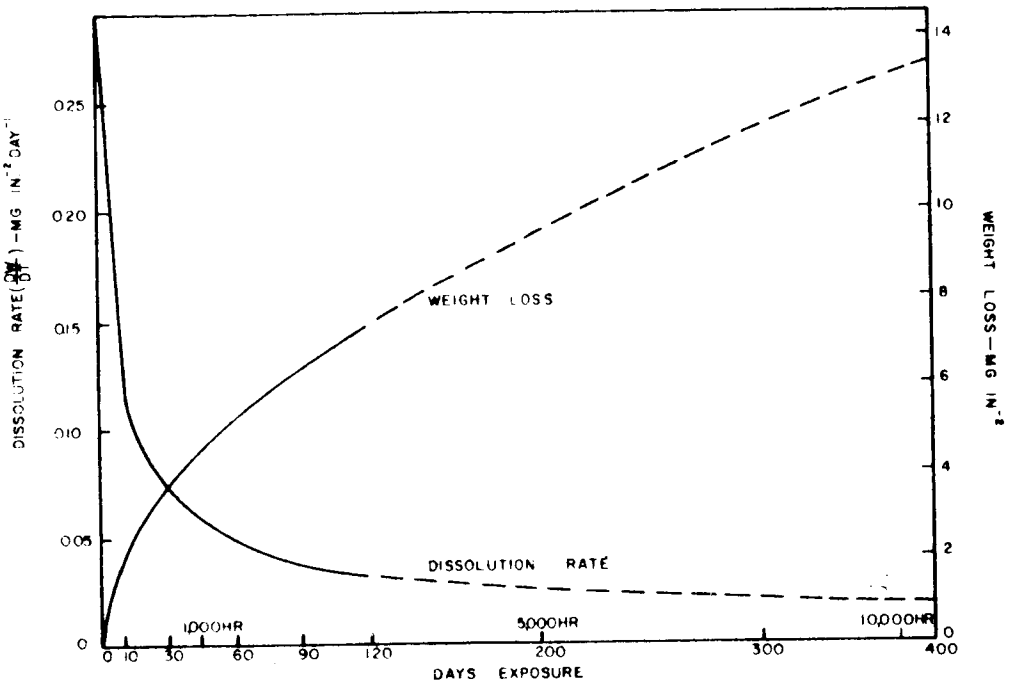
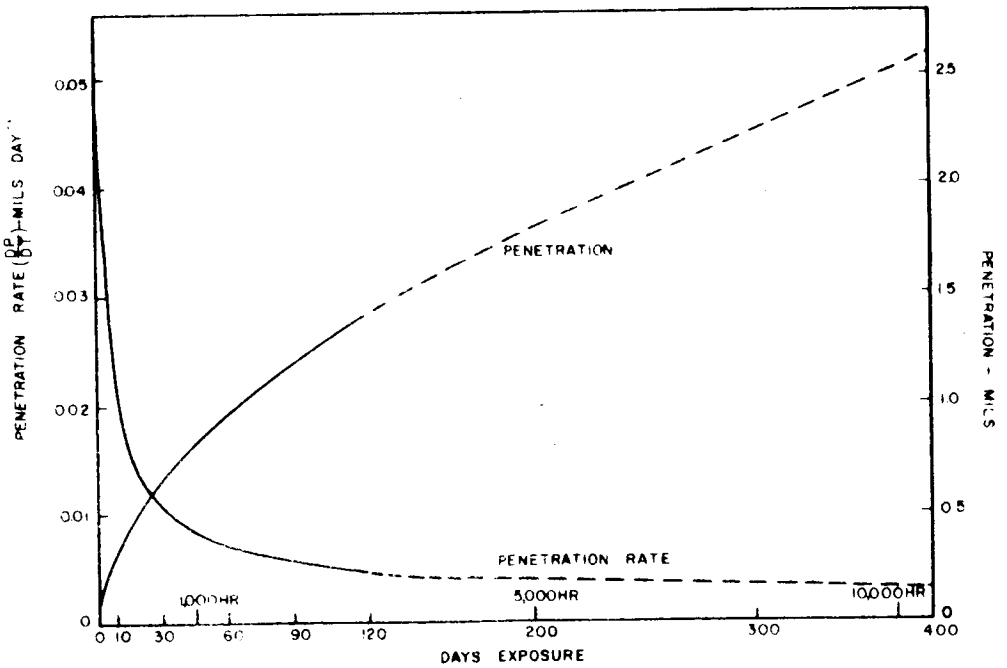


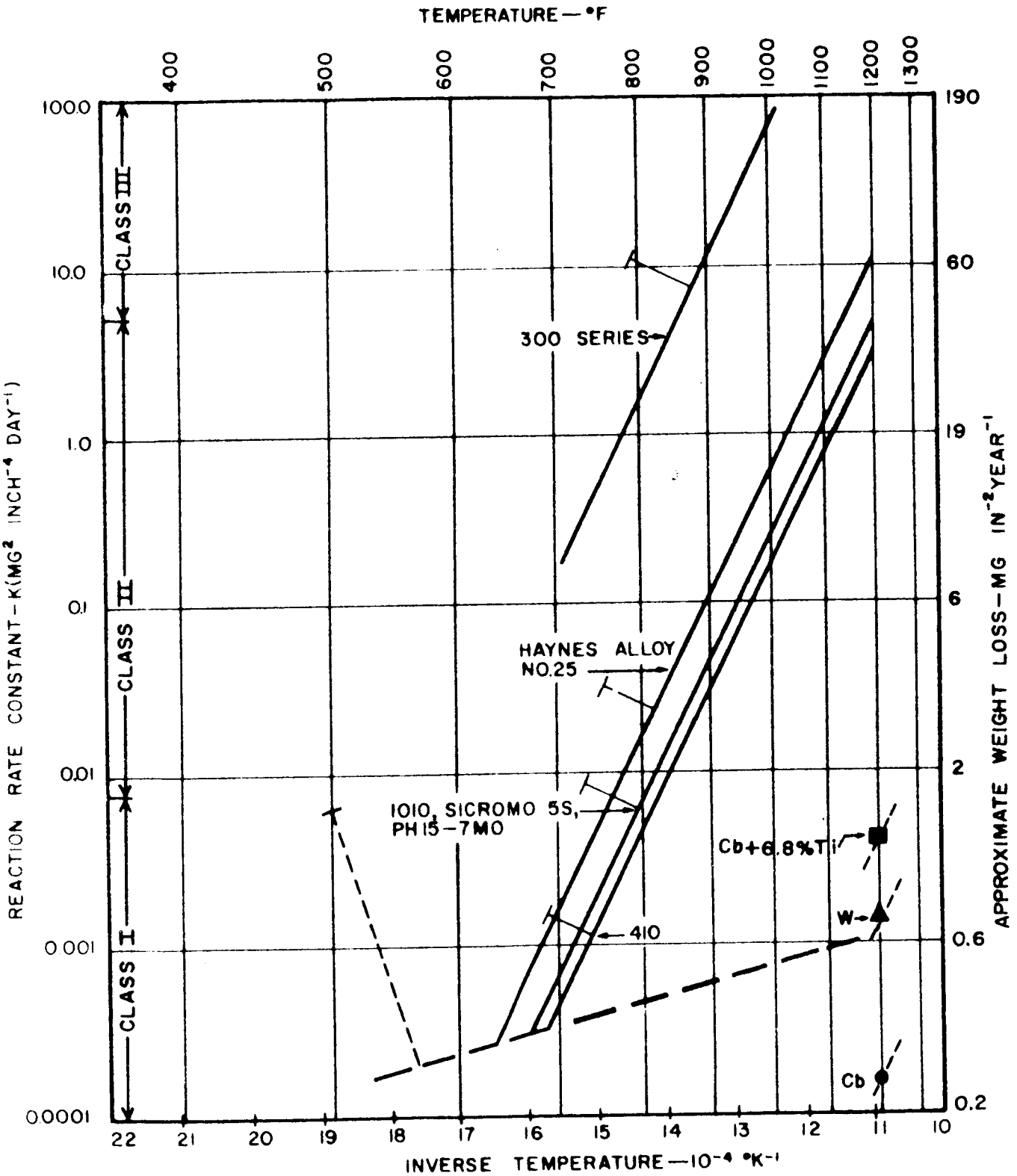
FIGURE 12

WEIGHT LOSS AND DISSOLUTION RATE VS TIME FOR HAYNES ALLOY NO.25 IN REFLUXING LIQUID MERCURY AT 900°F.



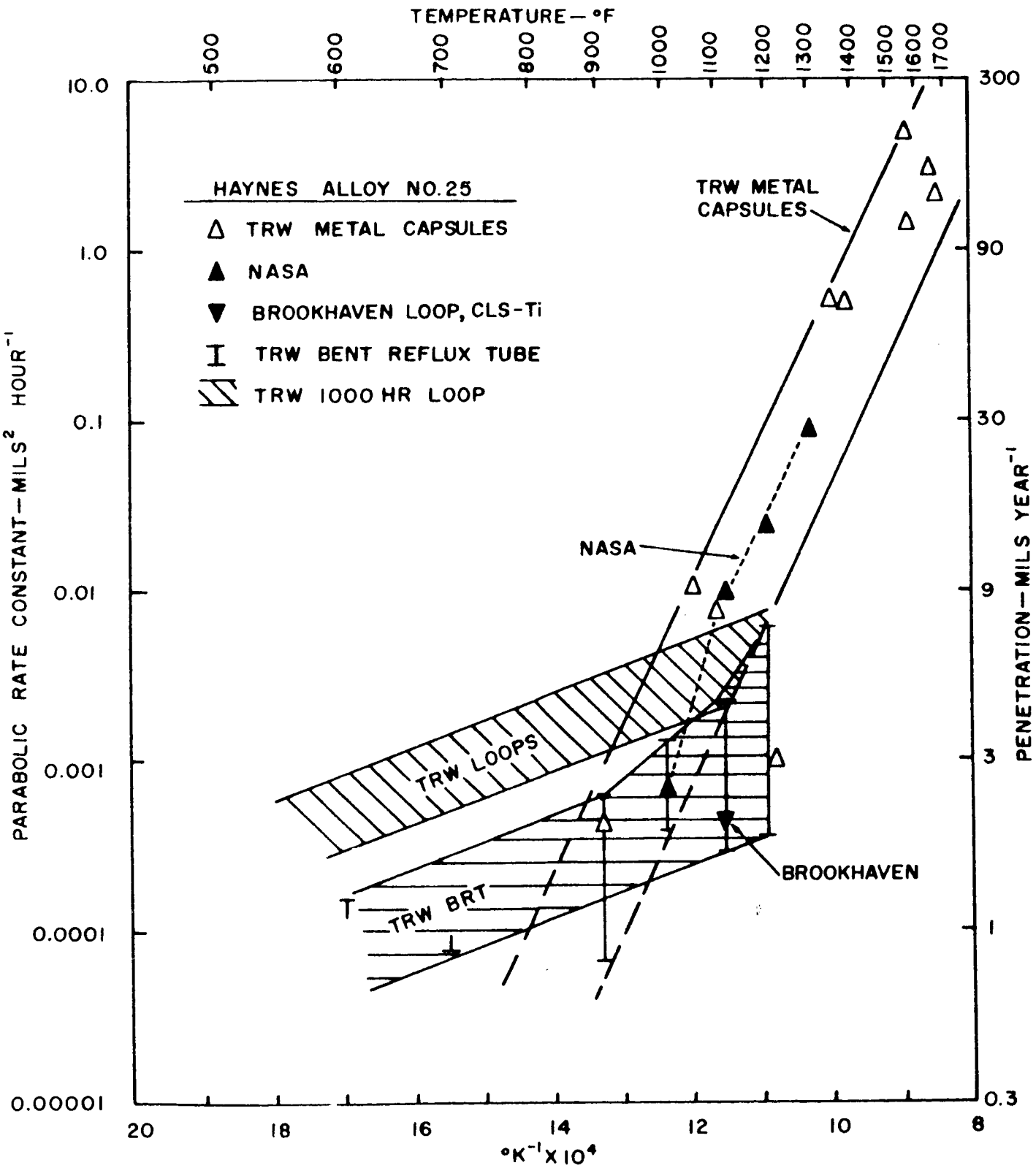
PENETRATION AND PENETRATION RATE VS TIME FOR HAYNES ALLOY NO.25 IN REFLUXING LIQUID MERCURY AT 900°F.

FIGURE 13



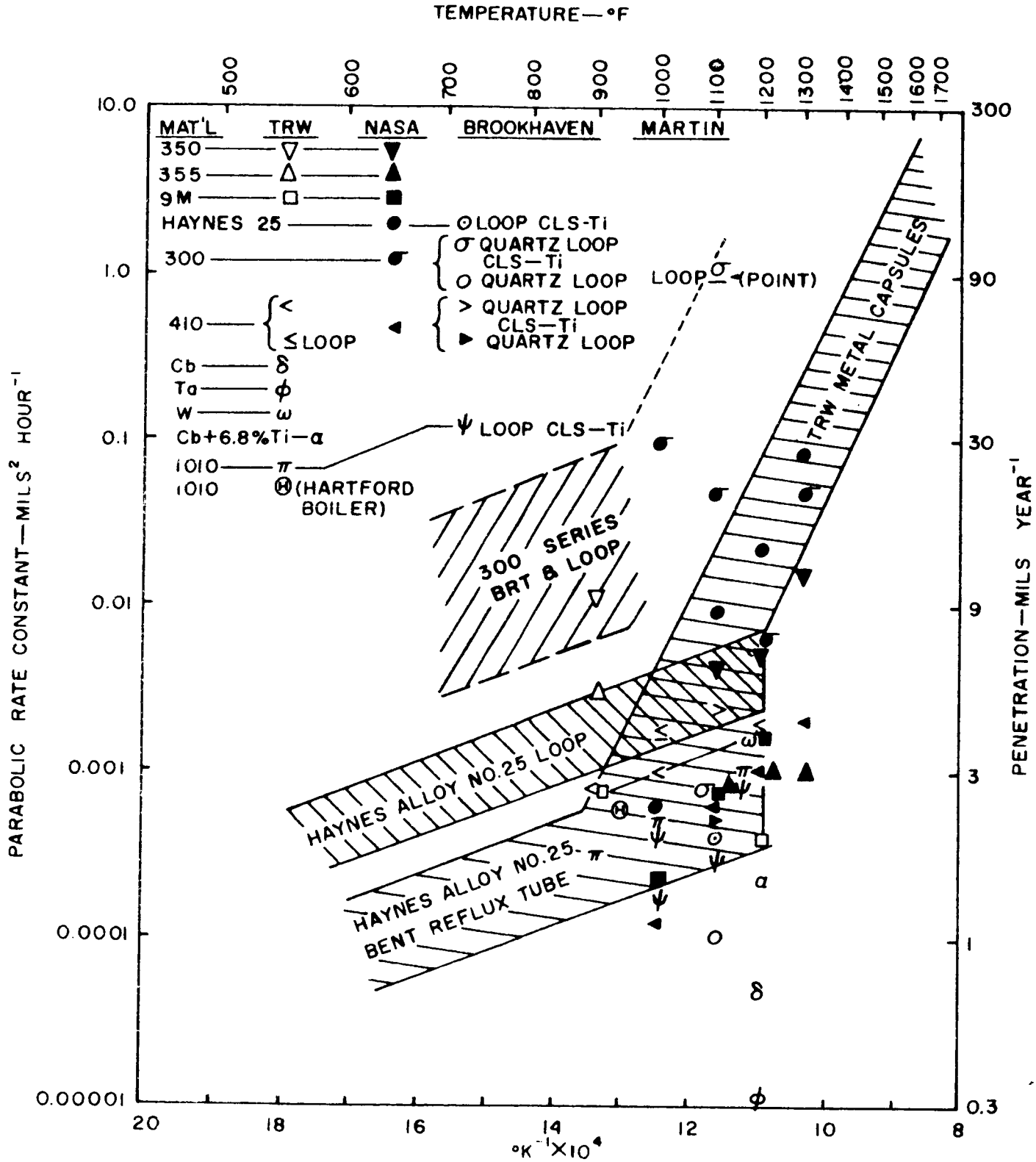
SUMMARY - WEIGHT LOSS vs TEMPERATURE

FIGURE 14



HS-25 PENETRATION vs TEMPERATURE

FIGURE 15



SUMMARY - PENETRATION vs TEMPERATURE
VARIOUS INVESTIGATORS

FIGURE 16

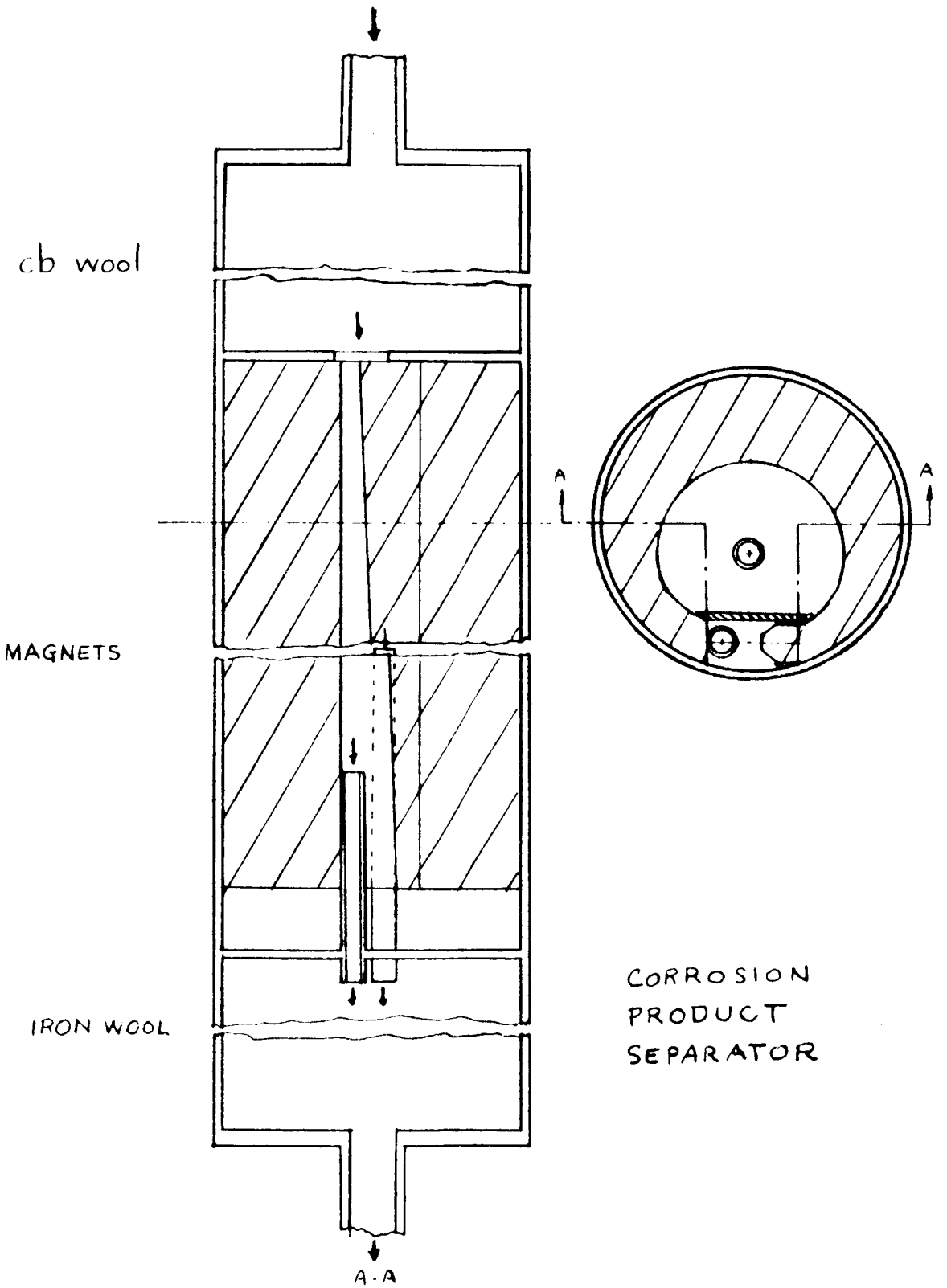
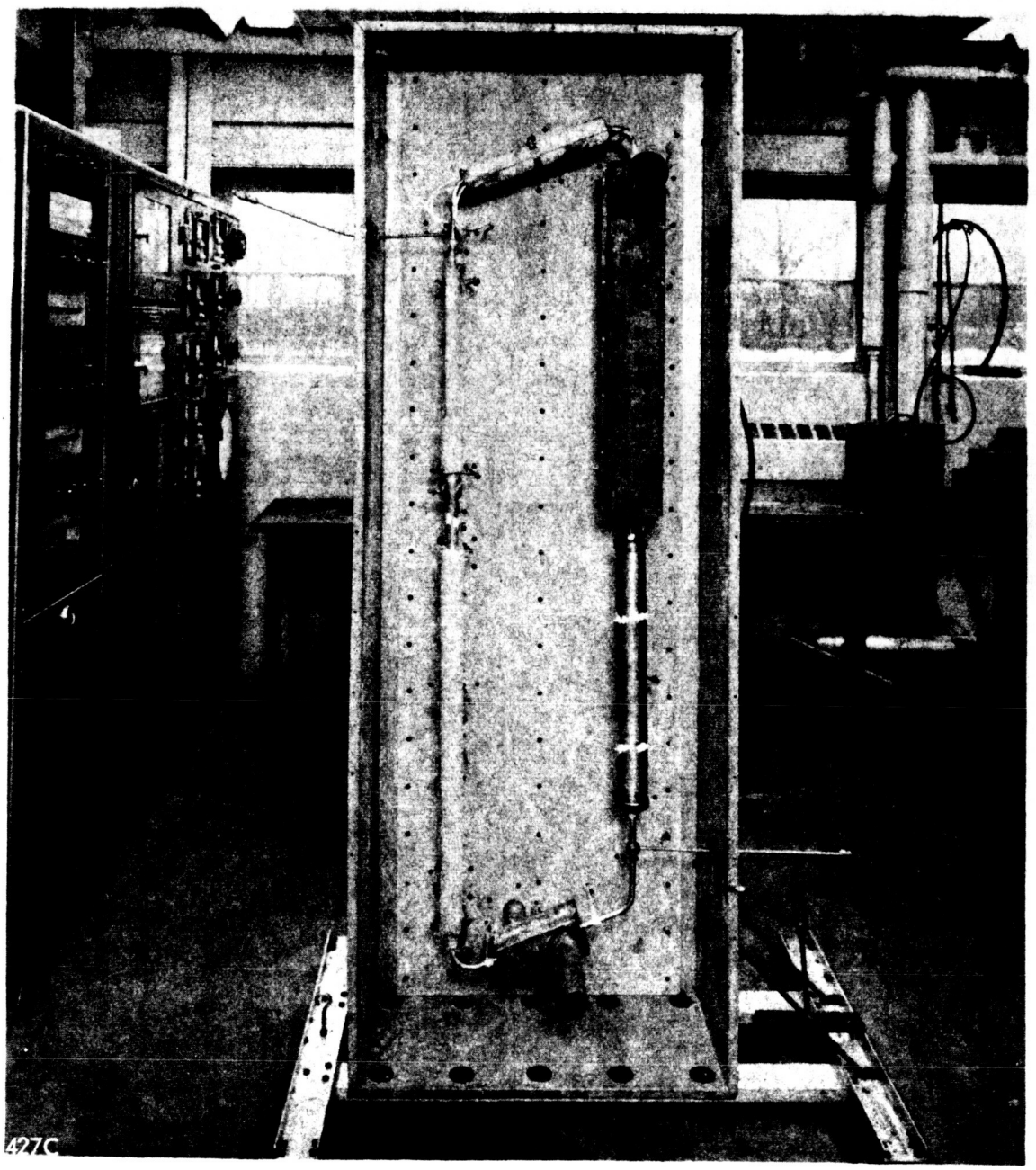
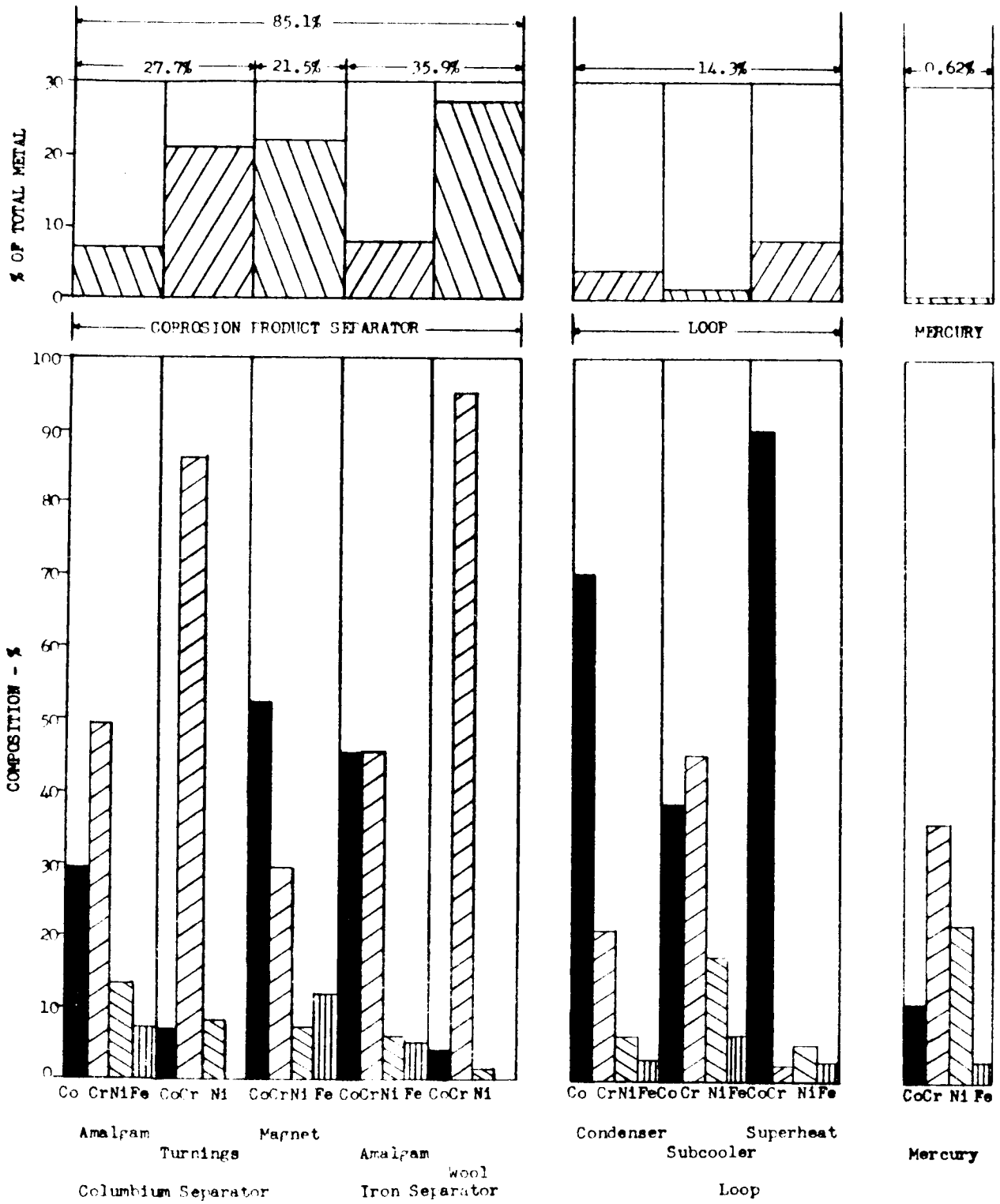

cb wool
MAGNETS
IRON WOOL
A-A
A
A
CORROSION
PRODUCT
SEPARATOR

FIGURE 17



HAYNES ALLOY NO. 25 LOOP WITH CORROSION PRODUCT SEPARATOR

FIGURE 18



Corroded Metal Deposit Location and Composition

FIGURE 19

System Compatibility to Mercury Corrosion Products

The preceding discussion has indicated the amount of corrosion products we may expect to be generated in one year's operation ofa mercury Rankine system. Correlation between the total internal plumbing area of the Sunflower system (regardless of temperature) and the material removal data of the preceding discussion at 1100°F would conservatively indicate a quantity of material removal of 2.6 cubic inches. Utilization of trapping concepts, as effective as the concepts employed in the reported loop tests, would reduce this by 85% to 0.39 cubic inches. Preconditioning of the system by pre-corrosion and oxidation will permit further reduction by a factor of 3, leaving a residual after one year's operation of approximately 0.13 cubic inches.

These numbers strongly indicate the tolerability of mercury Rankine systems to the corrosion products which will be formed in a Haynes 25 system with the above noted provisions and precautions. The picture can be made even more reassuring by reviewing the indicated compatibility of system components, which has been exhibited in the developmental tests of systems under much less favorable conditions.

Due to the combination of economy, availability and timing of the identification of superior materials, most of the development test rigs at TRW have been fabricated of 300 series stainless steels. As indicated in the preceding section, this material will yield ten times the amount of corrosion products at similar operating conditions as will be yielded by Haynes 25. Yet, under these very adverse operating conditions, we have accomplished several 500 hour runs on SNAP 2, a 2500 hour run on SPUD and the current Sunflower run in excess of 1400 hours. These runs have been characterized by freedom from spurious influences of corrosion product deposition in the rotating packages; with a single exception being the mercury pump on the SPUD package. This exception can be explained by excessive air leakage. In this test copious air leakage occurred through the alternator bore seal, since mercury was kept out of the alternator stator by keeping a greater-than-atmospheric pressure on the alternator and permitting gas flow inward through the faulty bore seal. This operating procedure introduced enough air to cause a bubble to form at the inlet to the pump of sufficient size to prevent successful pump operation. Even under these conditions, such possibly critical elements as the hydrosphere bearings exhibited no degradation with time or corrosion product accumulation whatsoever.

In the above noted SPUD endurance test, a .001 to .002 inch deposit of contaminants was observed on disassembly on the first stage nozzle vanes. This buildup did not cause an observable change in the turbine performance of that unit. However, in the last few days of the Sunflower test, the turbine flow-pressure conditions have indicated a similar buildup in that unit.

Results of the several 500 hour SNAP 2 tests have been free from indications of corrosion product deposition problems in the rotating package. In recognizing these facts, it is germane to note that the rotating units under discussion incorporate a number of flow restrictions and orifices, especially in the bearing feed areas. These include both static and dynamic restrictions. The freedom of these restrictions from blockage under these adverse conditions is significant.

Problems of corrosion product blockage have been observed in other areas of TRW's developmental rigs and hardware, however. It has been observed that flow restrictions which occur in cold portions of the flowing system may frequently be subjected

to deleterious accumulation and even blockage. Examples are; manually operated external flow regulating valves, jet pump nozzles, external flow regulators and flow metering orifices. The significant difference between these restrictions and similar trouble free restrictions in the package is the thermal condition. Specifically, blockage is observed to occur where the material of the restriction is colder than the folowing mercury. This is not surprising since a portion of the corrosion products are carried in solution and would tend to precipitate out where the mercury is cooled. This hypothesis has been checked by such means as employing electrical heaters on the housings of such system elements. It has generally been observed that, while it is difficult to clear up blockage which has occurred, heat application can effectively prevent the containment accumulation. Examples include package drain jet pumps which are employed in the SNAP 2 system which chronically caused trouble prior to the employment of this technique. Identical techniques have been employed on flow regulators, perhaps the most notable one being the flow regulator included in the sealed SPUD system which successfully passed checkout, transportation, re-checkout and launch. This flow regulator was exhibiting symptoms of blockage which were arrested by the addition of heat.

This knowledge identifies a number of effective controls of potential corrosion product accumulation difficulties. In the Sunflower system it appears that jet pump nozzle blockage can be eliminated by permitting the jet pump driving fluid to reject sufficient heat to space, to reduce its temperature slightly below the temperature of the jet pump hardware.

Our current conceptual thinking is based primarily on reducing the quantity of corrosion products formed, and circulation in the system to the minimum. In addition, all the flow regulators in the bearing lubrication lines will be eliminated, retaining only the modulated flow regulator at the boiler inlet. This area can be well insulated and supplied with a few watts of electrical heat to similarly prevent contaminant accumulation in its sensitive elements.

The above discussion has stressed the positive aspects of our knowledge.

There are two areas of incomplete knowledge in the reassuring summary presented above.

1. The compatibility testing which has been accomplished to date has been limited to single temperature conditions ($T_{boiling} \simeq T_{Condensing}$) and to lower velocity, lower heat flux conditions than will be experienced in operating systems. These variables may influence the comptatibility data. Pumped loop experiments are being initiated at TRW and Aerojet to provide closer analogy to system requirements. A second and more relevant check would result from the long term operation of a HS-25 Sunflower near-prototype system.

2. Corrosion product deposition characteristics will be influenced by zero gravity conditions. It is apparent that 1 g conditions will strongly tend to accumulate corrosion products, especially at liquid vapor interfaces, and that the better dispersion which will occur under 0 g conditions will improve the system compatibility. This consideration, together with the excellent corrosion product trapping results indicate that 0 g operation will not adversely influence the system. We cannot claim, however, to have operated long term 0 g tests of systems.

Thus, TRW's current conclusions on the mercury compatibility question may be summarized as follows:

1. The use of Haynes 25 throughout the system supplemented by a preconditioning operation and also supplemented by the incorporation of corrosion product trapping provisions will reduce the amount of contaminants with which the system must contend to a very low value, conservatively estimated at 0.13 cubic inches.

2. Developmental experience at TRW has indicated that all elements of the system except cold flow restrictions are compatible without measurable deterioration to corrosion product content several orders of magnitude higher than that hypotesized in the above defined system.

3. The "cold restrictions" exceptions of item 2 above can be effectively negated by avoiding cold restrictions.

It will be a major objective of the forthcoming Sunflower test to demonstrate validity of the above conclusions with one major exception. The system will employ 300 series stainless steel throughout and will thus be exposed to the significantly higher corrosion product formation. Thus, successful demonstration of this system will be even more significant.

Hydrogen Containment

Hydrogen Containment Data

The relatively high efficiency of the heat sink in the Sunflower system is dependent on maintaining a high percentage of lithium hydride in the boiler assembly. Under the anticipated conditions of operation the partial pressure of hydrogen over the molten LiH at 1600°F is approximately 1 atmosphere and this results in a substantial loss of hydrogen through the container walls. A relatively high permeation of hydrogen through the boiler into space will produce a serious loss in the heat sink capacity by decreasing the LiH/Li ratio and could also produce problems in pump section of the assembly.

The purpose of this discussion is to briefly summarize the experimental effort which has been directed toward evaluating the permeability of hydrogen through constructional materials and to present several methods which provide current solutions to the hydrogen containment problem.

A large quantity of data is available on the basic permeability of metals to hydrogen. Figure 20 presents the permeability as a function of temperature for several pure metals. There is a wide spectrum of hydrogen permeability values present in metals with columbium, for example, having a permeability to hydrogen which is about three orders of magnitude greater than that present in molybdenum. As a general rule, the permeabilities obtained by alloying pure metals are simply additive functions of the metals which compose the alloy. For example, an alloy of iron and molybdenum would have a permeability to hydrogen which is intermediate between the permeability obtained in pure iron and pure molybdenum, however current fabrication technology eliminates the use of this metal for a boiler material due to its brittleness. As a point of reference when discussing the subsequent experimental data, it is well to keep in mind that the permeability of materials to hydrogen must be at least as good as molybdenum to be useful for the Sunflower application.

Since the existing metals do not afford an adequate barrier to hydrogen loss, consideration must be given to oxide and glass coatings as barrier systems.

Data on the permeability of hydrogen through oxides and glasses is relatively sparse, particularly when the additional conditions of chemical and mechanical integrity under cyclic temperature conditions are also considered. The major experimental effort on this program has therefore been directed towards evaluating the permeability of hydrogen through metal-coating systems. The permeability is measured with a modified Sieverts type apparatus at temperatures ranging from 1600°F to 1200°F under a pressure head of 1 atmosphere.

A. Oxide Coatings

Typical results obtained with oxide coatings that are unstable are presented in Figure 21 which show the permeability of hydrogen through an oxidized stainless steel diaphragm. During the first heating cycle, the oxide coating provides a substantial barrier to hydrogen; however, as the specimen is cycled the effectiveness of the coating is rapidly reduced until the permeability of the coated specimen approaches the uncoated condition.

A relatively stable oxide coated is Al_2O_3 which is obtained by aluminizing Haynes 25 and oxidizing the aluminized surface. The

permeability of hydrogen through this barrier is presented in Figure 22 for two methods of aluminizing. The aluminizing process which employs pack cementation (Chromalloy) provides the most effective barrier. Although there is a slight degradation in the barrier properties on the first heating-cooling cycle, subsequent cycling causes practically no change in the hydrogen permeation.

B. Glass Coatings

Glass coatings are very effective barriers to hydrogen flow; however, they are also mechanically unstable when exposed to the cyclic temperature conditions. Although numerous glasses have been evaluated, they appear to have comparable barrier capabilities when they do not undergo mechanical spalling. The best glass from a combined long-time stability and permeability standpoint is the Solaramic coating. Data obtained on specimens coated with Solaramic are presented in Figure 23. Also included in this figure (dashed area) are recently published data from an independent source on the Solaramic coatings. An extremely good bond is obtained between the base metal and coating and this results in relatively good reliability over long time periods and under cyclic temperature conditions.

The permeabilities of several coated specimens are presented for comparison in Figure 24. Both the aluminized Haynes 25 and the Solaramic coatings (glasses) have permeabilities which are lower than molybdenum, hence they represent realistic laboratory solutions to the hydrogen containment problem.

The logical extension of the laboratory data is to employ it to predict hydrogen loss after long time exposure and in actual lithium hydride containing systems. The results of long time tests are presented in Figure 25 where the permeability of hydrogen through the Solaramic-coated specimens is evaluated as a function of test time. Although the data fall in a scatter band, a moderately good extrapolation can be performed which indicates that after 10,000 hours, which is the design life of the system, the barrier properties of the coating are still comparable to those obtained with molybdenum. There is, of course, the additional advantage of even lower permeabilities in the time interval up to one year. Using a Solaramic coating and neglecting the advantages obtained when the boiler is in the shade cycle, the calculated loss of hydrogen in the present Sunflower system is less than 3 lbs. per year.

In many instances, certain data obtained under idealized laboratory conditions is not applicable to actual operating conditions where the complicating effects of corrosion produce a very high hydrogen activity and an attendant increase in hydrogen flux. To evaluate the ability of the hydrogen permeation parameters for predicting actual loss of hydrogen produced in lithium hydride containers, actual capsule tests were conducted under cyclic temperature conditions. The loss of lithium hydride determined experimentally in capsule tests was compared to the value calculated from the laboratory derived permeability parameters. The results presented in Figure 26 indicate that a good correlation is obtained between the two methods and the permeability parameters can therefore be used to realistically

predict lithium hydride containment.

The current status of the hydrogen containment problem indicates that the Solaramic coating and the aluminized Haynes 25 provide adequate barriers to hydrogen outgassing. With these coatings less than 3 lbs. of hydrogen is lost per year through the boiler section, and approximately 4×10^{-4} lbs. of hydrogen is lost to the pump section.

The future work in the hydrogen containment area will be aimed at:

1. Developing coatings with improved barrier properties,

2. Evaluating and improving the long-time stability of the coatings.

A significant development in either of these areas will produce an even lower degree of hydrogen loss and a decreased weight of the lithium hydride section of the Sunflower.

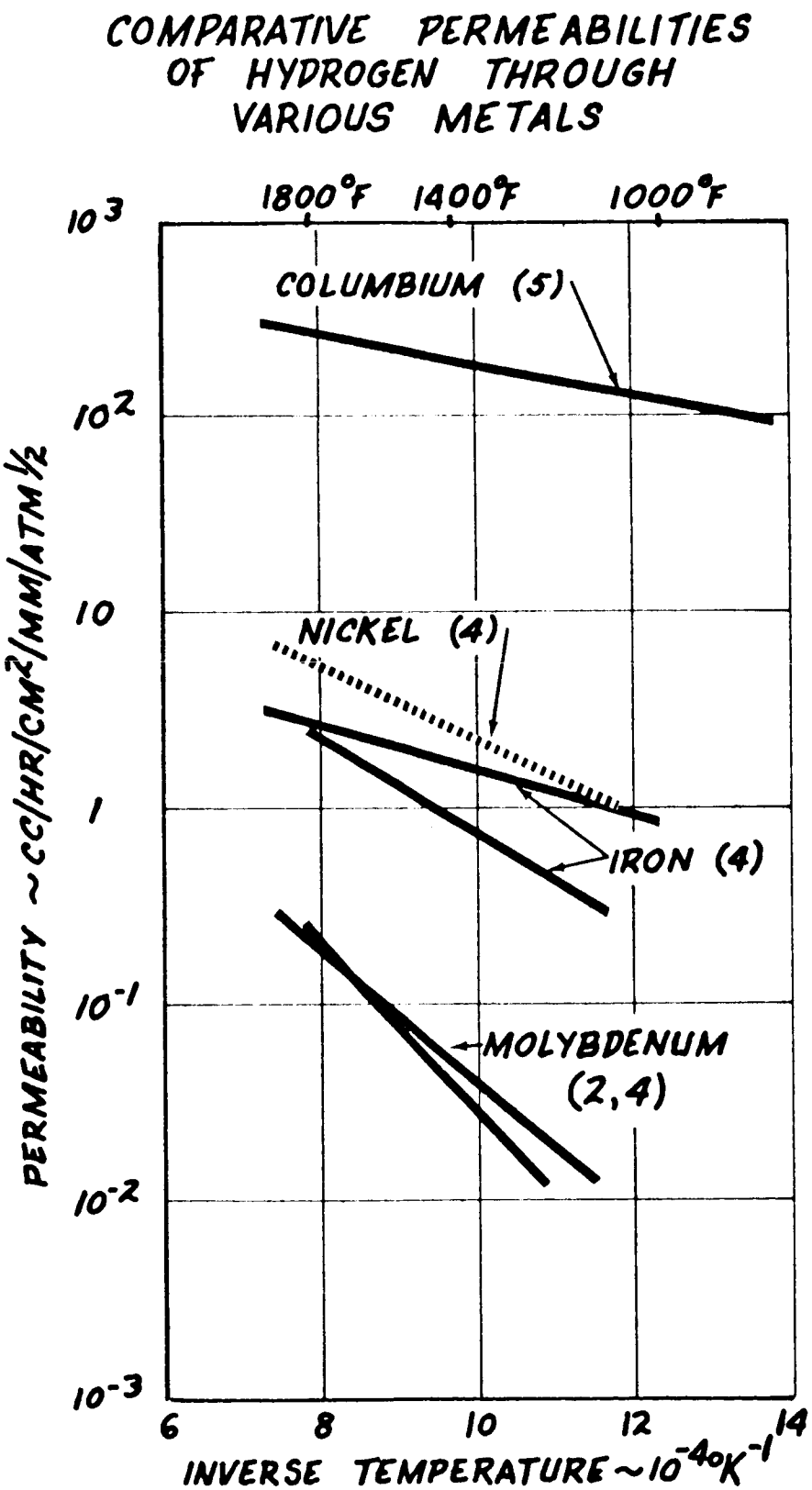

COMPARATIVE PERMEABILITIES
OF HYDROGEN THROUGH
VARIOUS METALS
1800°F
1400°F
1000°F
COLUMBIUM (5)
NICKEL (4)
IRON (4)
MOLYBDENUM
(2,4)
PERMEABILITY ~ CC/HR/CM²/MM/ATM½
10³
10²
10
1
10⁻¹
10⁻²
10⁻³
6
8
10
12
14
INVERSE TEMPERATURE ~ 10⁻⁴°K⁻¹

Fig. 20

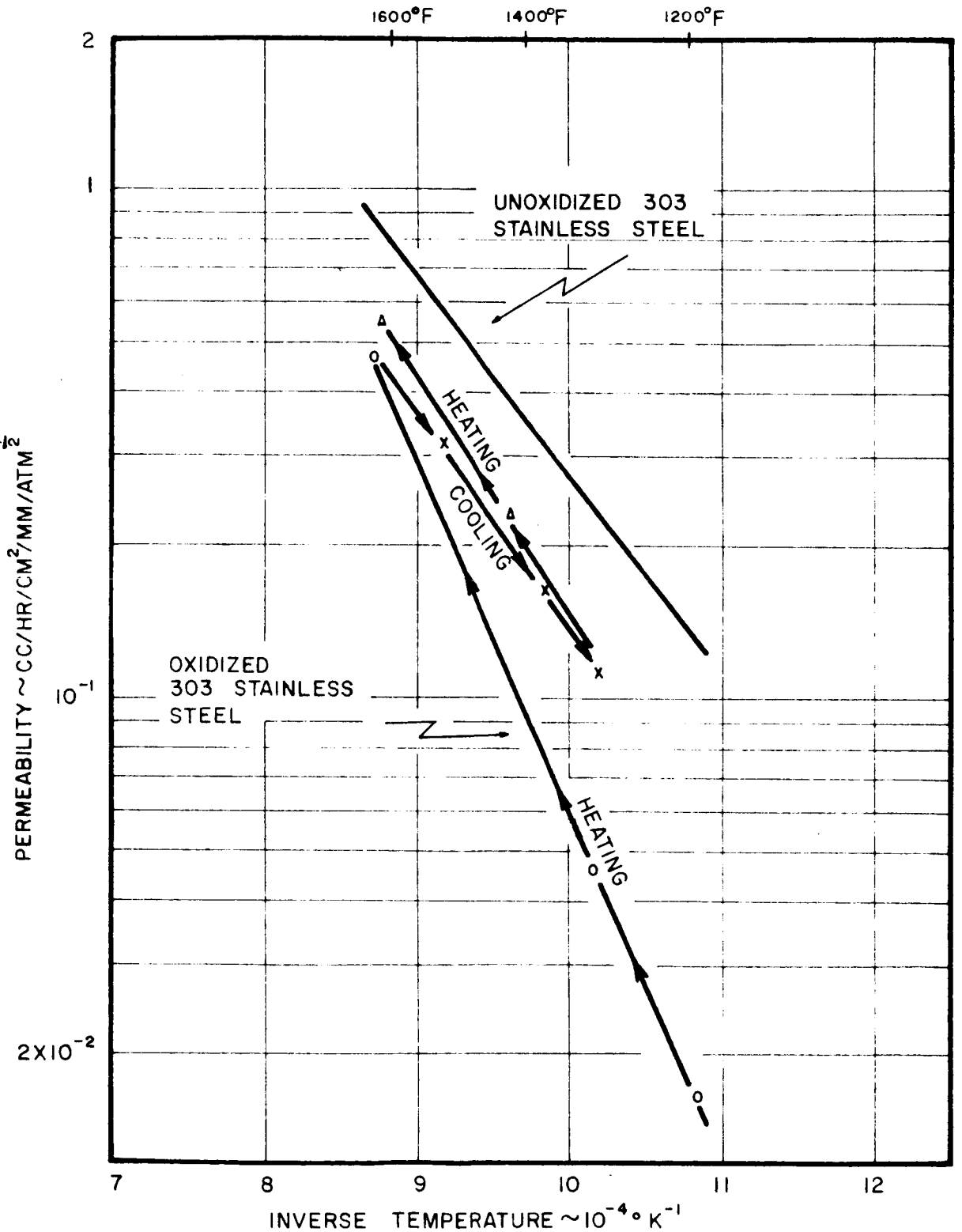


FIG.21: PERMEABILITY OF OXIDIZED 303 STAINLESS STEEL TO HYDROGEN.

PERMEABILITY OF HYDROGEN THROUGH ALUMINIZED AND OXIDIZED HAYNES 25

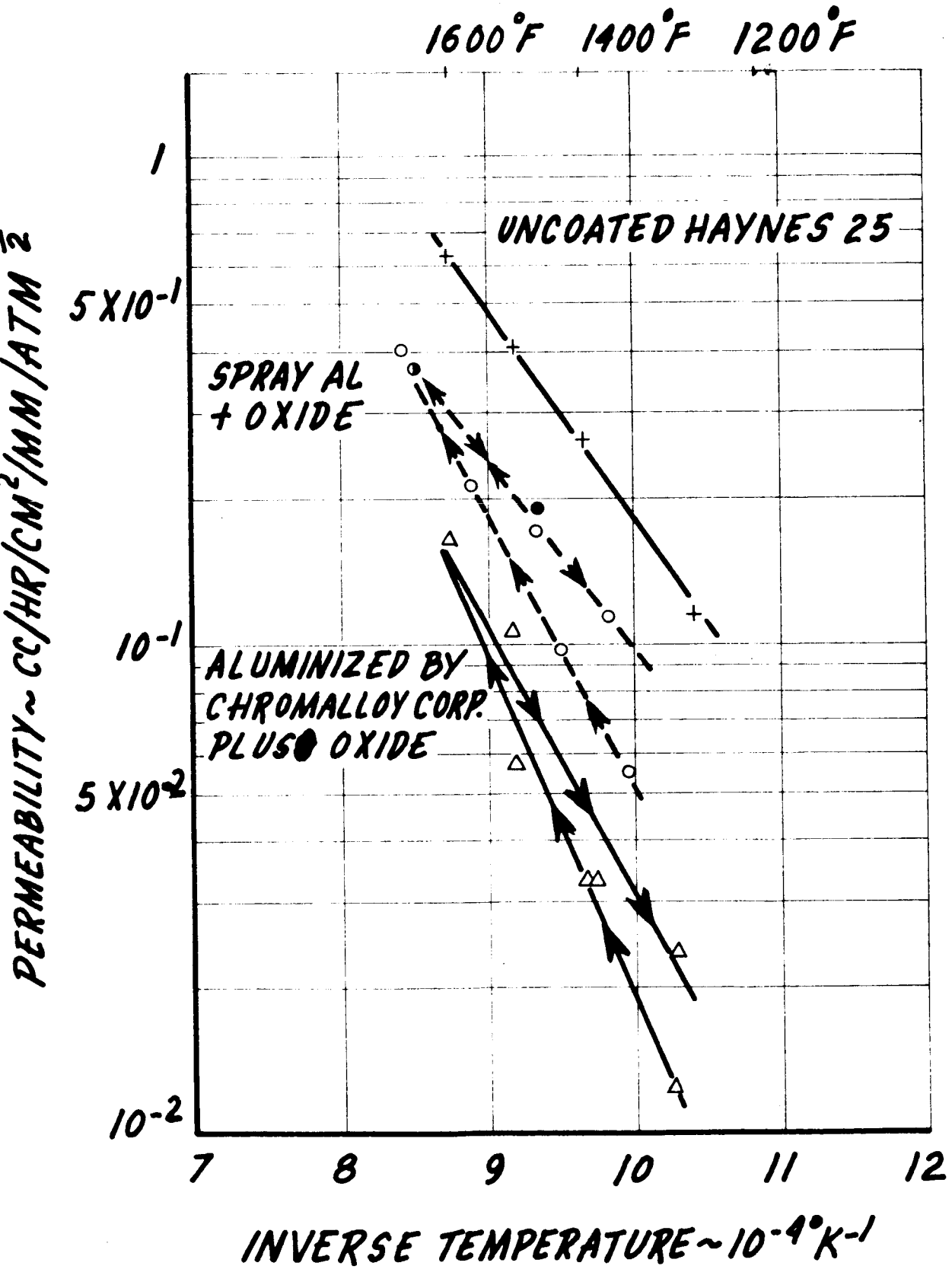


Fig. 22

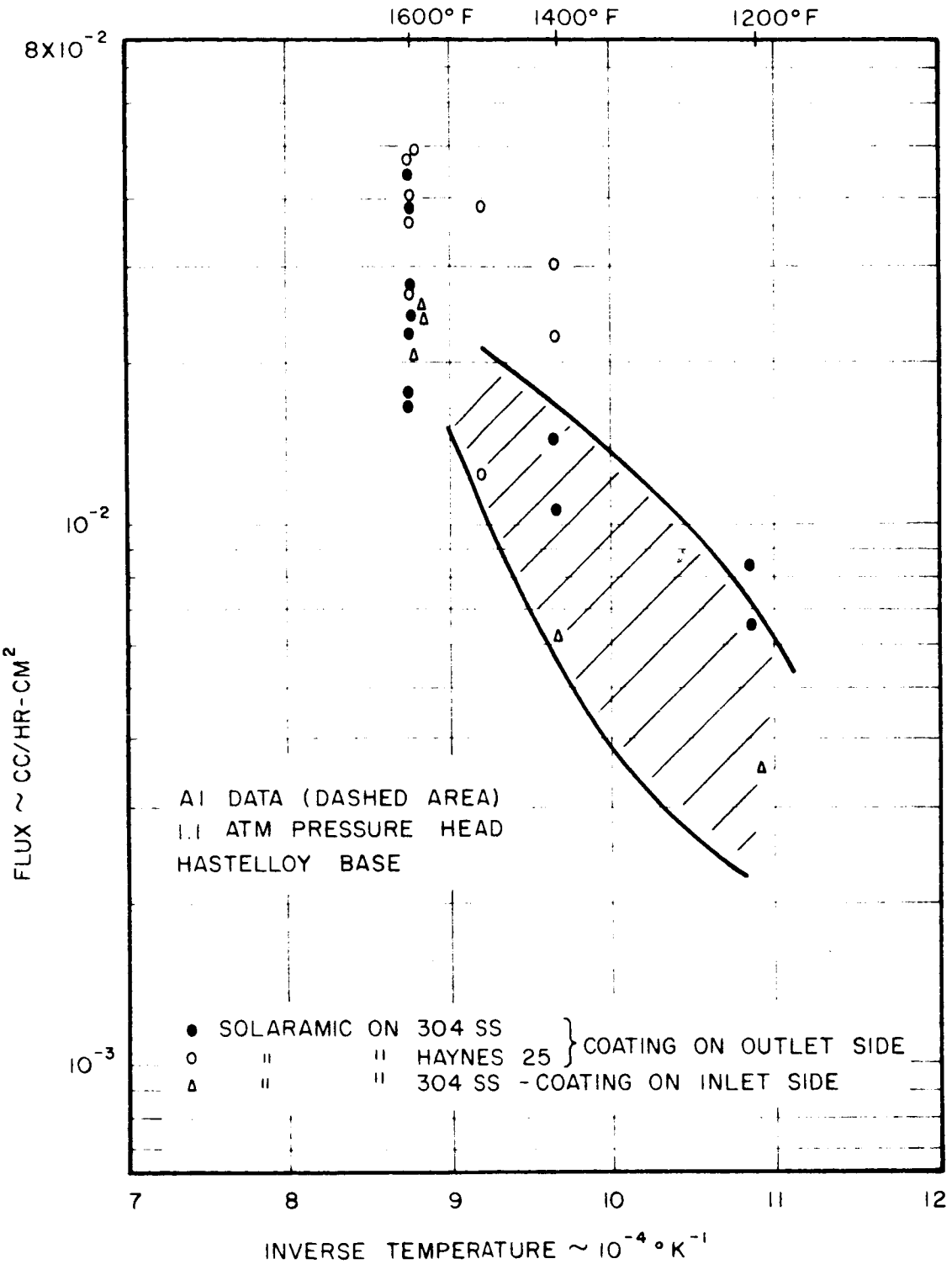


FIG. 23: COMPARISON OF TAPCO HYDROGEN PERMEABILITY DATA FOR SOLARAMIC-COATED CHAMBERS WITH ATOMICS INTERNATIONAL DATA.

PERMEABILITY DATA FOR VARIOUS MATERIALS

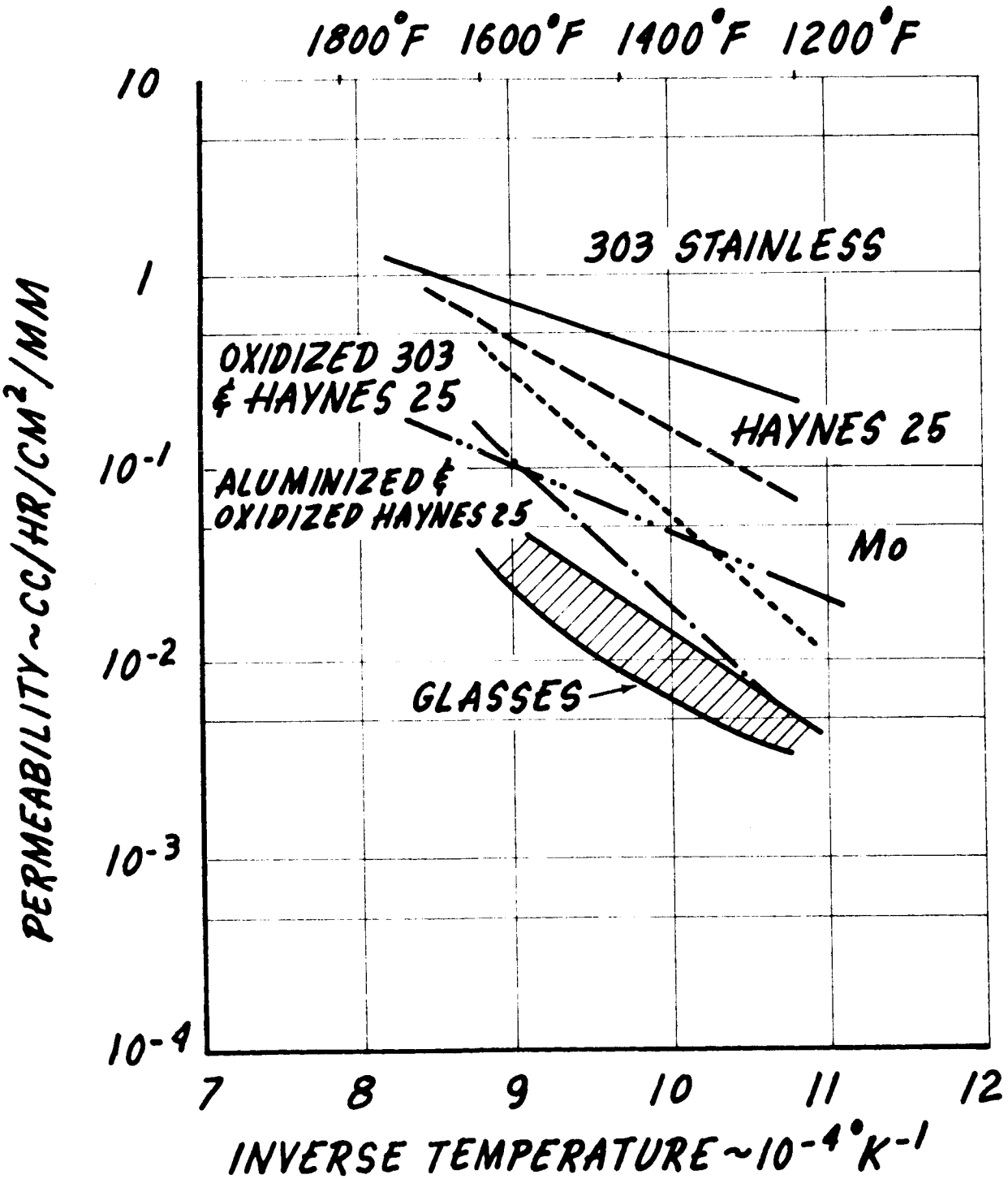


Fig. 24

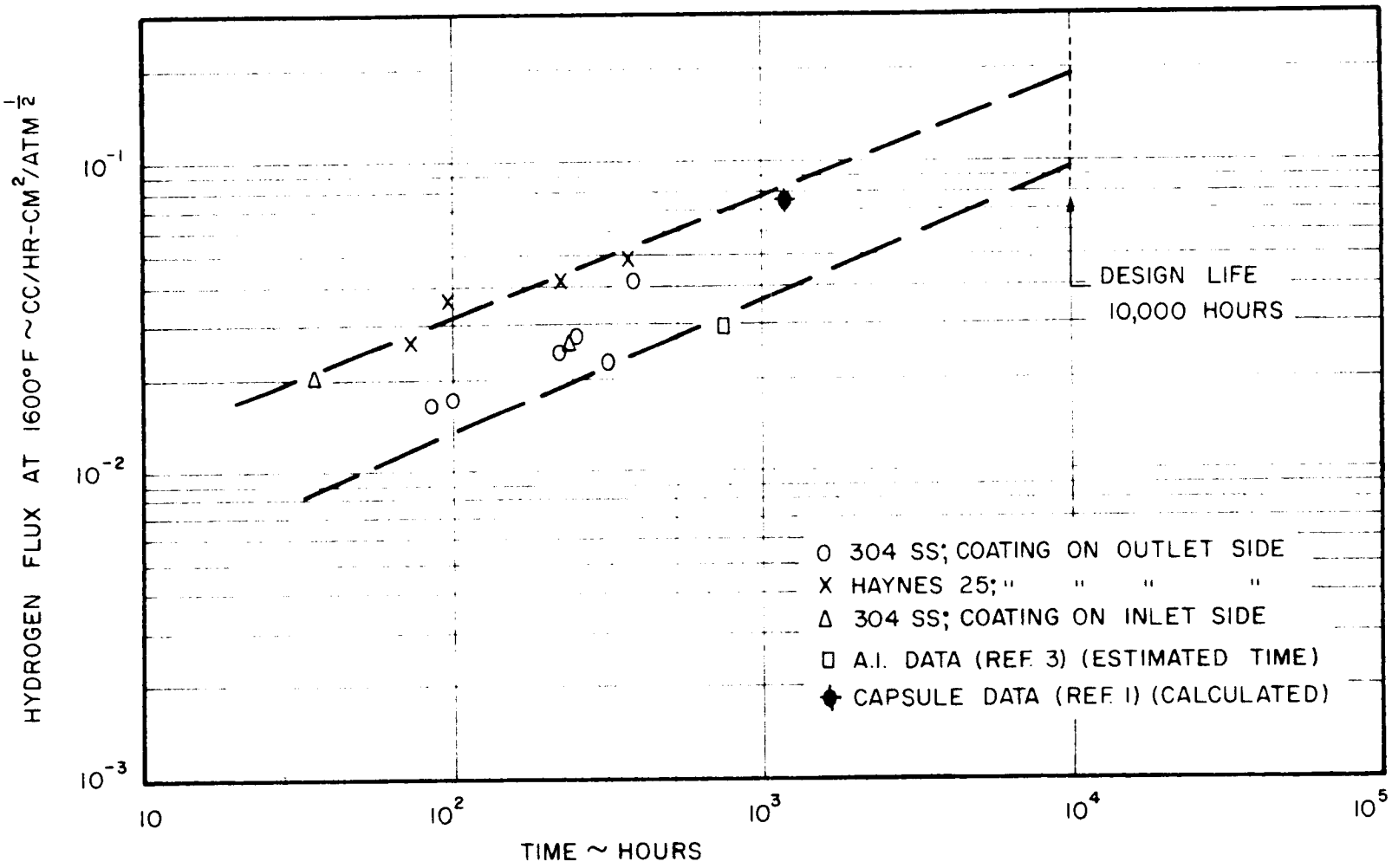


FIG.25: VARIATION IN HYDROGEN FLOW THROUGH SOLARAMIC-COATED SPECIMENS AS A FUNCTION OF TIME.

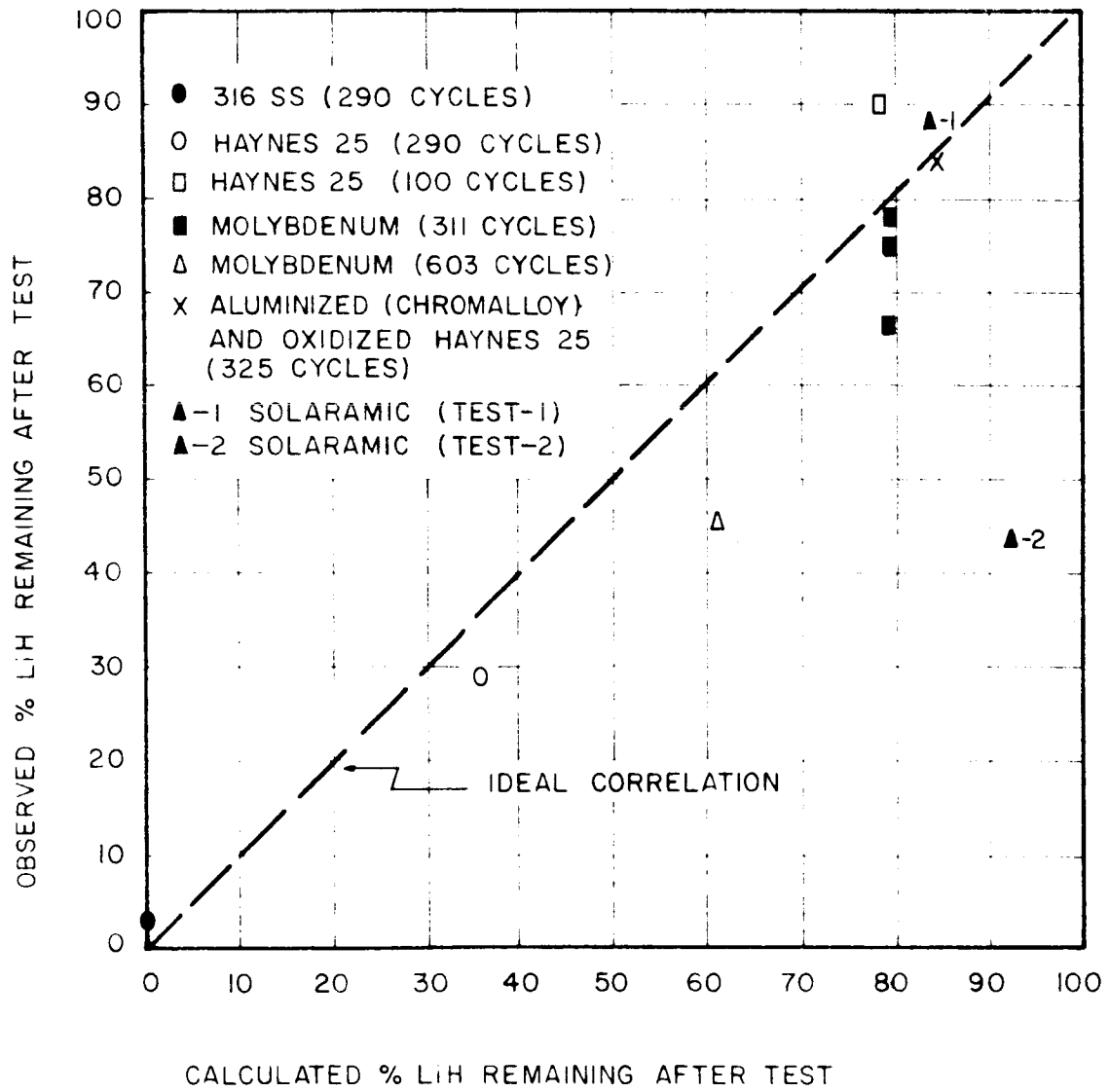


FIG. 26: CORRELATION BETWEEN OBSERVED AND CALCULATED LITHIUM HYDRIDE IN ACTUAL CAPSULE TESTS.

System Compatibility to Hydrogen

These experimental studies on hydrogen containment have served to establish rates of hydrogen diffusion through various material coating combinations. Taking the most promising of these coatings, solaramic and aluminum oxide, it may be calculated that the hydrogen diffusion rate, or loss, will be 2.8 lbs. per year for loss through the boiler inner shell based upon a continuous temperature of 1600°F. Of this amount, 0.2 lbs. per year is diffused through the boiler tubes into the mercury side of the system. The remainder is lost to the space environment and represents a system penalty. A less conservative calculation of total hydrogen loss yields a value of 0.6 lbs. per year. This calculation takes into account the variation of the boiler inner shell temperature from nominal values of 1250 to 1600°F during the sun portion of the orbit and accounts for the absence of loss during the shade period due to the natural barrier afforded by the frozen LiH at these surfaces. The calculation assumes a nominal log temperature mean between these values and accounts for the lower hydrogen dissociation pressure at this mean. For a molecular weight of LiH of 8.0, approximately 5 lbs. of additional LiH will be required to compensate for this loss. Using the conservative value of 2.8 lbs. per year hydrogen loss, 20 lbs. of additional LiH are required. The 0.2 lbs. per year diffusion into the mercury system is a conservative value, since it is also based upon a continuous source temperature of 1600°F and 1 atmosphere of pressure, compared to an average mercury boiling temperature of 1100°F.

System hydrogen compatibility can be defined in terms of component performance in the presence of hydrogen gas. Hydrogen diffusion into the system through the boiler tubes can be expected to pass from the boiler to the system condenser. During this phase the hydrogen gas will be mixed with mercury vapor and is expected to have little effect upon performance of the boiler, turbine and condenser components. Following condensation, two general conditions can be conceived:

1. The hydrogen gas can experience separation, accumulate and eventually pass to the pump in the form of a gas bubble.

2. The hydrogen gas can become entrained in the liquid mercury without separation and pass to the condensate pump in this state.

Condensate pump performance under these conditions becomes the limiting factor in determining hydrogen capability.

Some preliminary tests have been made to determine, in general, the bubble swallowing capacity of a pump operating at flow and head conditions comparable to Sunflower conditions. It was found in these tests that air bubbles as large as .03 in^3 in volume could be passed through the pump and demonstrate full recovery capability at inlet pressures of 4.0 to 6.0 psia.

Further evaluation of the effects of hydrogen gas upon pump performance is planned using a basic "workhorse" mercury loop, Figure 27. These tests are planned to give basic information on the sensitivity of the boiler feed pump to hydrogen in the form it will be delivered to the pump. The basic characteristics of these tests are as follows:

1. A prototype, 40,000 rpm, centrifugal pump, jet pump booster will

be used for fluid circulation.

2. Means will be provided to introduce hydrogen into the boiling section of the loop at accurately measured values and measure natural permeation from the tubing in the condenser and subcooler section.

Means of active removal of hydrogen from the system will also be provided in the "workhorse" loop. The centrifugal separator and overboard diffusion disposal path concept shown in Figure 28 have the following design characteristics: The area of columbium tube available for hydrogen egress is overdesigned by a factor of 1000. The centrifugal separation action provided is capable of removing bubbles down to a diameter of 0.0024 in. in the separator dwell time at a 1-g centrifugal effect. The velocities provided cause centrifugal accelerations of 12 g's. These over-design factors are intuitively felt to suffice for reservations which have been recognized for the possible reduction of permeability by the deposition of products of corrosion on the columbium surface. The design can be made even more conservative with little additional inventory or pressure drop. (The mercury inventory of this separation as shown is approximately one-half pound.)

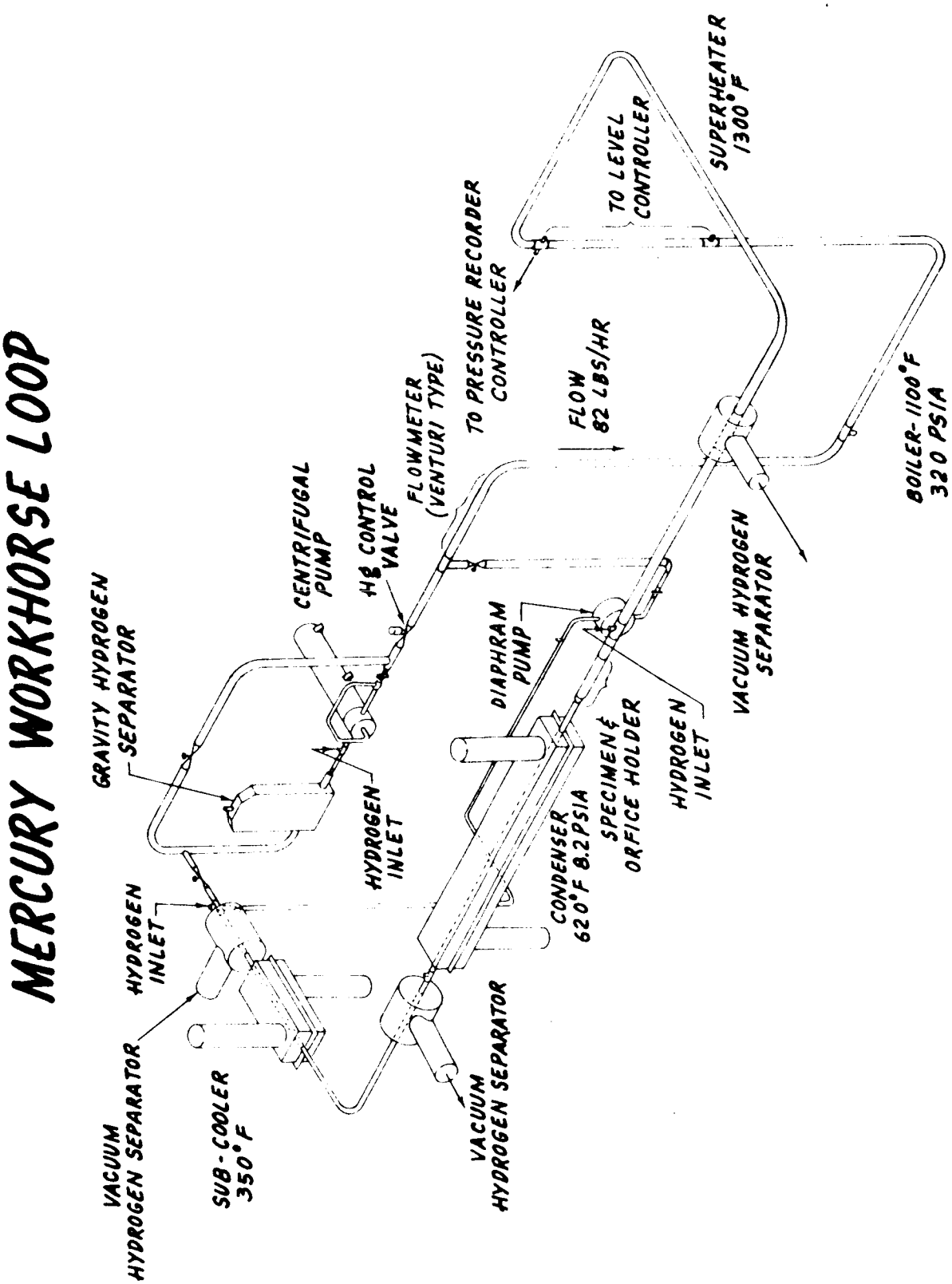

MERCURY WORKHORSE LOOP
VACUUM HYDROGEN SEPARATOR
HYDROGEN INLET
SUB-COOLER 350°F
GRAVITY HYDROGEN SEPARATOR
CENTRIFUGAL PUMP
Hg CONTROL VALVE
FLOWMETER (VENTURI TYPE)
TO PRESSURE RECORDER CONTROLLER
TO LEVEL CONTROLLER
SUPERHEATER 1300°F
FLOW 82 LBS/HR
BOILER-1100°F 320 PSIA
VACUUM HYDROGEN SEPARATOR
HYDROGEN INLET
DIAPHRAM PUMP
CONDENSER 620°F 8.2PSIA
SPECIMEN ORFICE HOLDER
HYDROGEN INLET
VACUUM HYDROGEN SEPARATOR

FIGURE 27

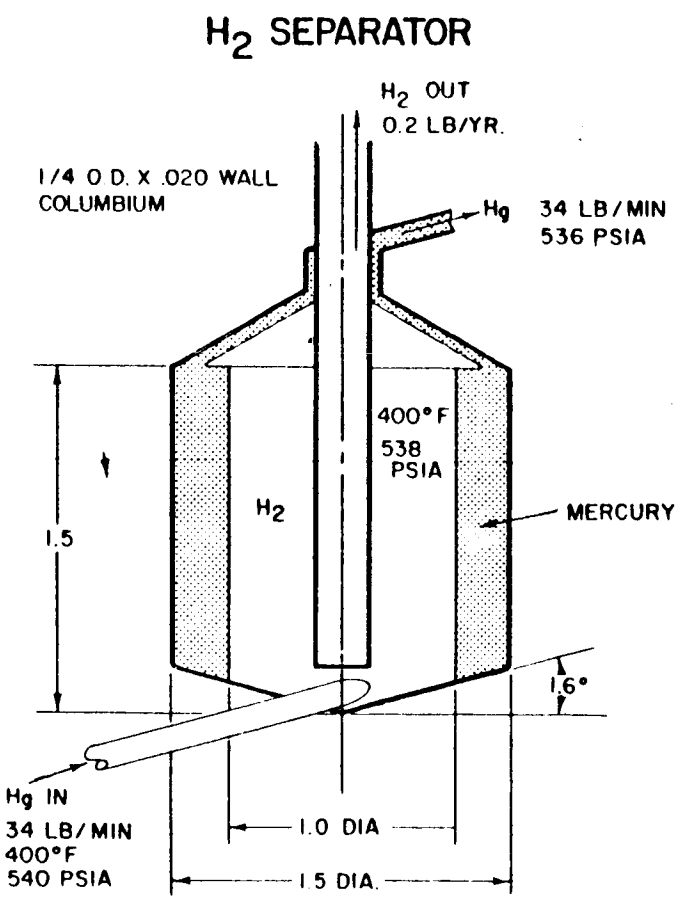

H2 SEPARATOR
H2 OUT
0.2 LB/YR.
1/4 O D. X .020 WALL
COLUMBIUM
Hg
34 LB/MIN
536 PSIA
400° F
538
PSIA
H2
MERCURY
1.5
1.6°
Hg IN
34 LB/MIN
400°F
540 PSIA
1.0 DIA
1.5 DIA.

FIGURE 28

Sunflower Solar Collector Status

The Sunflower collector developmental status may be summarized as follows:

1. Preprototype Collector II-2 is fabricated and assembled. A photograph of this assembly is shown in Figure 29.

2. Optical inspection has been performed on each of the individual sectors.

3. The assembled collector is currently undergoing optical inspection.

4. Deployment, vibration and single petal performance testing are scheduled to be completed during the next few months.

5. Petal thermal behavior and fabrication development has progressed to the identification of the details required for required insensitivity. Confirmation of the adequacy of these factors is in progress by means of a computer analysis of the entire paraboloid as a structure.

Detailed indications of the status of the various performance and weight elements of the collector development may be obtained by reference to Figures 30 and 31. In reviewing the achieved weight tabulation, it may be noted that the current sectors weight 5.9 lbs. compared to an objective of 5.0 lbs. per petal. This difference between achieved weight and design objectives results from the difficulty which has been encountered in avoiding buckling on the front and back faces of the honeycomb layup. Stresses formed in the skins during layup tend to relieve themselves causing buckling after completion of the curing process. This has been corrected in the II-2 petals by providing reinforcing doublers along the edges of the part. These doublers account for the additional 0.9 lbs/sector. Petals without doublers have been fabricated at design weight of 5 lbs/sector. It is concluded that a light prestretch operation will reduce residual stresses in the faces and will eliminate the surface deviations caused by edge buckling.

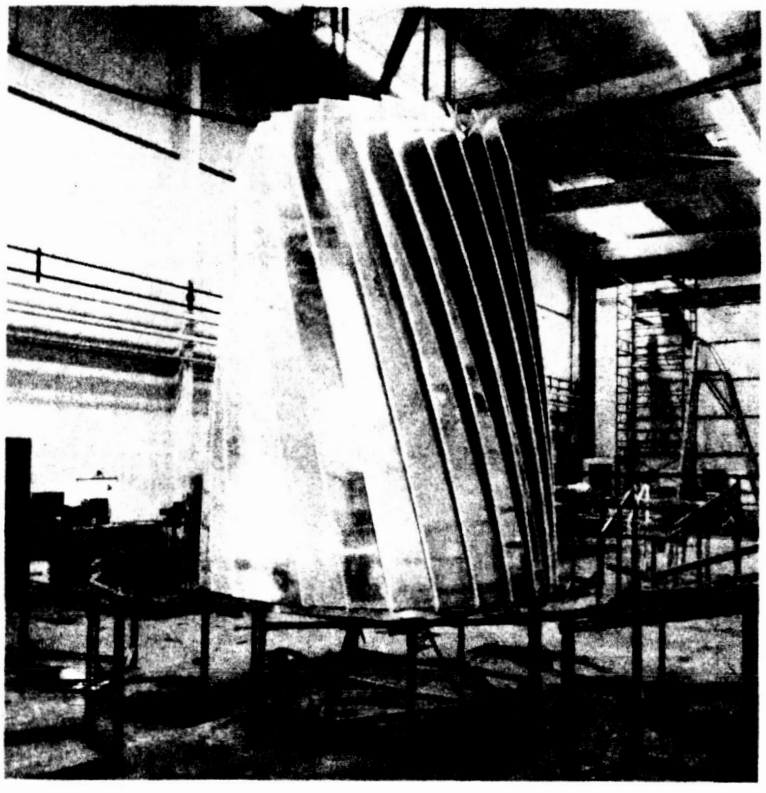
The indicated weight reduction objectives of the lock and hinge hardware will be straightforwardly accomplished by reduction in wall thickness of these components.

The similar comparative optical performance status summary in Figure 31 is easily interpreted with the possible exception of the tooling, waviness and spring back entries under fabrication errors. The large difference between achieved and objective in this category results from the basic definition of the II-2 Collector in the development.program. At the time of redirection of the Sunflower program in January of 1962, budget limitations were such that the II-2 Collector was defined as primarily a structural integrity development copy. At the time of initiation of the petals for this Collector, the tooling waviness and spring back errors were known and could have been corrected by barbering of the layup tool. This was not done due to the cost and schedule aspects of such an operation.

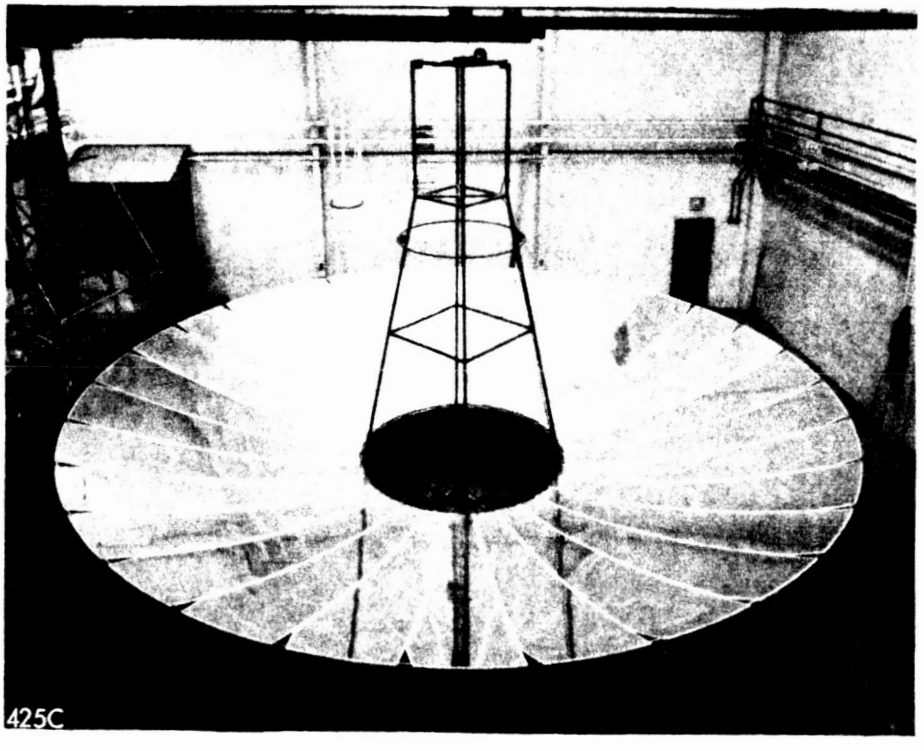
As noted above, thermal distortion of the petals has been investigated both analytically and experimentally. Analysis and tests have been conducted to investigate

the heat transfer characteristics of honeycomb sandwich material of various adhesive and core preparation details. The effect of these modifications has been experimentally correlated both for thermal conductivity and with resultant thermal distortion. Results of these tests have been incorporated into a computer program which has provided a reliable basis for identifying design requirements. In addition to the conductivity conclusions of the small specimen testing, these analyses have indicated two additional design requirements. It has been preliminarily indicated that incorporation of two intermediate compression pad engagements on each petal would significantly reduce the distortion of the assembled paraboloid under the influence of the thermal conditions. In addition to this assembly provision, analyses have indicated the desirability of incorporating a 3 to 6 micron thickness of transparent silicon oxide on the reflective surface of the solar collector to increase its infra-red emissivity. This provision in conjunction with minimization of infra-red emissivity off the back face of the collector and the above noted detailed provisions will suffice to meet the thermal distortion objective of 0.1° maximum distortion.

SUNFLOWER SOLAR COLLECTOR ASSEMBLY



STOWED



DEPLOYED

FIGURE 29

SUNFLOWER SOLAR COLLECTOR WEIGHT

	ACHIEVED PRE-PROTOTYPE COLLECTOR II-2	FLIGHT DESIGN
SECTOR WEIGHT (AVG)	5.9 LB.	5 LB
LOCK WEIGHT	.3 LB/SECTOR	.15 LB/SECTOR
HINGE & ACTUATOR WEIGHT	.4 LB/SECTOR	.35 LB/SECTOR
TOTAL COLLECTOR WEIGHT	198 LB	165 LB
COLLECTOR SPECIFIC WEIGHT BASED ON INTERCEPTED AREA	.26 LB/FT^2	.22 LB/FT^2

FIGURE 30

TAPCO a division of Thompson Ramo Wooldridge Inc.

SUNFLOWER SOLAR COLLECTOR OPTICAL PERFORMANCE

			MEASURED DATA COL II-2	FLIGHT DESIGN
SURFACE DEVIATIONS	FABRICATION ERRORS	HONEYCOMB HEX MARKOFF	.14°	.10°
		TOOLING WAVINESS	.25°	.20°
		SPRING-BACK	.38°	
	ASSEMBLY ERRORS	DEPLOYED ASSEMBLY	NOT YET EVALUATED	.10°
	ENVIRONMENTAL ERRORS	THERMAL DISTORTION	1.2° (CALCULATED) LOCKS AT RING ONLY	.10° CALCULATED 3 LOCKS PER SECTOR
REFLECTIVITY	TOTAL REFLECTIVITY		90.7%	91%
OVERALL EFFICIENCY	ZERO MISORIENTATION		NOT YET EVALUATED	90%
	3/4° MISORIENTATION		»	74%

FIGURE 31

TAPCO a division of Thompson Ramo Wooldridge Inc.

Sunflower Boilers and Condenser Status

Three boiler heat storage demonstration units have been constructed. Two of these have been loaded with lithium hydride and ground tested. The material of construction is 316 stainless steel throughout, with 1/4 inch thick shell walls and a heavy closure ring with a minimum thickness of 1½ inches. The design is purposely heavy to afford safety in handling and testing the lithium hydride.

Three types of tests were performed on both units, steady-state, storage capacity, and cyclic thermal input corresponding to the 300 mile orbit. In addition, flow startup tests were conducted on the second unit with the breadboard start system.

The steady-state tests were run to confirm design concepts and the boiling correlations. The storage bath must be designed to boil the mercury for the 70 minutes of shade time encountered in the 20,000 mile orbit and operate in an almost continuous transient at the 300 mile orbit. Therefore, the storage capacity tests were conducted over the expected range of mercury flow rates with zero net heat input. The results confirmed a storage capacity sufficient to boil the design flow rate of mercury for 72 minutes.

The cyclic tests were intended to simulate the 60 minutes of sun time and 36 minutes of shade time encountered in the 300 mile orbit. Sufficient heat was transferred into the storage bath in 60 minutes to boil mercury continuously for 96 minutes. At least three cycles were completed to demonstrate repeatibility.

The startup tests on the second unit indicated stable and normal flow and pressure conditions at the end of 18 seconds. These results indicate that the boiler heat storage demonstration unit design has successfully met all performance objectives.

Two condenser subcooler units have been constructed and tested. The first unit was a flightweight model which featured an exit quality from the primary radiator of one percent. This unit was tested with the condensate flowing vertically upward. This condition is the most severe of the current specification. Stable operation was not achieved with this design. Design changes were made for the second unit. These changes included alteration of the exit quality from the primary radiator to a value of approximately 15 percent and addition of a single tube secondary radiator to condense the remainder. Further, the manifolding at the exit of the primary radiator was modified to provide smooth continuous flow. The number of tubes was reduced to increase the fluid velocity and the tube exit diameter was maintained greater than the critical diameter. Finally, the fins on the second unit were sized for ground test.

The second unit was tested over a range of flow rates from 7 lbs/min. to 14 lbs/min. in the same attitude as the first unit. Stable condenser operation was achieved over the entire flow range and with excursions from the design point of 15 percent primary exit quality and 94 ft/sec. exit velocity to as low as 8 percent exit quality and 45 ft/sec. exit velocity. These excursions from the design conditions give an indication of the ability of the condenser to operate under adverse off design conditions. The successful operation of a full scale once through condenser with flow against gravity is considered a significant milestone. The capability to operate stably at off design conditions enhances the usefulness and importance of the design.

The heat rejection in the ground test was reduced by the presence of tube heaters which resulted in a higher condensing temperature and pressure at design flow than anticipated.

Component Modifications and Improvements

The boiler and condenser component weights are influenced by the Sunflower system specifications. The multiplicity of orbits from 300 miles to 20,000 miles contributes significantly to the weight of the boiler heat storage unit. There must be sufficient storage capacity to boil the mercury continuously for 70.5 minutes shade time in the 20,000 mile orbit. On the other hand, the hydride heat input flux must be sufficient to transfer heat equivalent to 51 percent of capacity into the bath during the one hour of sun time in the 300 mile orbit.

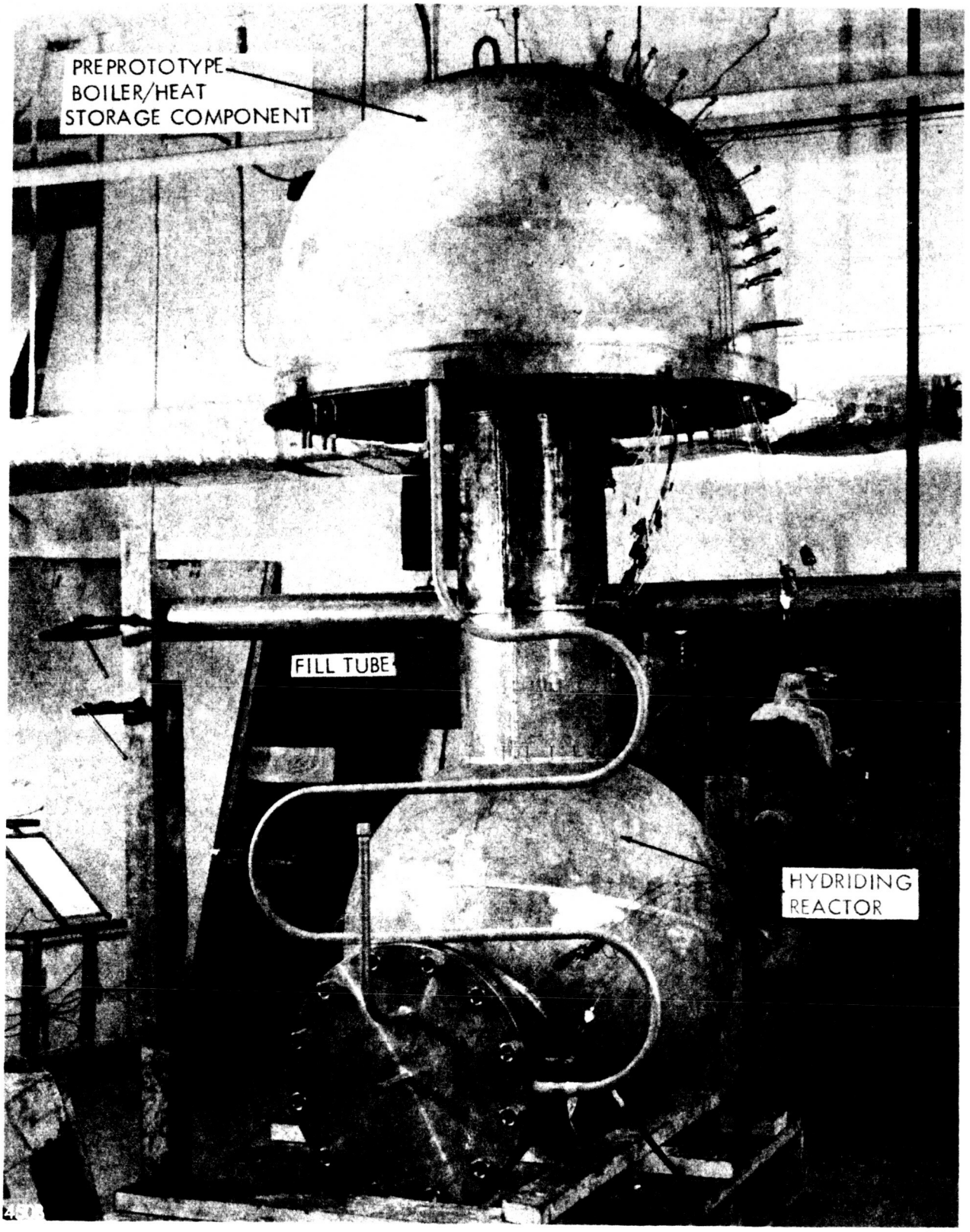
Design and operation of the 3.0 KW Sunflower system for a single 300 mile orbit would permit the storage capacity to be reduced to the 36 minute shade time of this orbit. Thus, the weight of lithium hydride can be reduced. In addition the length of the boiler tube can be altered to mate with the 36 minute shade time. The container and outer shell attachment volume and weight can be reduced correspondingly. The net effect of these alterations is to reduce the weight of the boiler heat storage unit by 120 pounds. Thus, the present requirement for a range of orbits from 300 miles to 20,000 miles adds 120 pounds or 67 percent to the weight of the boiler heat storage unit.

At low altitude orbits which require high heat absorption rates, an alternate type of container construction becomes attractive. The present design consists of two spherical shells open at one end, and the end is closed by a toroidal ring. Another type of construction which appears promising is a honeycomb box. The ends of the honeycomb are closed by the spherical shells as in the present design. However, the sides of the honeycomb act as fins to promote heat transfer into the hydride bath. In addition, the honeycomb provides a rigid structure and adds strength to the container, thus permitting thinner shells than in the present design. It appears that the heat input flux may be increased from the present 10,000 BTU/Hr-Ft^2 to as high as 20,000 BTU/Hr-Ft^2. This increased heat flux would allow a reduced cavity surface area and a more compact container. The smaller volume container should weigh less provided the honeycomb weight is not excessive. The amount of increase in the heat flux with honeycomb must be determined experimentally. In lieu of actual test data, estimates were made based on Haynes 25 honeycomb at the 20,000 BTU/Hr-Ft^2 flux, and the results indicated a potential reduction of about 33 pounds. The potential use of honeycomb appears attractive for development and offers alternatives to the present design. (Figure 37)

At the high altitude orbit, even though the LiH capacity is increased, the component can be kept compact with the current design concept because the low heat flux requirement permits lengthening the heat flow path, thus using a thicker hydride configuration.

The condenser subcooler component is influenced by the current Sunflower system specification to operate in 0 g and $\pm$ 1 g. Operation in the -1 g environment has been successfully achieved by the condenser as a component, but the velocity required to overcome the force of gravity contributes to a higher condenser pressure drop. With a fixed minimum outlet pressure, a higher pressure drop in

the condenser means a higher turbine back pressure and less output for the system as a whole. Modification of the specification to operation in 0 g and + 1 g only would permit ground test of the system and is comparable to ot other system requirements in orbit. This modification has been employed in the systems described later and results in reduced fluid velocities and a reduced pressure drop. Also, liquid interface location and design are less critical and need only consider the effects of 0 g operation.



PARTIAL ASSEMBLY PREPROTOTYPE BOILER -
LITHIUM HYDRIDE FILL FIXTURE

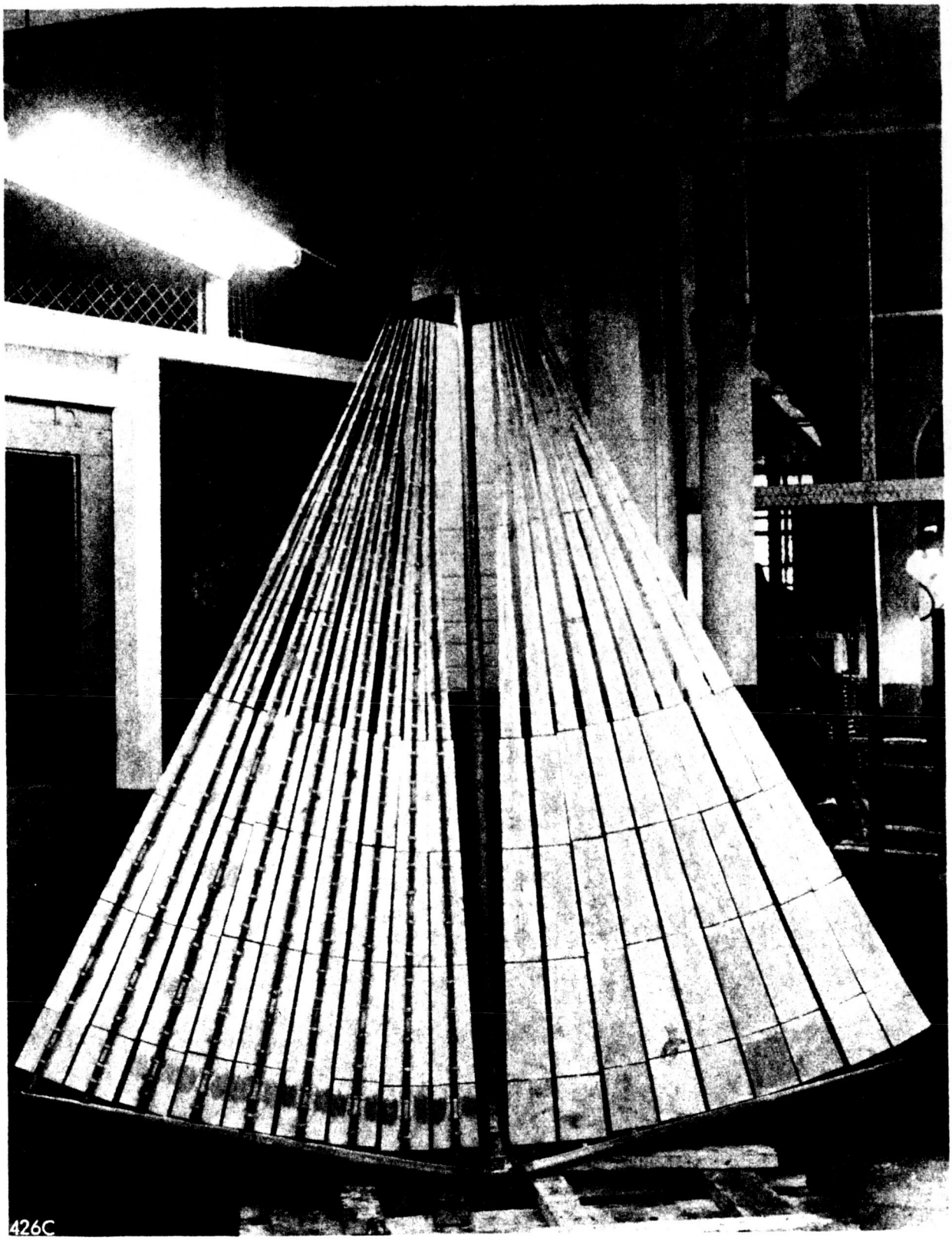
FIGURE 32

COMPONENT STATUS REVIEW
BOILER/HEAT STORAGE

	WEIGHT		PERFORMACE		TO DO
	TARGET	ACHIEVED	TARGET	ACHIEVED	
BHS ASSEMBLY	260 #	430 # (II-1 DESIGN) 320 # (REDUCTION OF SHELLS TO .030" PER III-1 DESIGN)			(1) LIGHT WEIGHT FABRICATION DEVELOPMENT (2) CONFIRM 1 YR STRUCTURAL INTEGRITY
ENERGY STORAGE AND TRANSMISSION			(1) ABSORB AT 66.5 KW AT $T_S \leq 1600°F$ (2) OPERATE FOR 72 MIN WITH NO EXTERNAL HEAT ADDITION (3) STABLE OPERATION DURING CYCLIC HEAT SUPPLY	CONFIRMED CONFIRMED CONFIRMED	
START-UP			TO DESIGN OUTLET PRESSURE IN 30 SEC	< 18 SEC — STABLE	
TEMPERATURE CONTROL			T MAX ≤ 1600° F WITH Q_{in} = 74 KW & UNMODULATED Q_{out} = 40 KW	DESIGN CONCEPT COMPLETED	EXPERIMENTAL DEVELOPMENT OF TEMPERATURE CONTROL DOOR ACTUATION
HYDROGEN CONTAINMENT			≤1.25 LB/YR H_2 LOSS	≤2.83 LB/YR EXTRAPOLATED FROM 1000 HR CYCLIC TEMPERATURE TEST	(1) CONFIRM 1 YR. INTEGRITY OF COATING (2) DEVELOP TUBE & SHELL APPLICATION TECHNIQUES (3) CONTINUE SEARCH FOR LOWER PERMEABILITY

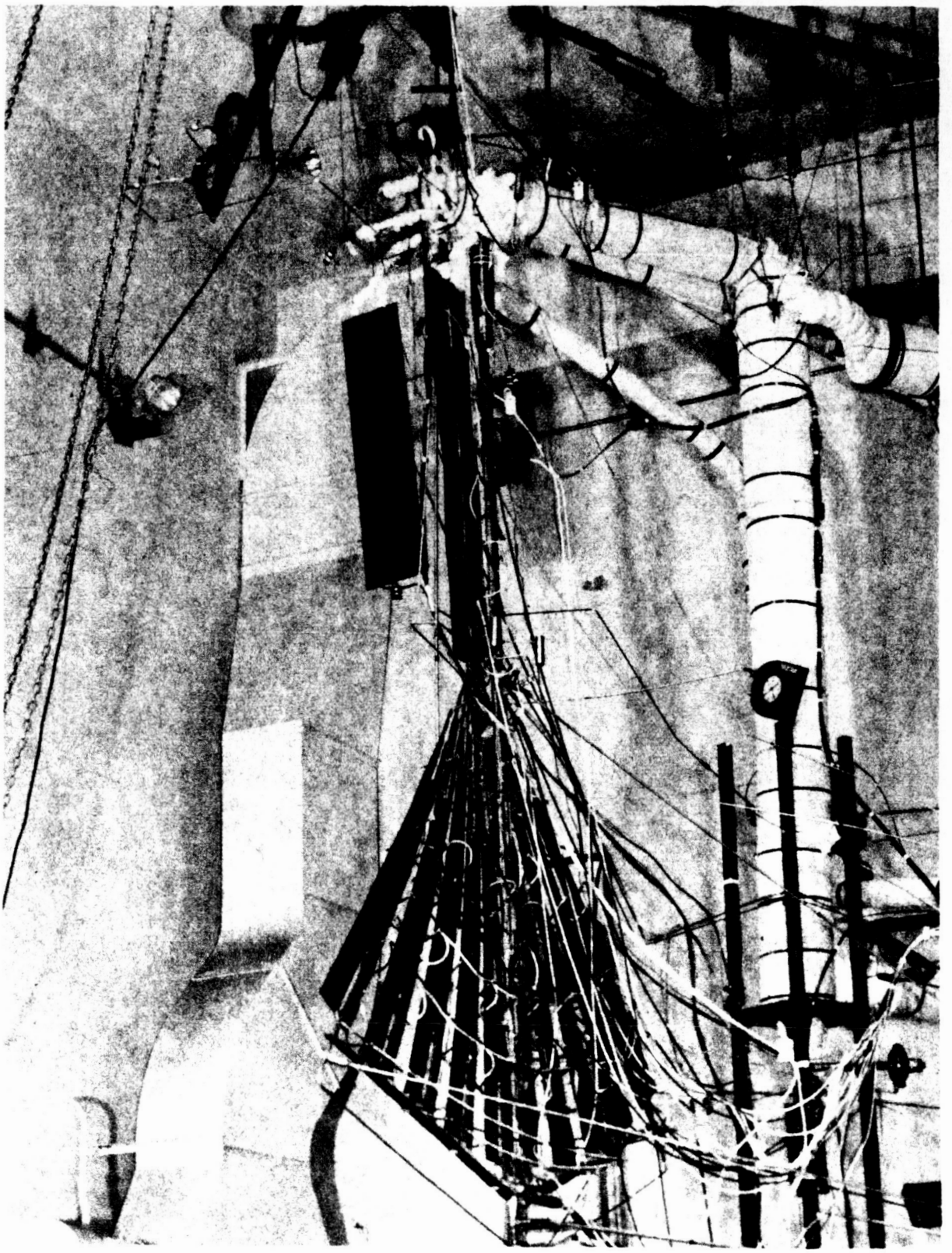
FIGURE 33

TAPCO a division of Thompson Ramo Wooldridge Inc.



PREPROTOTYPE RADIATOR I-1

FIGURE 34



CSC I-1A CONDENSER

FIGURE 35

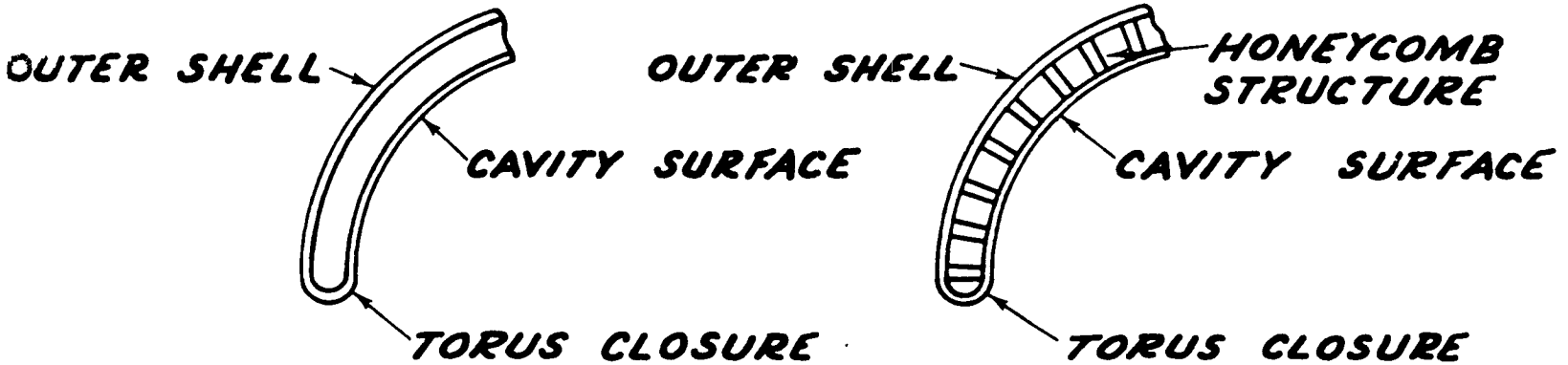
COMPONENT STATUS SUMMARY
CONDENSER-SUBCOOLER

	WEIGHT		PERFORMANCE	
	TARGET	ACHIEVED	TARGET	ACHIEVED
ASSEMBLY 10 TUBE UNIT	62 LBS	62 LBS (II-1 DESIGN)	STABLE THERMAL & FLUID DYNAMIC OPERATION AT $\Delta P \leq 2.5$ PSID $X_E = 15\%$ $V_E = 90$ FT/SEC	STABLE OPERATION CONFIRMED OVER FLOW RANGE OF 7.0→14.0 LB/MIN WITH $X_E \geq 8\%$ AT $V_E \geq 46$ FT/SEC
THREE TUBE BREADBOARD				THREE TUBE BREADBOARD OPERABLE AT $X_E \geq 15\%$ AT V_E AS LOW AS 12.5 FT/SEC
SINGLE TUBE BREADBOARD			STABLE OPERATION $X_E \geq 1\%$ & $V_E \geq 60$ FT/SEC AGAINST GRAVITY $\Delta P \leq 1$ PSID	CONFIRMED DOWN TO $X_E = 0\%$ & $V_E \approx 0$ FT/SEC VERTICALLY UP (& DOWN) $\Delta P \leq 1$ PSID

FIGURE 36

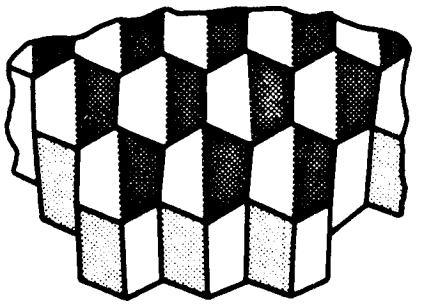
TAPCO a division of Thompson Ramo Wooldridge Inc.

BOILER CONTAINER CONSTRUCTION



PRESENT DESIGN

MODIFIED DESIGN



TYPICAL HONEYCOMB STRUCTURE

FIGURE 37

TAPCO a division of Thompson Ramo Wooldridge Inc.

REVIEW OF SYSTEM AND COMPONENT PERFORMANCE IMPROVEMENT AREAS

Alternator

The status of the alternator development is divided into two major areas. The first part of the discussion will present the status of the permanent magnet alternator development. The second part presents the status of our electromagnetically excited brushless alternator. In each case, performance of existing units will be established at power levels well above the Sunflower rating.

Before discussing the detailed alternator performance, a brief review of the problems associated with the development of alternators for turbine driven space power systems is in order. The problem of designing an alternator considering only the power level is relatively simple. However, if we add the conditions imposed by the rotating package, we end up with an alternator performance specification that represents an advance in the state-of-the-art. First, the alternator must operate at turbine speed. Also, the rotor design is restricted since its length, mass, and construction can seriously affect the rotor and bearing designs of the package. In addition, the alternator must be capable of operating at temperature of 700°F and higher in a metal vapor environment. Experience has added many more detailed requirements to define the alternator as a difficult development problem that must be considered as an integral part of the rotating package.

The characteristics of a permanent magnet alternator are attractive for space power applications particularly at relatively low power outputs. The permanent magnet rotor eliminates the need for rotating windings and brushes and offers high efficiency for a low weight and volume. In the polyphase unit, the rotor losses are relatively low and eliminate the need for rotor cooling thereby simplifying the package design.

In Figure 40, the cross section of the permanent magnet alternator shows that the design offers advantages in solving the high temperature mercury vapor seal problem. The stator is enclosed in a non-magnetic housing except in the bore area. A high temperature glass is bonded to the closed slot laminations and seals the stator. The maximum allowable leakage rate with a pressure differential of one atmosphere has been set at 1.07×10^{-7} cc/sec of helium. Over 80% of the stators meet this requirement without requiring any rework. Shock and vibration tests have not effected the integrity of the seal. Stators have also been subjected to a 250°F thermal shock by water quench and have remained leak tight.

In the final analysis, the alternator performance is measured by extended operation in the high temperature mercury vapor environment. This alternator design has operated successfully during thousands of endurance hours in the SNAP II and Sunflower rotating packages.

Alternators for high temperature operation are necessarily designed with low conductor losses to minimize the insulation problem and also reduce the temperature gradient from the hot spot to the housing. For polyphase operation, the stator iron, rotor surface, and windage losses remain essentially constant with load. Therefore the change in the total loss is due to the conductor loss. The polyphase winding also offers more efficient utilization of stator iron and copper as compared to single phase operation. Figure 41 shows a comparison of single phase and three phase performance for the SPUD alternator. Single phase operation also introduces large rotor surface losses that vary directly with the load. The comparison shows that the power output of the SPUD alternator can be increased from 1 KW to 1.5 KW

BOILER DESIGN MODIFICATIONS
WEIGHT SUMMARY

	PRESENT S/F	3 KW S/F SINGLE ORBIT	3 KW S/F SINGLE ORBIT
LITHIUM HYDRIDE	118 LBS.	61 LBS.	61 LBS.
BOILER TUBE	40	24	24
CONTAINER	97	64	40
DOORS & CONTROLS	15	12	12
ATTACHMENTS	32	21	12
TOTAL WEIGHT	302 LBS	182 LBS.	149 LBS.

FIGURE 39

TAPCO a division of Thompson Ramo Wooldridge Inc.

BOILER DESIGN MODIFICATIONS

DESIGN CRITERIA

	PRESENT S/F	3KW S/F SINGLE ORBIT	3KW S/F MODIFIED
ORBIT	300m 20,000m	300n.mi	300n.mi
STORAGE CAP.	70.5 MIN	36 MIN	36 MIN
INPUT REQ'D.	51% CAP.	100% CAP.	100% CAP
CONSTRUCTION	SHELL	SHELL	BOX
INPUT FLUX	10,000 BTU/HR-FT^2	10,000 BTU/HR-FT^2	20,000 BTU/HR-FT^2

FIGURE 38

TAPCO a division of Thompson Ramo Wooldridge Inc.

by rewinding the stator for three phase operation.

Figure 42 shows efficiency curve for the present Sunflower alternator. This data was taken with the alternator operating at rated speed and a bore temperature of 650°F. All alternators are tested at temperature prior to assembly in the rotating package. The test procedure includes efficiency at "off design" points and a continuous leakage test on the stator. Although rated at a net output of 3 KW, the alternator can provide 7 KW of unity P.F. at an efficiency of 90%. To operate at this load, an increase in coolant flow in the stator can be provided to limit the alternator bore temperature to the present Sunflower condition. Recent experience in the development of a 1000°F motor for WADD has verified the fact that insulating materials with higher thermal conductivity than those of the Sunflower alternator can be used to compensate for the increased conductor loss and limit the temperature gradient increase. The voltage regulation will also increase with load. However, should it be necessary to hold close voltage tolerance from no load to full load, an existing voltage regulator can be used. Output voltage is held constant by controlling the saturation level of the stator back iron.

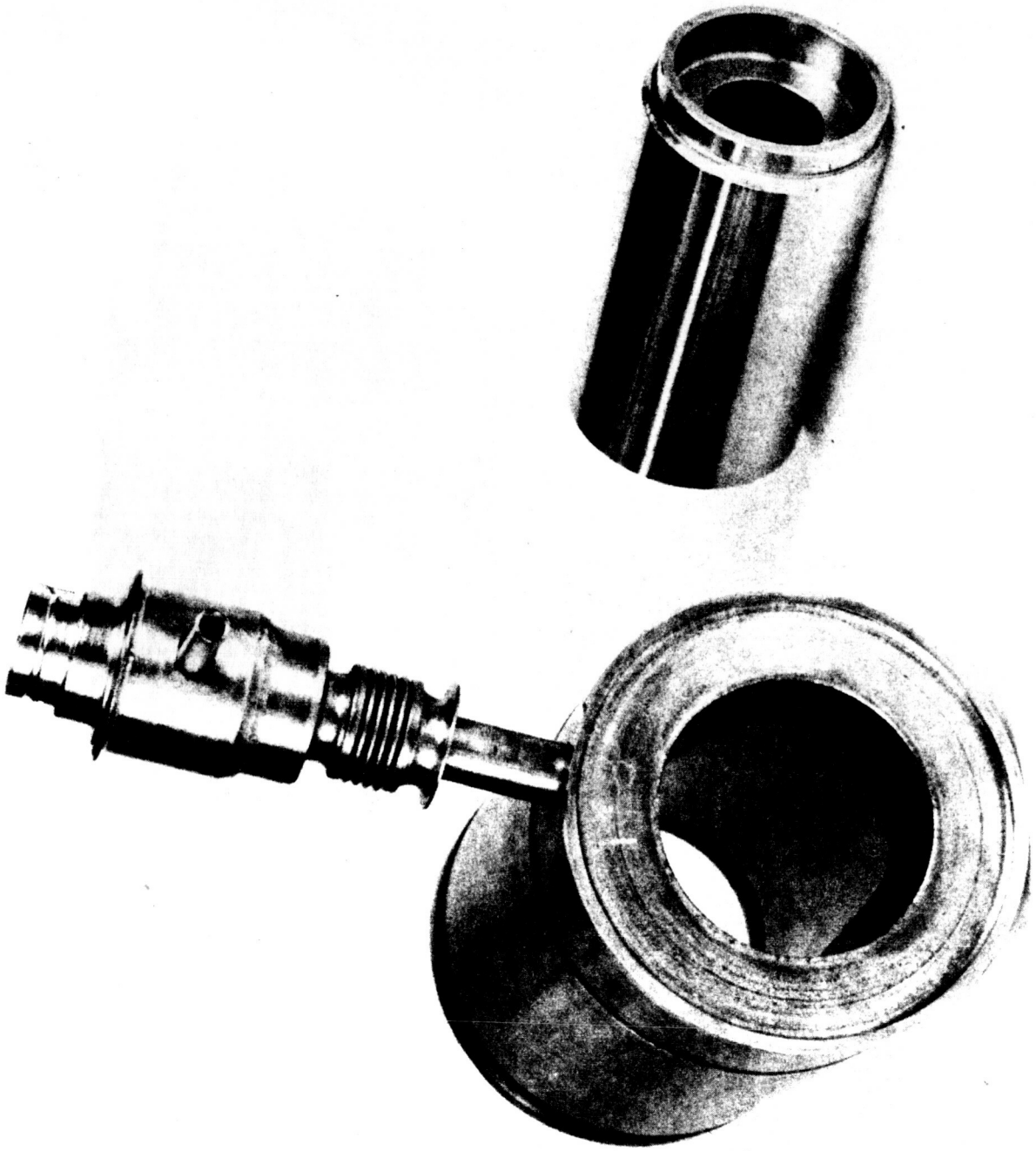
As the output power requirements increase, the permanent magnet alternator has definite limitations. For this reason, a detailed study of the various types of electromagnetically excited alternators was made. Figure 43 shows the cross section of the alternator design resulting from the study. The design is simple and incorporates many of the advantages realized by the permanent magnet design. It should be noted that the stator design is similar to that of the permanent magnet alternator and can use the same bore seal design. Since the unit is electromagnetically excited, it can operate with a large air gap which affords more latitude in the sealing of the stator from the high temperature mercury. However, as in the permanent magnet machine, the seal is tested as an integral part of the alternator. The loss distribution is essentially the same as that of the permanent magnet alternator.

The advantages of the alternator are realized primarily by the design of the rotor shown in Figure 44. The design is optimized by a trade-off of magnetic and mechanical designs. For a given rating, the size of any alternator is a direct function of speed. Existing alternators are operating at peripheral velocities of 525 ft/sec. Rotors have recently passed spin tests at velocities of 700 ft/sec. Known design improvements should realize a capability exceeding 800 ft/sec. The peripheral velocity of the Sunflower alternator rotor at rated speed is 370 ft/sec.

Alternators exist for ratings from 500 watts to 15 KW. We are presently under contract to develop ratings of 22 KW and 125 KW. Figure 46 shows the performance characteristics of the 15 KW machine.

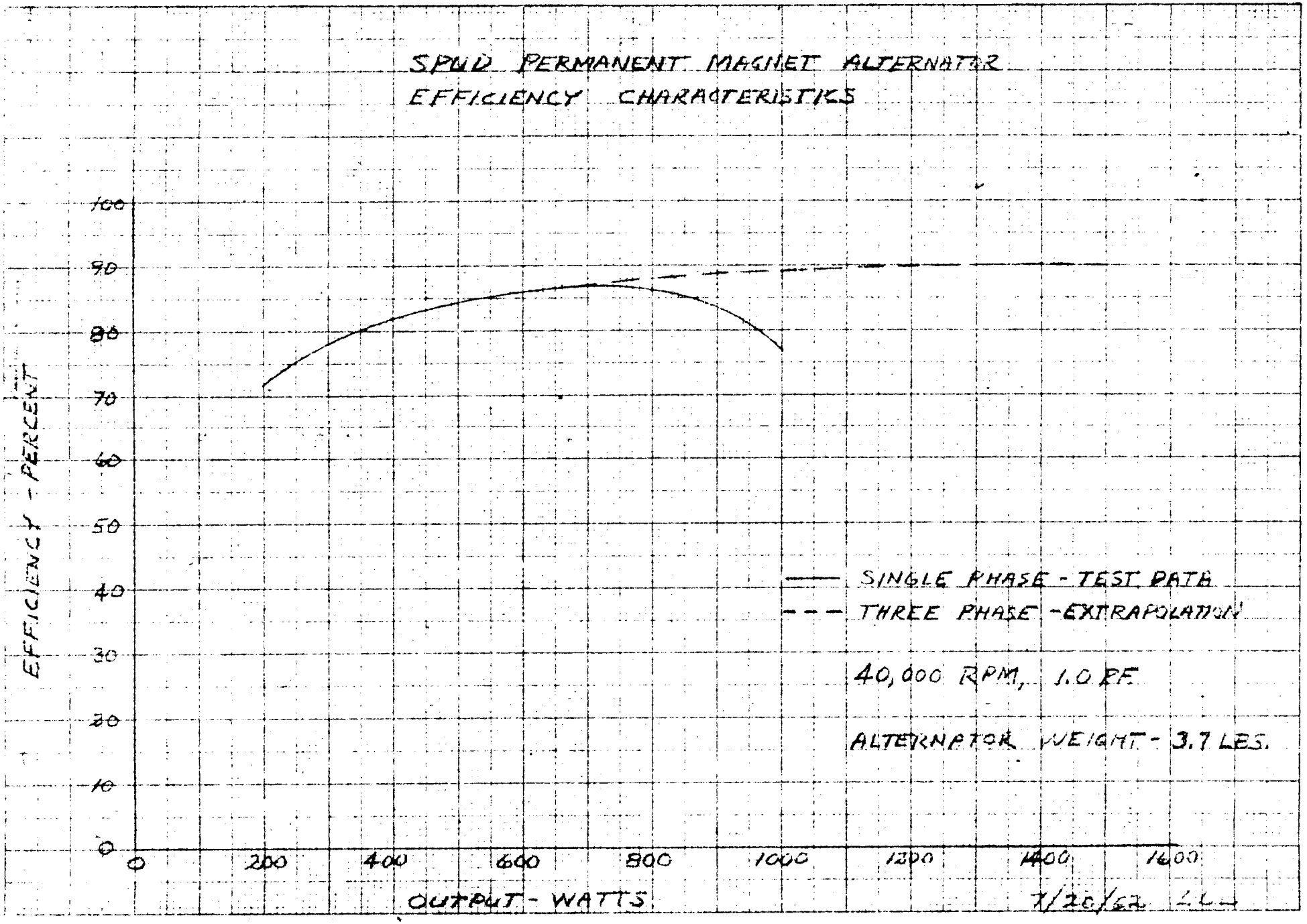
It should be noted that the 40,000 rpm operation realizes a specific weight ratio of less than one lb/KW. The 75,000 rpm curve represents our present design objectives with a rotor surface velocity of 820 ft/sec. The specific weight for this conditions is approximately 0.5 lbs/KW.

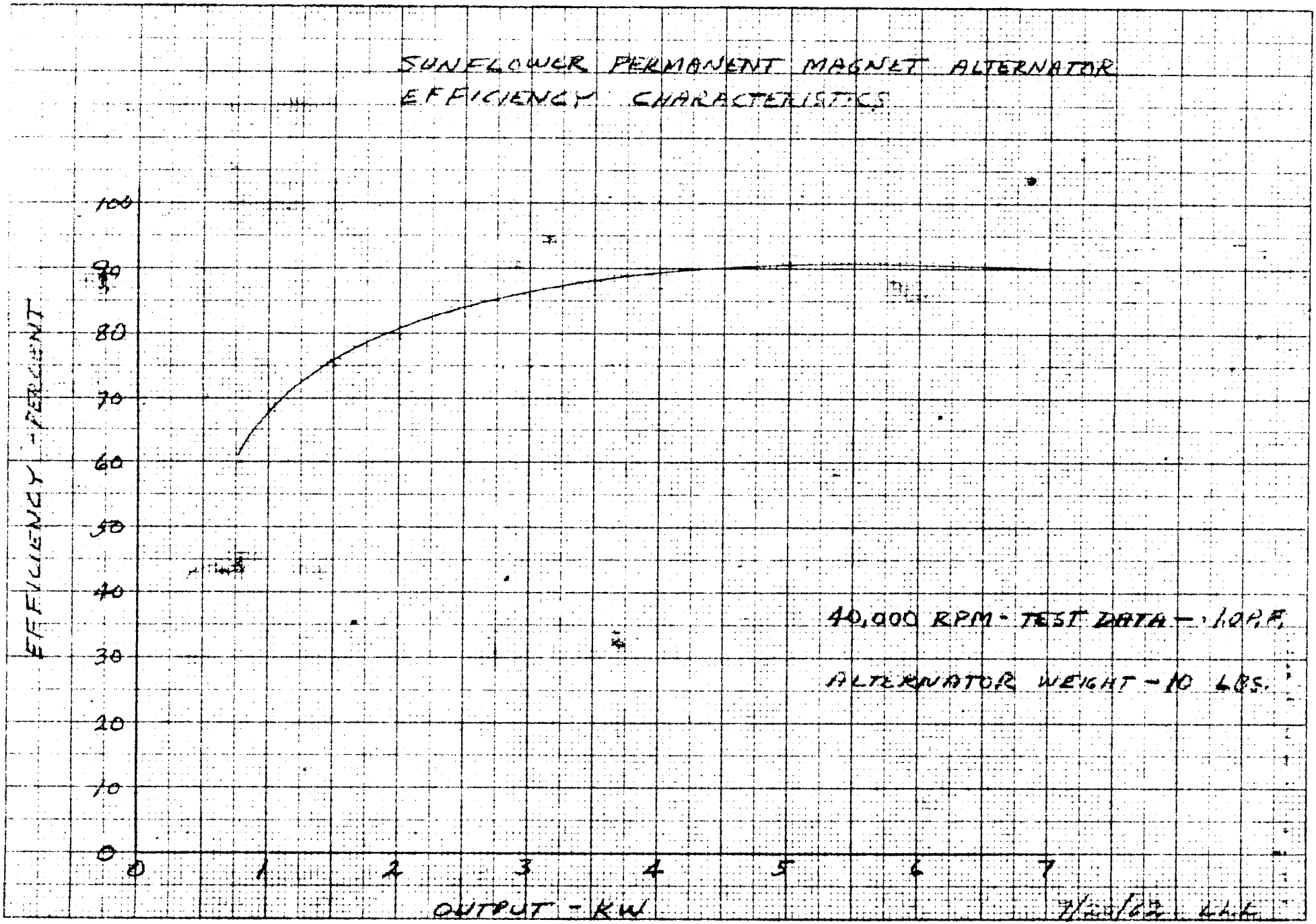
Figure 47 summarizes the existing alternator ratings that can be applied to Sunflower type power systems and the package sizes required to accommodate the alternators.



SNAP II AND SUNFLOWER ALTERNATOR
FIGURE 40

K&E 10 X 10 TO THE INCH 359-11
KEUFFEL & ESSER CO.




SUNFLOWER PERMANENT MAGNET ALTERNATOR
EFFICIENCY CHARACTERISTICS
EFFICIENCY - PERCENT
100
90
80
70
60
50
40
30
20
10
0
0
1
2
3
4
5
6
7
OUTPUT - KW
40,000 RPM - TEST DATA - 1 H.P.
ALTERNATOR WEIGHT - 10 LBS.

CROSS SECTION OF ALTERNATOR

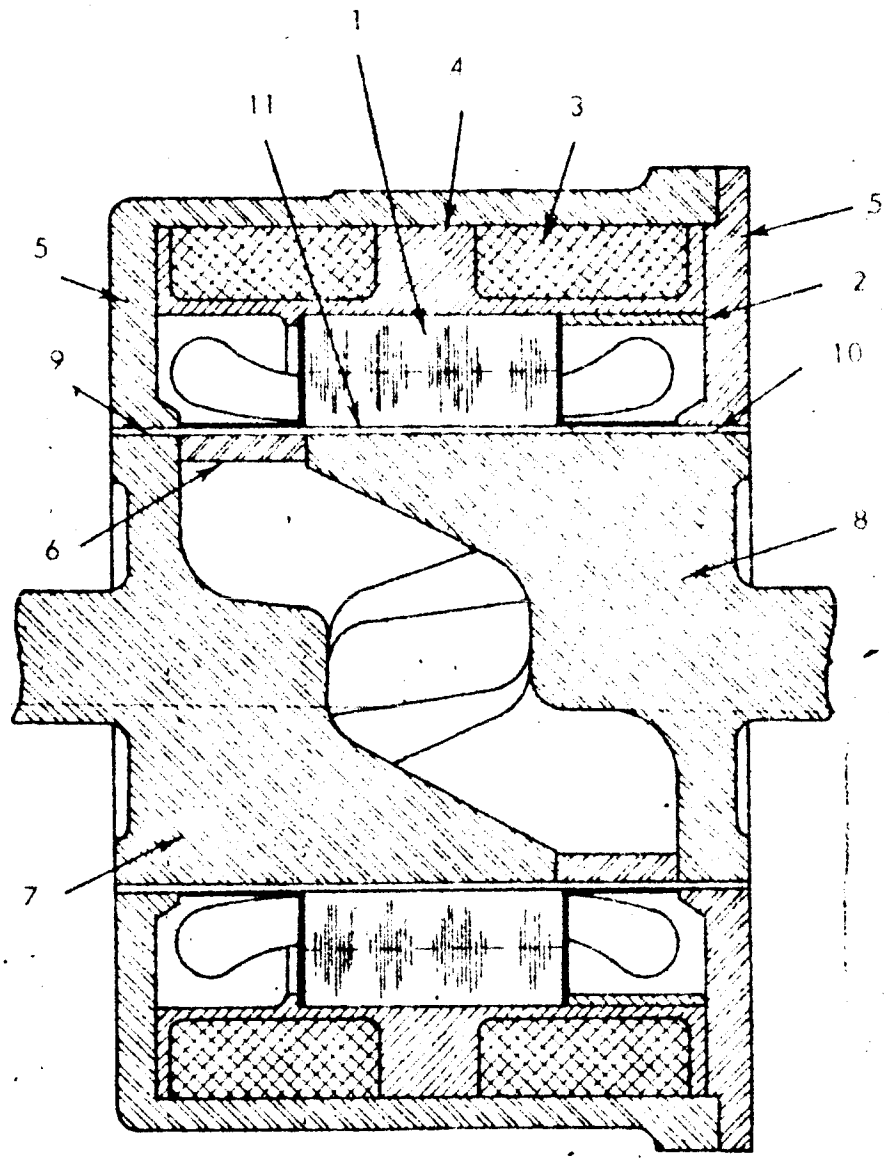


FIGURE 43

ROTOR CONSTRUCTION SCHEMATIC

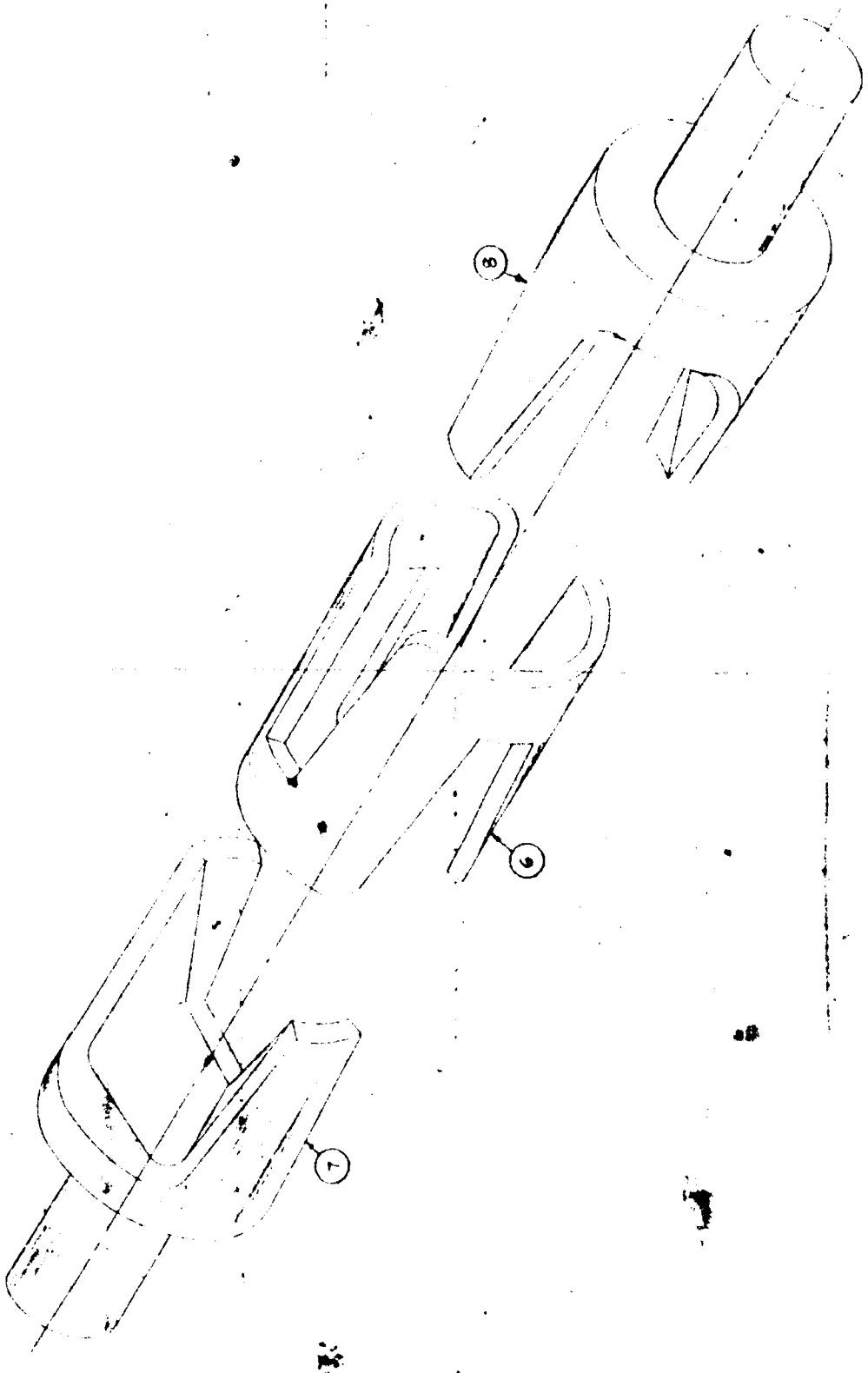


FIGURE 44

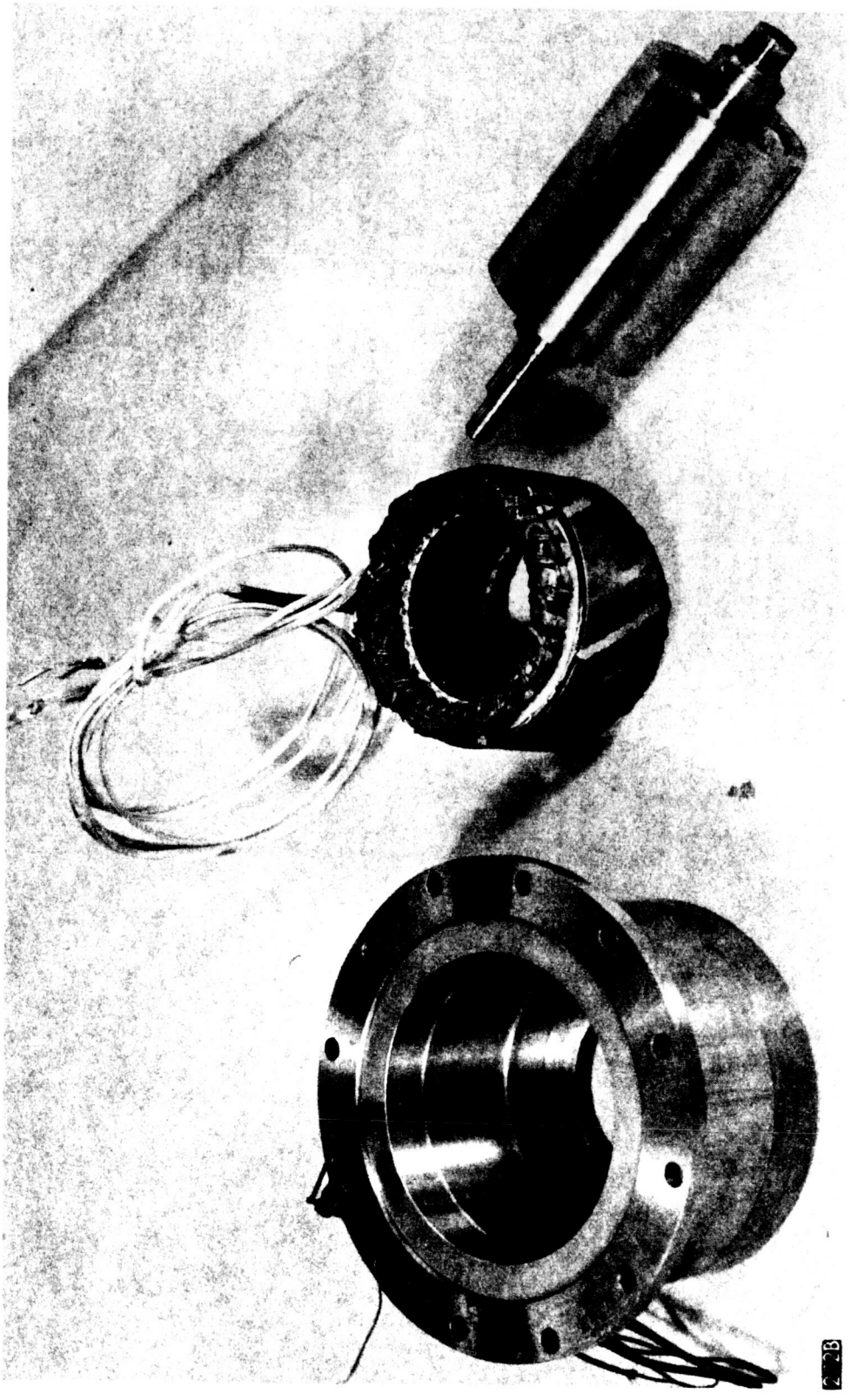
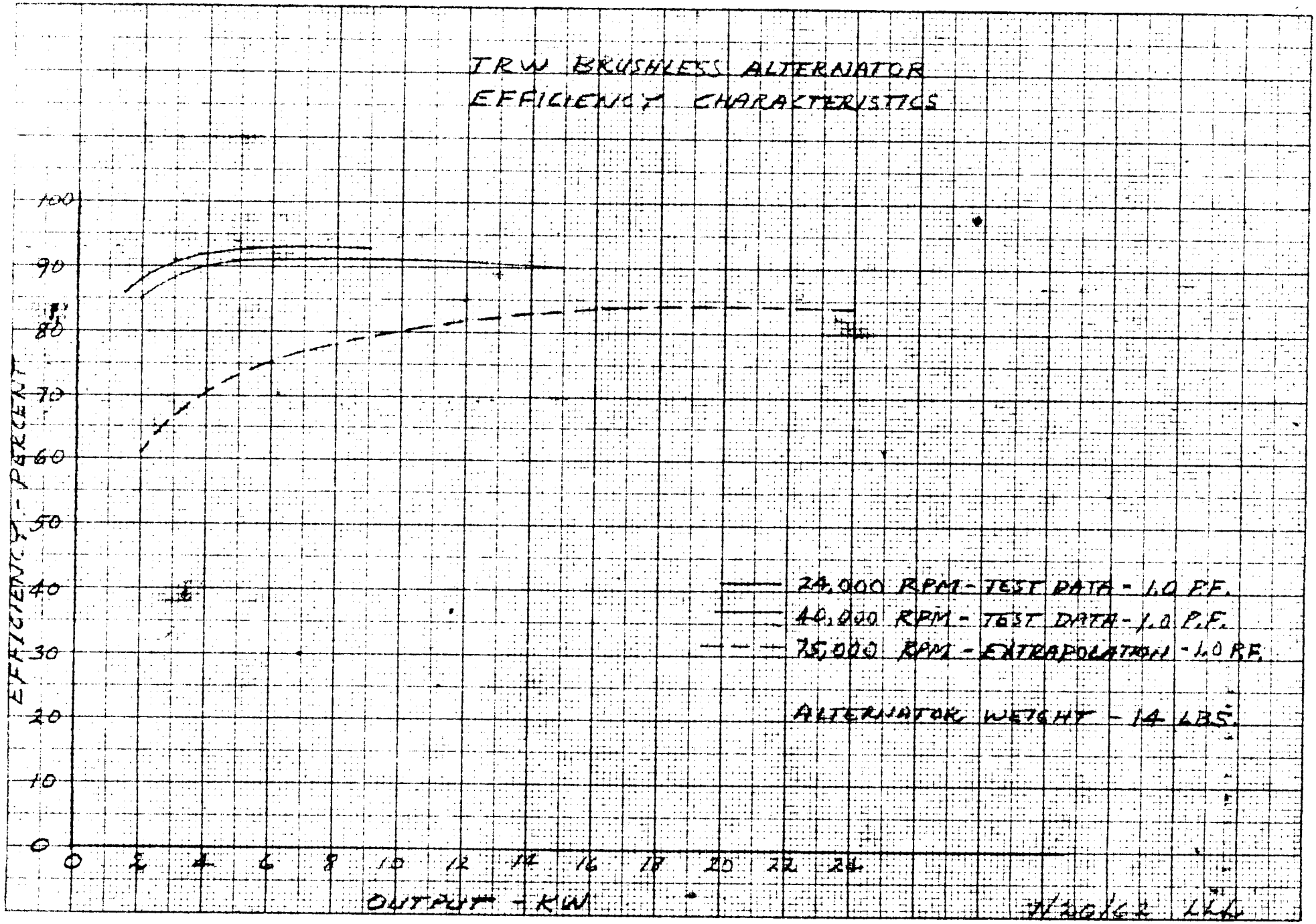


FIGURE 45


TRW BRUSHLESS ALTERNATOR
EFFICIENCY CHARACTERISTICS
EFFICIENCY - PERCENT
100
90
80
70
60
50
40
30
20
10
0
0
2
4
6
8
10
12
14
16
18
20
22
24
OUTPUT - KW
24,000 RPM - TEST DATA - 1.0 P.F.
40,000 RPM - TEST DATA - 1.0 P.F.
75,000 RPM - EXTRAPOLATION - 1.0 P.F.
ALTERNATOR WEIGHT - 14 LBS.

ALTERNATOR SUMMARY

TYPE	KW	RPM	PHASE	EFFICIENCY	WEIGHT	COMPATIBLE ROTATING ASSEMBLY
Permanent Magnet	1.5	40,000	3	90%	3.7 lbs.	SPUD
TRW Brushless	3.0	40,000	3	90%	7.3 lbs.	SPUD
Permanent Magnet	7.0	40,000	3	90%	10.0 lbs.	Sunflower
TRW Brushless	15.0	40,000	3	90%	14.0 lbs.	Sunflower
TRW Brushless	15.0	60,000	3	90%	12.0 lbs.	Sunflower

FIGURE 47

Additional System Factors

Some of the areas of potential performance improvement have been directly implied in the preceding component discussions. Before proceeding to a presentation of the results of these implications, some additional factors related to detailed system specifications need to be noted.

Perhaps the major details of the current Sunflower program and specifications which restrict design flexibility are:

a) Operability, without modification, at any circular earth orbit between 300 and 20,000 nautical miles.

b) Operability during accelerations of up to one g in any direction.

c) Virtual budgetary requirement to retain SNAP 2 designs in the turbo-alternator, to retain component development support.

d) Design for 3 KW output.

The following paragraphs discuss performance improvements which can result from departing from some of the above requirements. Specifically, the results of the following assumptions are discussed.

a) Pre-establishment of approximate orbital altitude to permit tailoring of the solar collector, boiler/heat storage component and start system.

b) Modification of the operating acceleration specification to permit accelerations of up to one g in a predicted direction. It is specifically assumed for illustration, that the total acceleration shall be $\leq$ 1 g, and that no component shall be in the aft direction.

c) Bearing and turbo-alternator developmental freedom is assumed.

d) Design concepts are presented for both greater and less than 3 KW.

In addition to the above program and specification assumptions, the following paragraphs present some "second thoughts" on system and component concepts.

Rankine cycle system performance improvements can be obtained by utilizing components of higher efficiencies and increasing the upper cycle pressure and reducing the condensing temperature.

More efficient components may straightforwardly be obtained by increasing the design power. Increase in total power output allows the use of more efficient alternators. The specific examples noted above include a permanent magnet machine of 90% efficiency at 7 KW and a TRW Brushless type alternator with an efficiency of 93% at the 15 KW level. These concepts are not design values but have been accomplished on actual hardware. The packaging of the 7 KW permanent magnet machine is identical to the current Sunflower unit. The 15 KW machine requires a larger diameter due to the excitation coil but can be incorporated into the package

with no change in bearing span, allowing use of the same bearings and shaft assembly as modified for the new rotor at the same, 40,000 rpm, rotating speed.

Increase in turbine efficiency to the 63% range at 7 KW and 70% at 15 KW results from the higher cycle weight flows. At these higher power levels, leakage losses lose significance, and the stages approach full admission. The higher power turbines also fit in the existing package designs. Axial length is unchanged, and only blade height and stage admissions change.

These factors permit the increase in power output of the current Sunflower turbo-alternator with very minor changes in package design, to 7 or 15 KW. These designs do not only benefit from higher turbine and alternator efficiencies. Since rotating speed, bearing load and pump power remain unchanged, the turbo-alternator package efficiency is further increased by the reduced significance of package parasitic power losses. In the present Sunflower unit, these losses constitute 18.5% of the turbine output. In the 7 KW example, these are halved to 9.25%.

Wider cycle limitations can also be utilized.

Conservative design limits the turbine inlet pressure to a maximum of 350 psia due to the influence of boiling temperature on the quantity of corrosion products formed. The 240 psia value of the present Sunflower design was largely determined by the maximum pump output pressure which had actually been demonstrated at proposal time.

The boiler output temperature must be maintained near the 1250°F temperature of the current Sunflower system to match the LiH melting point.

Condensing pressure minimums continue to be dictated by the design limitations of jet-centrifugal pumps. However, the choice of a known acceleration direction on zero g operation permits reduction. The known acceleration direction allows placement of the pump in a position to avoid acceleration induced NPSH reduction and allows relaxation of condensate drop transport requirements permitting lower condenser ΔP.

The demonstrated NPSH operating limits of Hg jet-centrifugal pump combinations is shown in Fig. [illegible]. Classical pump design and operating experience with this type of pump has shown that the pump will operate for extended periods of time with jet pump capacity ratios up to M = 2.2. (M is defined as pump net useful flow ÷ jet pump flow.) Short term operation can be tolerated to lower NPSH conditions, limited by accumulated implosion damage due to operation in the cavitation region. For example, a test which was conducted to determine the minimum NPSH point at which the prime was lost is noted on the curve. It is observed that this is well to the left (lower NPSH) side of the stated capability limit.

Other system improvements are suggested in the start system preheating concepts. One concept employs the use of pyrotechnic heaters. After orienting the collector and traversing through one sun cycle the condenser radiator is at a temperature of approximately 30°F. The energy required of the chemical pyrotechnic heater is that necessary to raise the temperature to 600°F.

Two mixtures have been investigated, a barium and a molybdenum mixture. The barium mixture becomes an unstable crystalline solid and liberates latent heat of crystalline change at approximately 725°F. The moly mixture liberates sensible heat of a solid residue.

The analysis indicates the barium mixture will bring the condenser tube to 600 + 15°F and maintain the temperature for approximately 235 seconds as shown in Figure 49. The moly mixture was insufficient to bring the tube to temperature with a reasonable amount of mixture.

A typical prototype pyrotechnic heater concept is shown in Figure 50. Electrical impulse would be used to fire the initiator and the reaction would be self-sustaining, burning at a rate of four to five seconds per foot.

The barium preheating system weighs approximately 44 pounds. This compares with a total preheating weight of nearly 100 pounds under the present Sunflower concept.

An attractive concept utilizes the primary source of energy, the LiH storage bath, to preheat the CSU and condenser. This system employs a separate motor driven pump to circulate a fluid such as Dowtherm past the boiler/heat storage unit to the CSU and condenser components. Preliminary calculations for a 7 KW unit indicate that a system of this type would require a flow rate of 35 lbs/min. of Dowtherm with a resultant pumping power of 170 watts. The required battery capacity is dependent upon preheat time. A typical sequence would consist of orienting the system toward the sun and, as the boiler/heat storage unit approaches the desired operating temperature, initiating the preheat system flow. Flow would be continued during the remaining sun and the following shade period. This would allow preheating during the shade portion with system operation to commence upon reentering the sun cycle. See Figure 51.

The weight elements of the preheat system are listed as follows:

Primary battery	3.7 Lbs. (Based on $\frac{50 \text{ Watt-Hr}}{\text{Lb}}$ for 1 hour)
Pump-Motor	4.0
Tubing	5.0
Manifolds	3.0
Accumulator	4.0
Dowtherm Inventory	3.0
	22.7 Lbs.

The numbers are based on a brief look at the concept, and although a more detailed analysis is required for a given system at a particular orbit, we feel the system could be designed with a weight of approximately 25 to 30 pounds.

Another feature of the system is that the heat exchanger passage formed around the radiator tubes can be utilized as a meteoroid bumper shield and would, in fact, allow a reduction in the wall thickness of the radiator tubing. To avoid having to protect the preheat system for long term meteoroid protection, the concept would employ a deliberate puncturing of the Dowtherm loop so that the radiator would not be influenced in its thermal operation should a puncture occur. The radiator design would be corrected for the effect of the bumper on the radiating area.

A further cycle improvement can result from the knowledge of the demands of the useful load requirements of the system. If the loads and time duration are known, a system can be designed to operate around the nominal load rather than the peak load.

To accomplish this power variation, a modulating flow control valve is incorporated into the boiler inlet line. This valve is modulated to control parasitic load power to a safe minimum regardless of variations in useful load demand.

The energy conserved as shown in Figure 52, results in a direct reduction of LiH heat storage material and a straightforward reduction in collector size.

The modulating valve is not sensitive to corrosion products since the signal received is proportional to actual system surplus power output. Therefore, should deposits form on the orifice and reduce flow, the resultant power reduction is sensed and the correcting error signal repositions the valve.

Other reductions of collector size can be realized by decreasing the reradiation losses from the cavity receiver. An aperture closure device can be utilized which senses the incident flux. When this flux is cut off, as while in the earth's shadow, the door would close over the aperture and reduce the reradiation loss. This results in a 5-8% reduction of collector area.

The same element could be utilized as the temperature controller for the boiler heat storage unit.

Another improvement which could be utilized, which again results in reduced collector area, is a more accurate attitude control system. The following curve, Fig. 52, shows the effect of attitude control on collector performance and the resultant gains in efficiency. Since some attitude control system is required to orient the system to the current $\pm 3/4^{\circ}$ accuracy, the penalty to orient to the tighter tolerance is limited to increased propellant. Since a useful propellant capacity of 20 lbs. suffices to orient a typical 3000 lbs. vehicle to $\pm 3/4^{\circ}$ for a year, the increased propellant requirements of a $\pm 3/8^{\circ}$ orientation for instance would be the quite minimal value of 20 additional pounds.

JET CENTRIFUGAL PUMP
INLET PRESSURE REQUIREMENTS VS SYSTEM FLOW

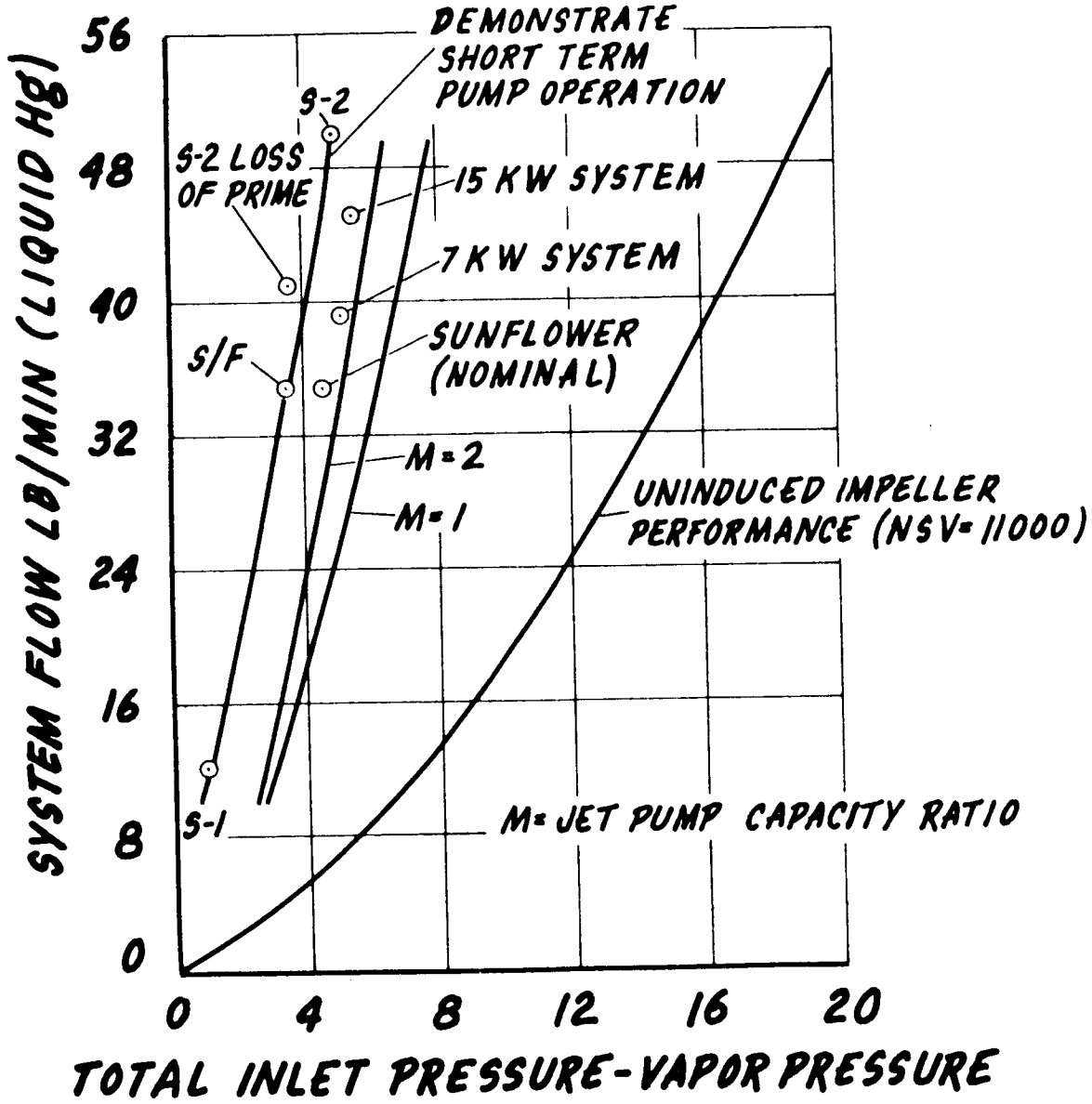
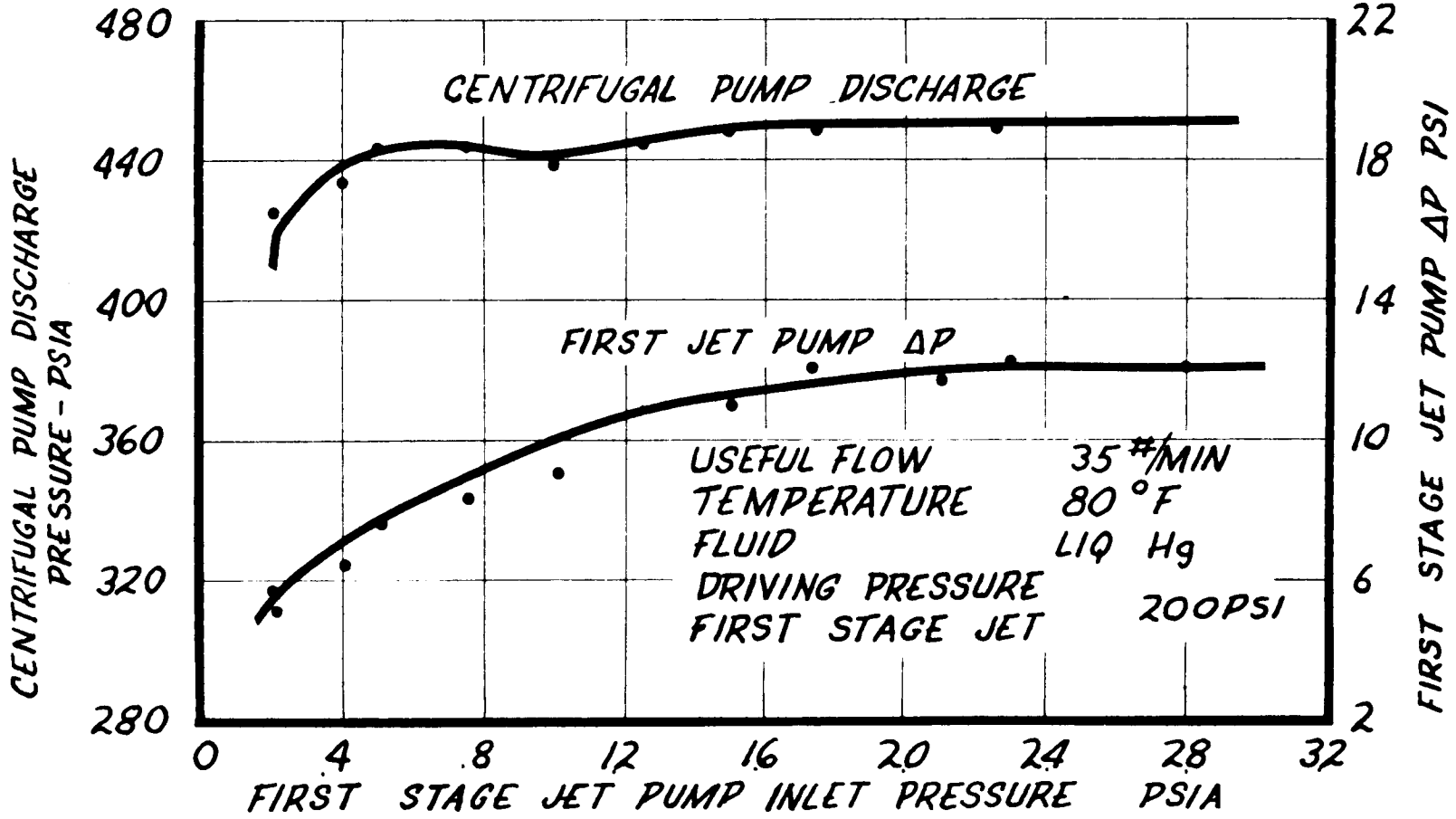


FIGURE 48

DOUBLE JET BOOST CENTRIFUGAL PUMP PERFORMANCE SUNFLOWER REQUIREMENTS



PYROTECHNIC HEATER RESULTS OF BARIUM-MIX

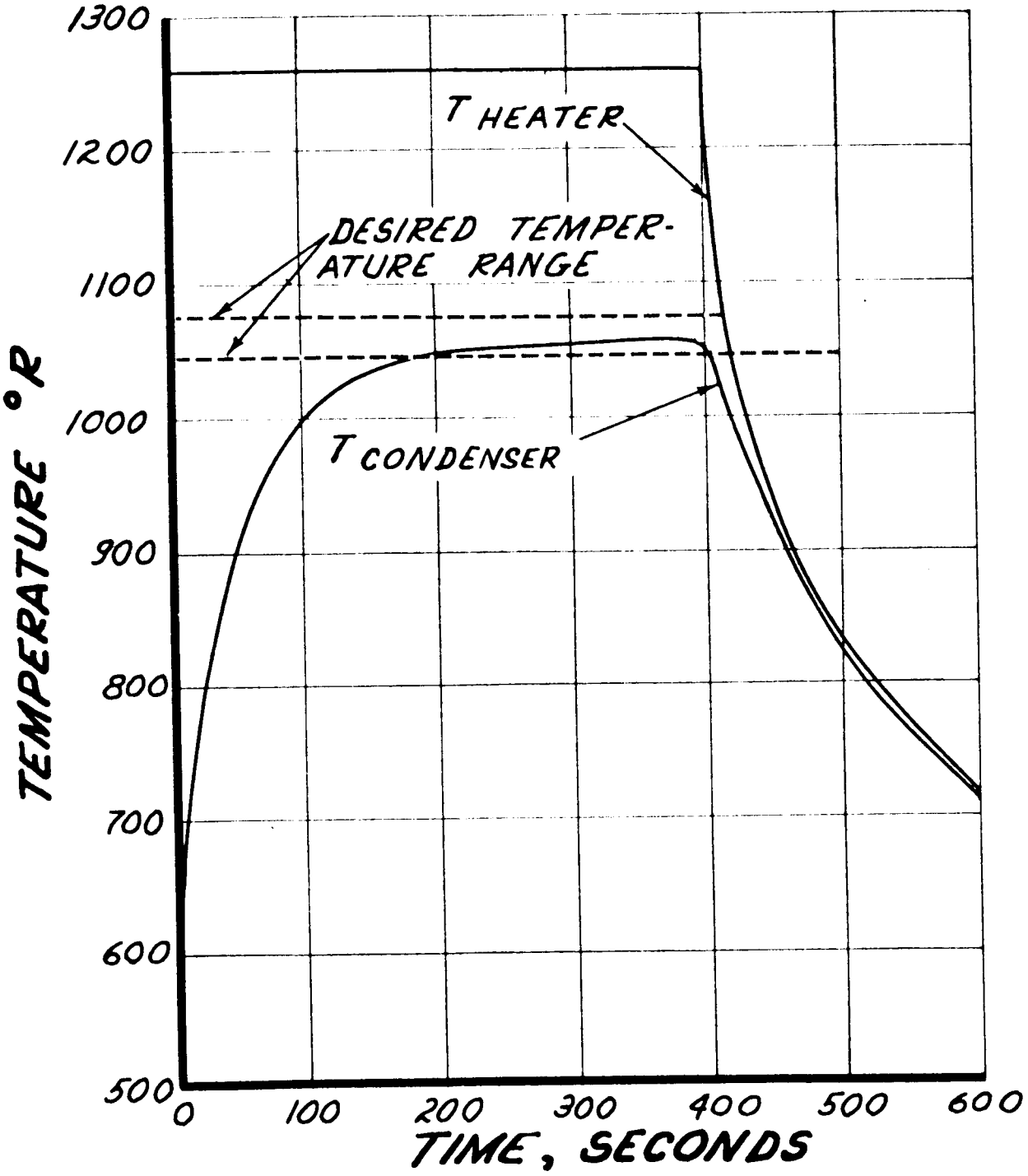
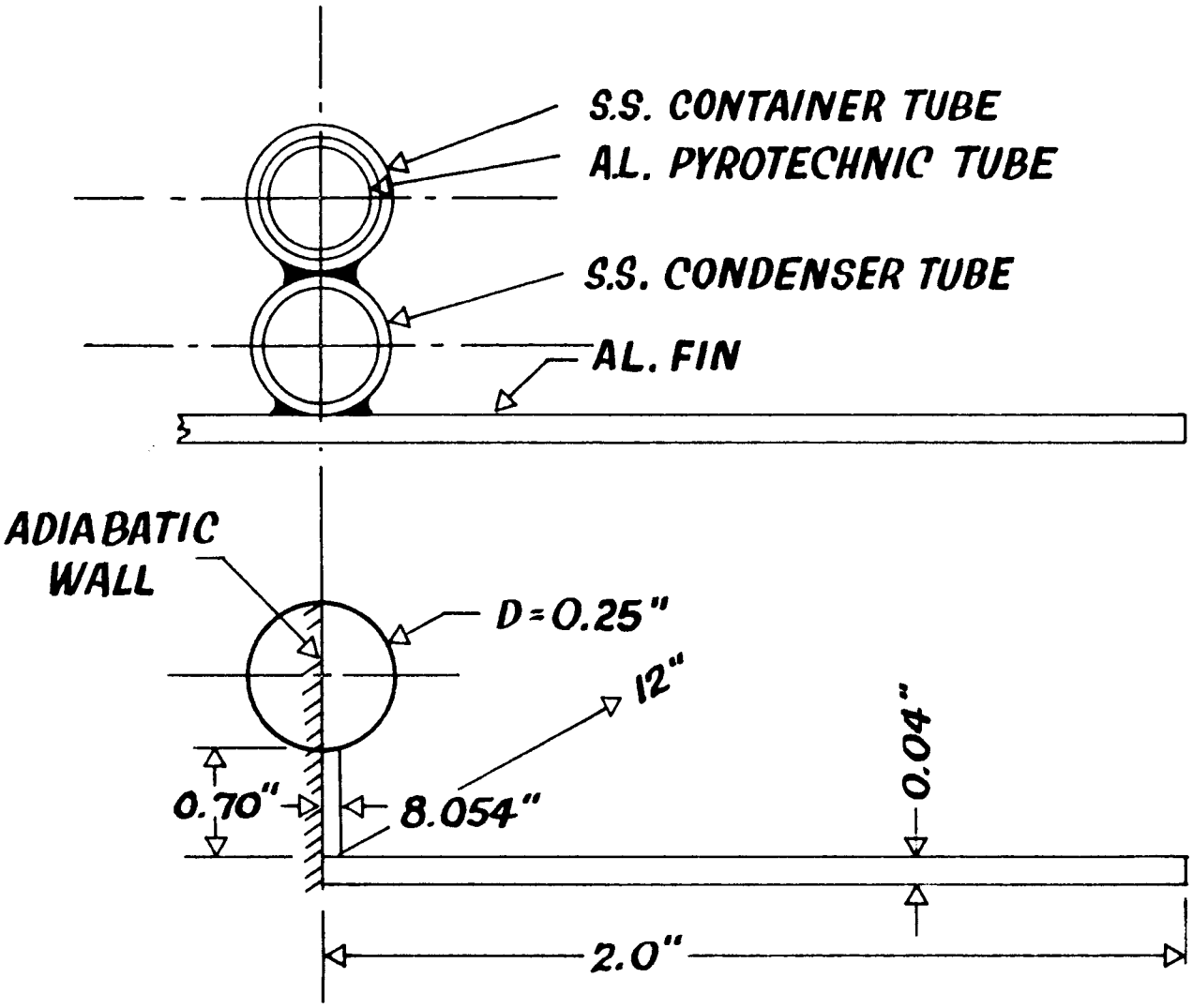


FIGURE 4?

HEATER-TUBE CONFIGURATION



NODAL POINT LOCATIONS

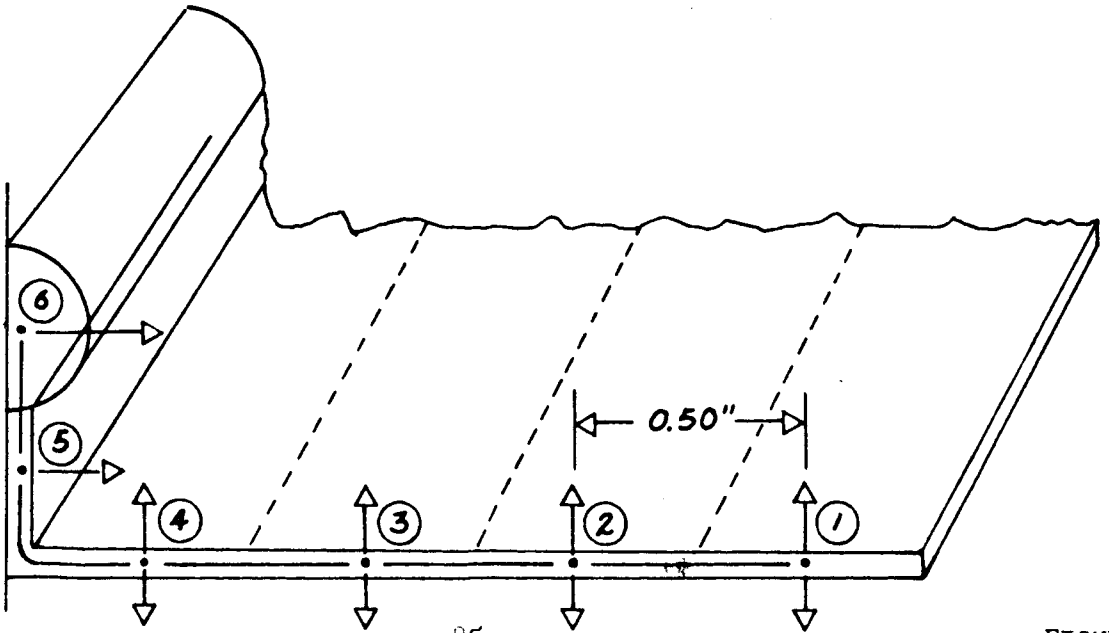
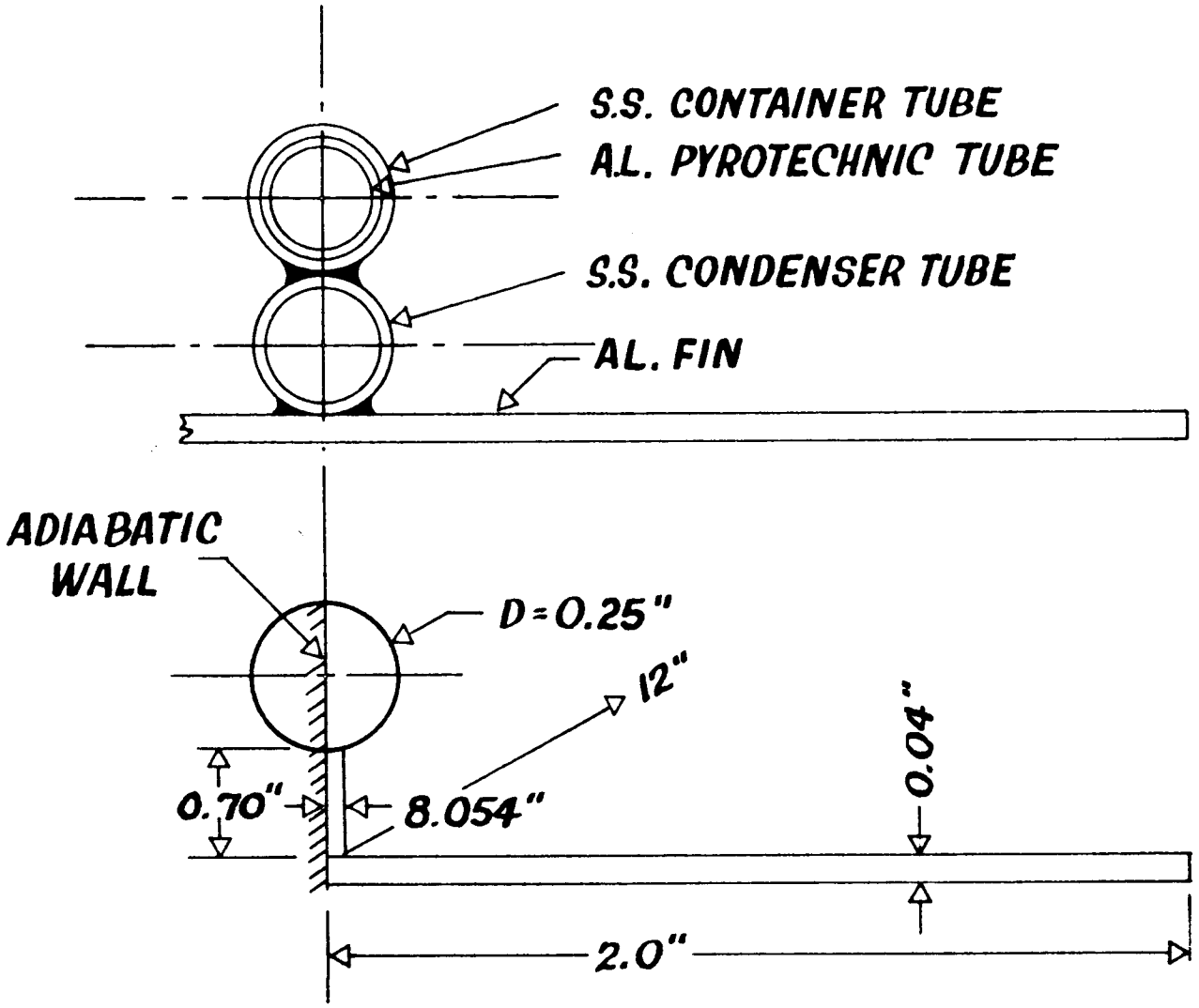


FIGURE 50

HEATER-TUBE CONFIGURATION



NODAL POINT LOCATIONS

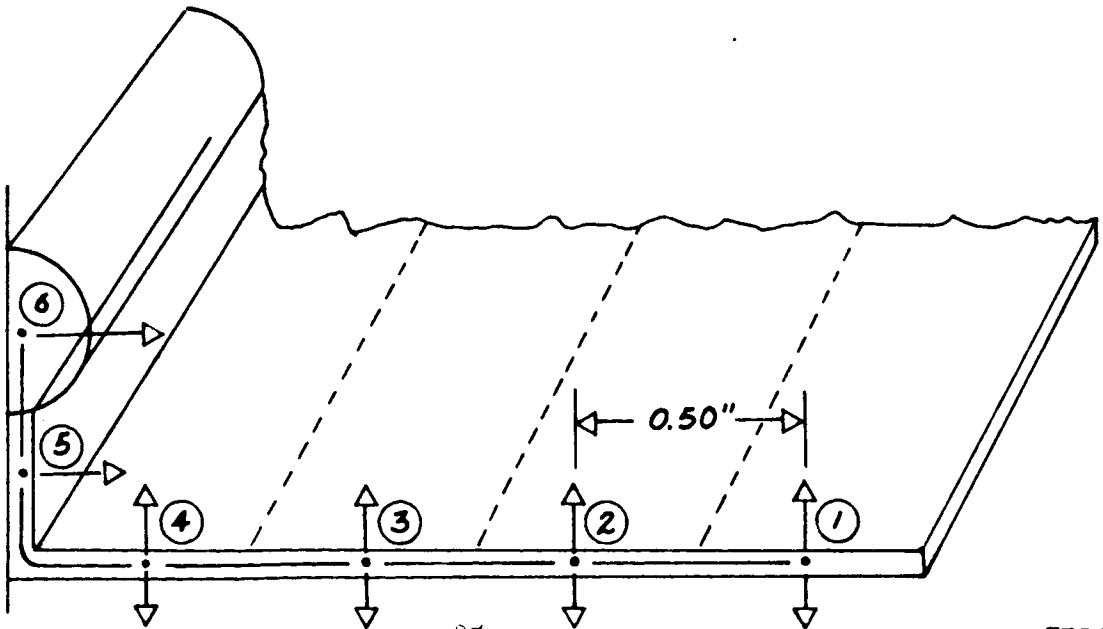


FIGURE 50

SEPARATE FLUID PRE-HEAT SCHEMATIC

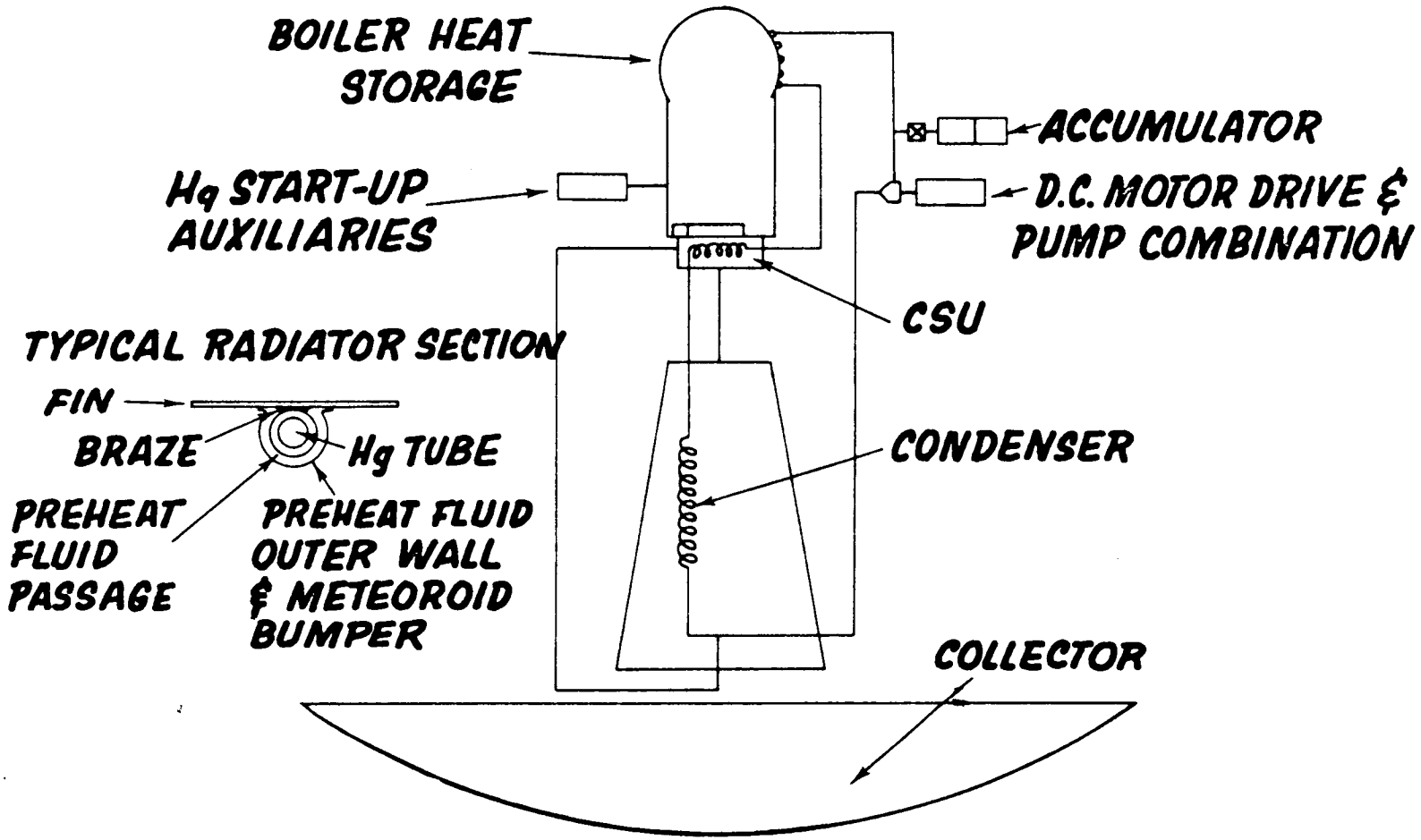


FIGURE 51

TAPCO
a division of
Thompson Ramo Wooldridge Inc.

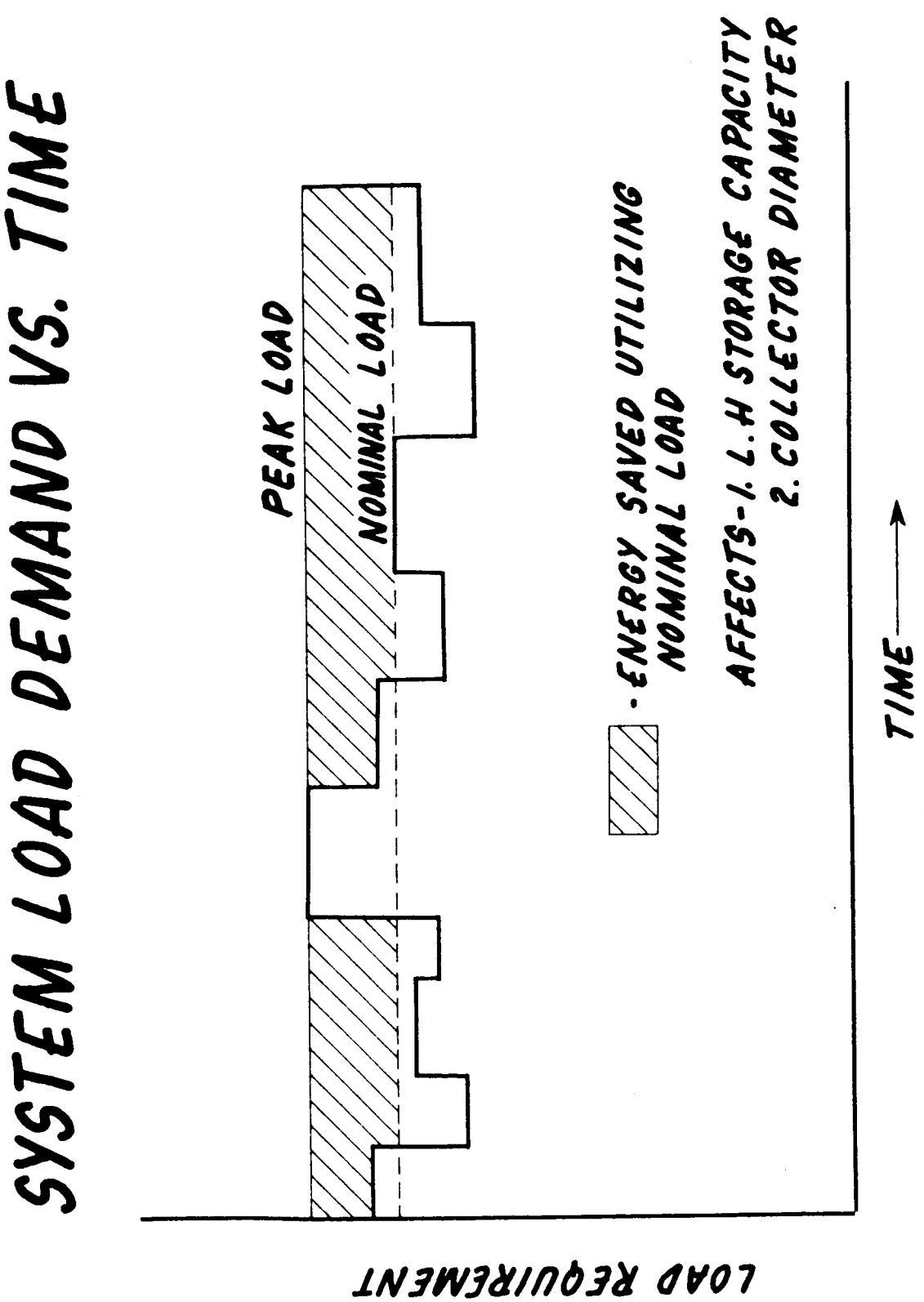
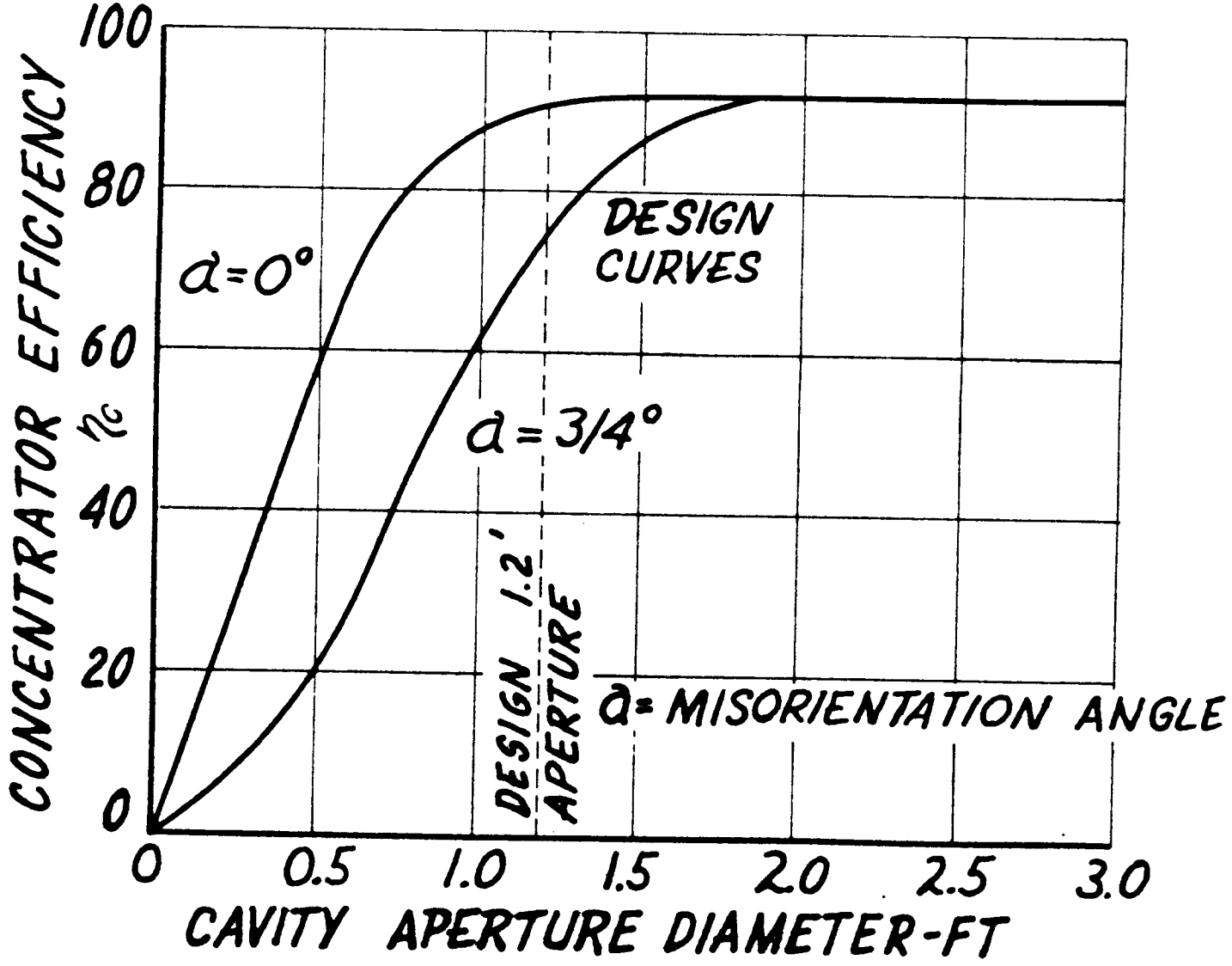

SYSTEM LOAD DEMAND VS. TIME
PEAK LOAD
NOMINAL LOAD
- ENERGY SAVED UTILIZING NOMINAL LOAD
AFFECTS- 1. L.H STORAGE CAPACITY
2. COLLECTOR DIAMETER
TIME
LOAD REQUIREMENT

FIGURE 52

COLLECTOR EFFICIENCY VERSUS CAVITY OPENING AT VARIOUS MISORIENTATION ANGLES



SYSTEM EXAMPLES

Shown on Figures 53 and 54 are system configurations of a 3.0 KW SPUD and a 7.0 KW Sunflower system. These systems have been conceived based upon the component and system performances discussed above. Figure 55 illustrates the versatility of packaging of the present 3.0 KW Sunflower system for a specific transfer mission for a low altitude orbit to the 24 hour circular orbit.

3.0 KW Extended SPUD

The system is conveniety packaged in a 5 ft. diameter space envelope of 14.5 ft. overall length. The system is designed for 0-g operation and capable of operating in a unidirectional 1-g environment for prelaunch checkout and orbital accelerations. The basic criteria for design are as follows:

1. Higher power is provided by a higher capacity and performance electro-magnetic alternator in the standard speed package.

2. The system incorporates a flow modulating valve at the boiler inlet and low parasitic capacity of 100 watts.

3. Component turbine efficiency of 57 percent.

7.0 KW Sunflower

The system is packaged in the current Sunflower space envelope, 9.6 ft. diameter cylinder, 8 ft. long, topped by a right circular cone of 15° half angle. The system design provides for operation in a unidirectional 1-g environment, with orientation of the force parallel to the longitudinal axis in the aft direction. The basic system design assumptions are as follows:

1. 7.0 KW of electrical power is provided by a higher capacity and performance permanent magnet alternator in the standard Sunflower package.

2. Boiler flow modulation to supplement a parasitic power capacity of 300 watts.

3. Component turbine efficiency of 70 percent.

4. Alternator efficiency of 90%.

3.0 KW Sunflower Orbit Transfer Vehicle

The system design layout illustrates the packaging flexibility of the present Sunflower system to meet a specific mission requirement. Shown is a system configuration for a transfer mission to the 24 hour circular orbit. The design provides for a mission travel time of approximately 120 days and useful payload of 800 lbs. Hydrogen fuel requirement for the low thrust transfer engine is 600 lbs.

In conjunction with the presentation of system layouts, system weight estimates have been prepared. These are shown in tabular form on Figure 56 and include estimates of a 1.5 KW SPUD unit and 15.0 KW Sunflower units. Given also are some of the significant parameters, along with assumptions on component efficiency.

The 1.5 KW SPUD system design is based upon extention of the present SPUD performance, generally through higher performance and capacity of the permanent magnet alternator. This is provided within the dimensional limitations of the SPUD package. System parameter limitations have been confined to increase in turbine inlet pressure and temperature to 350 psia and 1250°F respectively. Lower cycle pressure and temperature, 2.5 psia at 522°F, are consistent with the present SPUD system and component requirements.

A straight extrapolation of the same cycle and performance criteria as used in the above systems yields a weight estimate at the 15 KW level of 1301 lbs. F Figure 57 shows a layout of the turbo-alternator for this system. As shown, this unit is the same as the current Sunflower unit except that the girth has been increased in the alternator area to employ the TRW brushless alternator vehicle we described in a preceding section.

At this higher power, it was also of interest to conduct a preliminary design of an improved system. The bases for cycle and component operating assumptions has been discussed in the preceding section. The major assumptions are repeated as follows:

1) Turbine exhaust pressure, 2.5 psia - sual jet pump

2) Four stage turbine, interstage reheat, η_T = 75%

3) Alternator efficiency - 93%

4) Altitude orientation - ±3/8°

The results of this investigation are also tabulated in Figure 56. The weight of this system is estimated at 1116 lbs. Weight of the start-up auxiliaries is based upon use of circulation of a 943 secondary fluid as discussed above for condenser preheat.

The primary consideration in going to lower exhaust pressure is available head to the condensate pump. Through use of dual jet boost pumps in series, condensing pressures of this magnitude become practicable and offer the advantage of higher thermal efficiency.

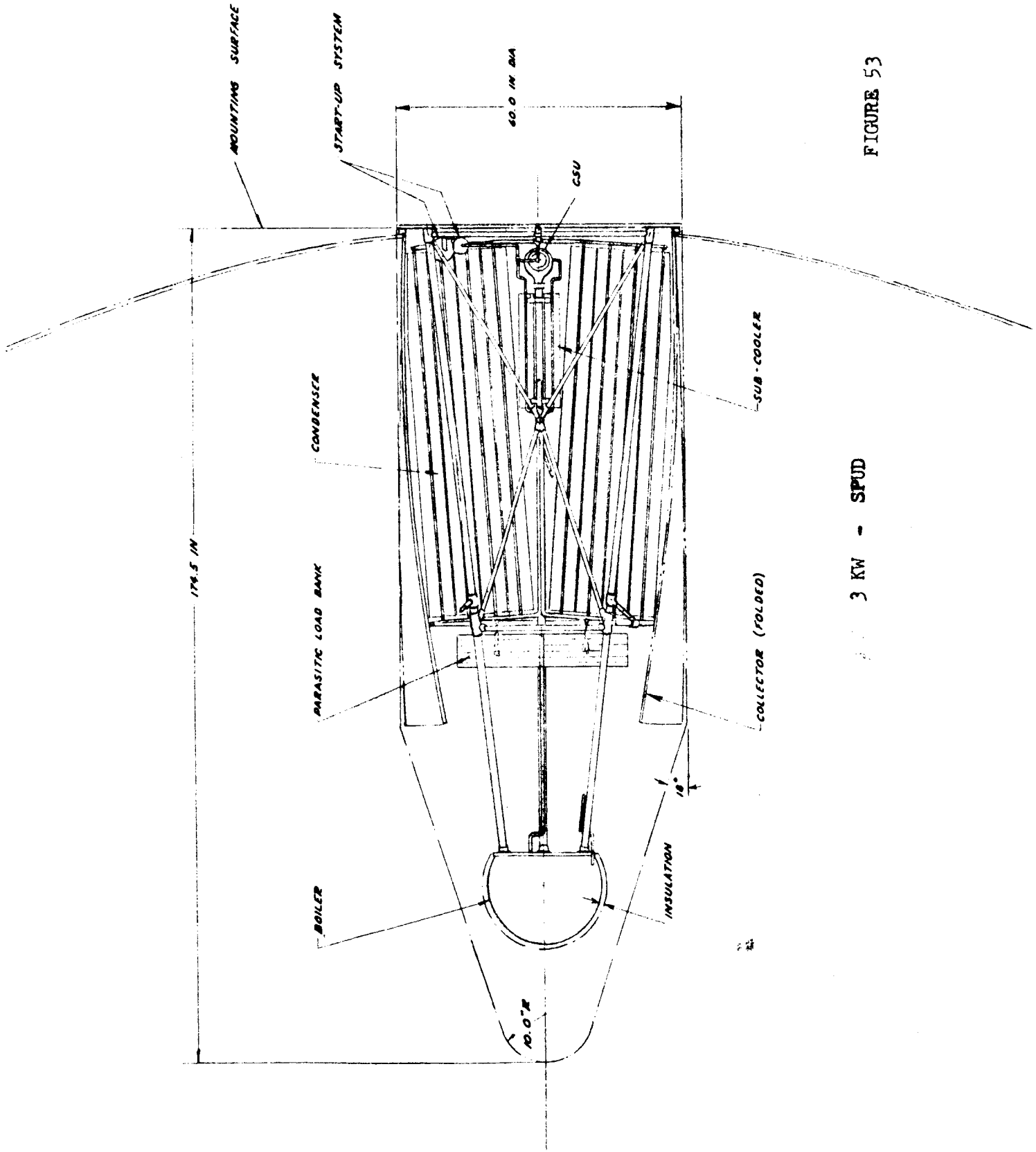


FIGURE 53

3 KW - SPUD

(Figure missing)

SUMMARY COMPARISON OF MERCURY RANKINE SYSTEMS FOR 300/N-MILE ORBIT

POWER-USEFUL (KW)	1.5	3.0	6.7	15.0	15.0
PARASITIC (WATTS)	50	100	300	500	100
WEIGHT (LB)					
COLLECTOR	38.0	74.0	215.0	410.0	244.0
BOILER HEAT STORAGE	52.3	82.9	196.0	349.0	247.0
CONDENSER/SUB-COOLER	19.7	27.7	88.0	177.0	167.0
TURBO-ALTERNATOR	15.0	15.0	40.0	45.0	45.0
RSC	20.0	25.0	30.0	40.0	40.0
START AUXILIARIES	25.0	35.0	65.0	110.0	35.0
STRUCTURE & MISC.	30.0	65.0	100.0	120.0	120.0
INVENTORY	8.0	15.0	30.0	50.0	45.0
TOTAL	208.0	339.6	764.0	1301.0	943.0
SPECIFIC WEIGHT (#/KW)	139.0	113.0	114.0	86.8	63.0
COLLECTOR AREA	175	340	980	1862	1110

FIGURE 56 A

TAPCO a division of Thompson Ramo Wooldridge Inc.

(Figure missing)

SUMMARY COMPARISON OF MERCURY RANKINE SYSTEMS FOR 300/N-MILE ORBIT

CYCLE PARAMETERS/KW	1.5	3.0	6.7	15.0	15.0
Q BOILER (KW)	9.1	18.1	44.6	84.5	59.8
Q CONDENSER (KW)	7.1	14.2	36.4	67.2	44.5
P_{oo} (PSIA)	350	350	350	350	350
T_{oo} (°F)	1250	1250	1250	1250	1250
P CONDENSER (PSIA)	1.3	2.6	7.0	7.0	2.5
ΔP CONDENSER	0.2	0.2	1.7	1.5	1.0
T CONDENSER (°F)	475	525	605	605	523
CYCLE FLOW (PPM)	3.29	6.55	17.9	33.8	23.8
CYCLE EFF. (η)	16.5	16.5	15.7	18.4	25.2
TOTAL FLOW	10.0	13.2	38.9	54.8	44.8
COMPONENT EFF.					
η ALTERNATOR	90	90	90	90	93
η TURBINE	54	57	63	70	75
η PUMP	25	30	30	30	30

15 KW TURBO-ALTERNATOR

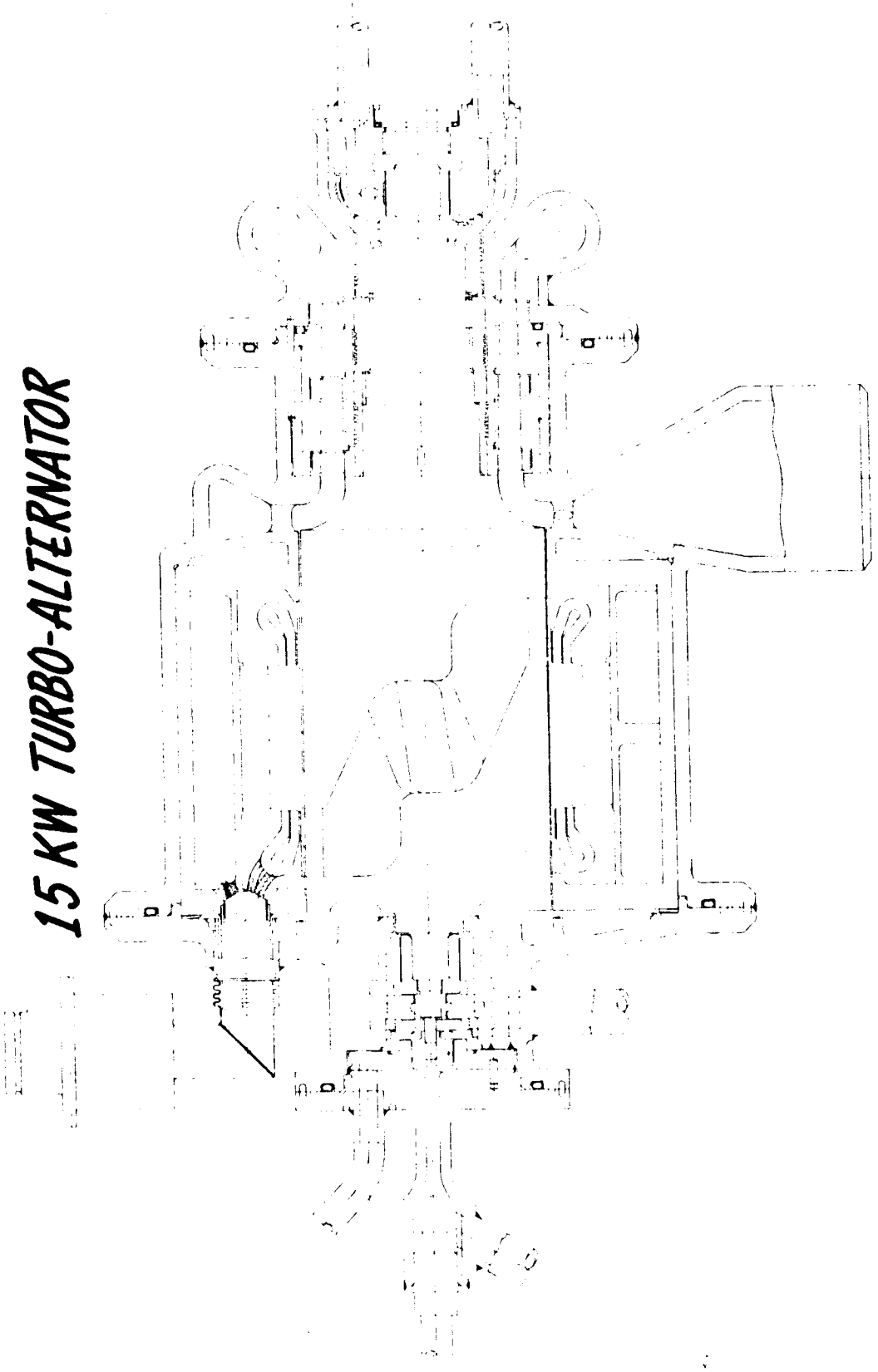


FIGURE 57

CONCEPT RELIABILITY ASSESSMENT

Successful operation of the Sunflower conversion unit for 1,500 hours, following the successful 2,500-hour endurance run of the SPUD conversion unit, provides an important demonstration of the capability of the Mercury Rankine solar power system for reliable, long endurance operation. The Sunflower unit endurance run is, in fact, continuing with no indication of performance deterioration and the SPUD unit was shut down by plan, with subsequent inspection showing the unit to be in good mechanical condition. These endurance demonstration runs, therefore, provide a very positive demonstration of capability for operation for one year, or longer.

Proof of reliability for this type of long endurance power system is difficult to obtain, however, by test alone. For example, successful operation of twenty-five (25) such power plants for one year, without a failure, would only statistically "prove" a 91% reliability, at a 90% confidence level. Obviously, time and expense require that additional techniques be used to predict operational reliability for this type of system.

The following discussion therefore presents several types of information which provides a basis for confidence that the Sunflower solar power system has the capability for achieving 95% reliability of operation for one year, as is required to justify initiating full scale development of this power system. These types of information are:

1) Summary of design features which have been included to attain reliability.

2) Assessment of reliability of the system, using recognized component reliability evaluations.

3) Discussion of techniques to be used in the development program to realize this reliability potential.

Attainment of reliable, long endurance operation was a major consideration in the Sunflower design and in the SNAP 1, SPUD, and SNAP 2 designs, from which the Sunflower concept grew. The Sunflower concept of power generation, therefore, already includes conservative design principles proven by extensive experience.

The first factor included in this background experience feature is that these Rankine cycle power plant designs have been based upon commercial steam and mercury power plants which have shown extensive capability for operating continuously for two or three years without shutdown. Forced shutdowns in commercial power plants occur only rarely during the life of the unit and the major cause of these shutdowns result from problems associated with the combustion side of the boiler and due to the fossil type fuels used. Recent studies of commercial power plant operation data (as described in Reference 1) show that, when the problems associated with fuel burning are eliminated, the turbo generator systems experience a forced shutdown only once every 2.9 years.

Direct reliability comparison of the Sunflower power conversion system with that of commercial refrigeration systems can also be made. Household refrigerators, for example, have sealed units guaranteed for five (5) years even though the units are continually started and stopped and have little or no cleaning of

built-up dirt deposits. In comparison, the Sunflower system is operated continuously at constant speed with little or no degradation due to accumulation of deposits on the condenser. In comparison to the household refrigerator, the goal of the Sunflower system is for 95% reliability for one year's operation.

The Sunflower and SNAP designs include further features to provide reliable, long endurance operation, in excess of that provided by commercial power plants. Briefly, these features may be summarized as follows:

1. Operates at conservative temperature and material stress limits.
2. Hermetically sealed.
3. No rubbing seals or brushes.
4. Working fluid is also the lubricant.
5. Journal bearings.
6. Low turbine tip speed.
7. Utilizes a single combined rotating unit.

It may be seen that these major design features have eliminated many components which would tend to wear out in service. The life of the power plant, therefore, depends upon such basic things as material compatibility with mercury, diffusion of lithium hydride, and erosion of turbine blades and bearings. These factors have been separately discussed and it has been shown that capabilities for component lives substantially in excess of one year are indicated by the numerous component tests and the system endurance tests which have been run.

To obtain reliable system operation, it is also necessary to eliminate the early life failure, due to an inherent flaw in the fabrication of a particular unit. This type of failure must be avoided by extreme care in fabrication and inspection, and by extensive acceptance check-out of each power plant which will be placed into operational use.

It remains to show that the properly inspected components, each having inherent capability of operating for the required time without "wearing out" will not have a high probability of failure due to random, undetectable causes. An assessment of system reliability, based upon random failure rate data, obtained from recognized sources, is therefore presented in the following paragraphs:

Two independent assessments of reliability are represented by the tabulations of Figure 58 . In the second column, no consideration has been given the system elements except the assignment of a judgment number of relative complexity. This number is selected from a range from 1 to 450 in increasing complexity and is based primarily on an estimate of the difficulty of the function performed, as well as consideration of the design to be employed in this particular concept.

Column 3 is then calculated from the assignments of complexity of column 2 by indicating a failure rate proportional to complexity, based on a 95% probability of one year's successful operation.

The tabulations of column 4, on the other hand are failure rates predicted from failure experience data of elements similar to those of the Sunflower system. These rates are from the AVCO Corporation (2) and are for Aerospace components. A comparison between Column 3 and Column 4 shows that for the most part the failure rates and assumed complexity failure rates are in approximate agreement. In the case of the alternator and bearings, however, prior engineering knowledge rates the complexity failure rates higher than justified for a mature well-developed system. With proper development, the alternator and bearings should be the most reliable components of the system. As previously mentioned, the problem in these areas are related to the development of suitable materials.

The predicted system failure rate and resulting 91.8% reliability in Column 4, although not as low as that required for 95% probability of success, is well within development capabilities. Since the system is essentially a mechanical design, we would expect that random failures may be virtually eliminated as a cause of system failure. The conservative design practices will insure that the wear-out limit is well beyond the system capabilities, and preflight checking and running will insure that early failure potential will be eliminated.

The small margin of difference between the predicted 91.8% and the desired 95% reliability growth potential. For example, using a conservative 86% learning curve (i.e., 14% reduction in the unreliability each time the program effort is doubled), the difference could be realized in 12 months.

Examples of reliability growth during four (4) typical development programs similar to the Sunflower are shown in Figure 59 . A simple percentage of runs free of unit-caused-stops is used as an index of program progress. This index changes during the course of the program due to the change in emphasis during the testing. On most programs, the initial reliability growth is small due to the dynamics of getting the system in operation. We would, therefore, expect early failures followed by a period of rapid growth as the design problems are resolved. Finally, we would expect that the system would gradually approach the reliability objective.

In the case of the Sunflower system, prior engineering knowledge from the SNAP and SPUD programs would naturally tend to put the Sunflower system on the rapid growth portion of the curve. This assumption is borne out by the current endurance run of 1,500 hours.

As an illustration of the Sunflower system design, we can compare it to the Bomarc APU.

	RPM	Turbine Tip Speed Ft./Sec.	Max. Turbine Temp. °F
Bomarc	60,000	1400	1300
Sunflower	40,000	390	850

By comparison to the Bomarc turbine, the conservative Sunflower turbine design indicates that the tabulated failure rate for the turbine, in Column 4 of Figure 58 , is high and could be reduced since the stress temperature relationship is low as compared to the proven Bomarc design.

Also, with respect to the condenser, the major failure mode is in the welds. A concerted quality control and inspection program, including 100% dimensional checks, helium leak detection, x-ray and dye penetrant, and proof pressure testing, will virtually eliminate weld failure as a contributing cause of system failure. We could, therefore, also expect that the estimated condenser failure rate of Column 4 could be greatly reduced.

Since the turbine and condenser estimated failure rates comprise approximately one-half the total system failure rate, reduction in these two components would greatly reduce the system unreliability.

In a fuel development program, the inherent high reliability of the Sunflower system will be kept at its maximum by comprehensive design reviews, quality assurance, and a detailed feedback of test data, inspection data and materials data. This will insure that, the design is satisfactory for the intended mission, the design will not be degraded during manufacture, and feedback of information will minimize any potential trouble areas.

Elimination of random failures resulting from partial tolerance build-up, undetected material weaknesses, hidden defective workmanship, and other similar factors can be insured through the application of proper quality control techniques. With normal mechanical wear-out, the equipment life can be more accurately predicted than if the failure is of a random nature. Designing the components with wear-out well beyond the life requirements will provide adequate wear-out safety margin.

In conclusion, this analysis indicates that all Sunflower system components are, inherently, sufficiently reliable for the required mission. The Sunflower system reliability objective of 95% can be met by, (1) utilizing conservative design techniques, (2) through design reviews, (3) adequate quality control and inspection, (4) feedback and analysis of all pertinent data, (5) comprehensive development, endurance, environmental and acceptance testing, (6) sufficient system break-in run to eliminate early failures.

Through the use of the basically reliable components in the design and by using the proven reliability techniques in conjunction with a well-planned development program, the 95% reliability for a one year life objective will be achieved in a very reasonable time.

Reference

#1 Edison Electric Institute, Turbine and Boiler Availability Report for the Period 1955 through 1958, New York.

#2 Reliability Engineering Data Series - Failure Rates, April 1962, Avco Corp., Research & Advanced Development Division, D. R. Earles and M. F. Eddings.

SUNFLOWER APPORTIONED & PREDICTED RELIABILITY

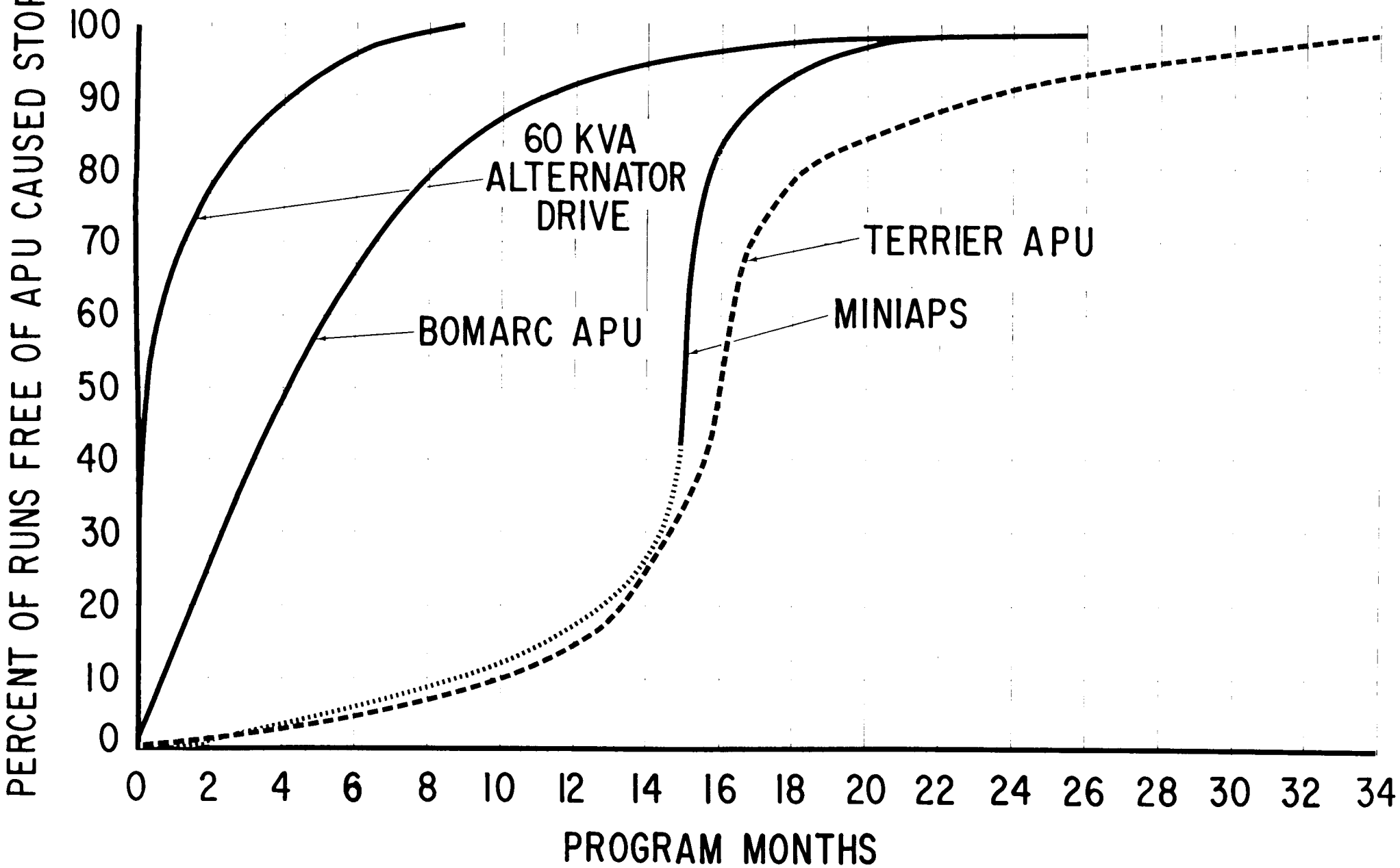
COMPONENT	ASSUMED COMPLEXITY	COMPLEXITY F.R. x 10^6	PREDICTED F.R. x 10^6
STRUCTURE	1	.002416	———
PUMP	50	.12080	0.68
BOILER FLOW REGULATOR	100	.2416	0.89
CONDENSER	250	.6040	2.21
BOILER	300	.7248	1.11
ELECTRONIC CONTROL	350	.8456	1.90
TURBINE	400	.9664	2.79
ALTERNATOR	450	1.0872	0.03
BEARINGS	450	1.0872	0.06
TOTAL	2351	5.68	9.67

$$R = e^{-t \times F.R} = e^{-8800 \times 9.67 \times 10^{-6}} = 91.8\%$$

START UP COMPONENTS: NITROGEN BOTTLE, 3 SQUIB FIRED VALVES, PRESSURE REGULATOR, START TANK, COMPONENT HEATERS, BATTERY & RELAY

RELIABILITY: 100% FOR STARTUP

RELIABILITY GROWTH DURING DEVELOPMENT



ADVANCED SYSTEMS

In order to provide a basis for exceeding the performance of solar mercury Rankine cycle space power systems, TRW began an extensive analytical and experimental investigation of other system possibilities approximately 18 months ago. Under this program some interesting conclusions were reached. These are as follows:

1) Cycle thermal directly effects the weight and size of solar systems. Since installation volume and weight are major limits in space power systems, it is of major importance to reduce size as well as weight.

2) Cycle efficiency improvement, obviously, requires operating the cycle over wide temperature ranges.

3) Since the solar energy receiver reradiates energy in proportion to the fourth power of the upper cycle temperature (and since light weight, precision collectors are difficult to fabricate and store) it is more advantageous to reduce the bottom cycle temperature than it is to increase the upper cycle temperature.

4) To avoid difficult material technology problems and, also, to utilize the unique high heat storage capability of lithium hydride, it is desirable to avoid top cycle temperatures of over 1250°F.

5) For reliability, endurance capability, and light weight, the conversion machinery must be a high speed turboalternator.

On the basis of these conslusions, establishment of the concept of a solar space power system using the binary Rankine cycle, with mercury as the upper cycle working fluid, follows as a natural result. To avoid the disadvantage of an excessive radiator weight due to low heat rejection temperature, a concept of utilizing the backside of the solar collector as a radiator also was established. In its simplest form, this system concept is shown in Figure 60. In this system, the rejected heat from a normal SUNFLOWER type mercury Rankine system is utilized to vaporize a second, low temperature, Rankine cycle working fluid. This vapor drives a second turboalternator and is then condensed in a compact condenser. Circulating fluid carries the waste heat to tubes attached to the back surface of the solar collector. The collector is constructed of aluminum sheet and acts as a finned tube radiator, rejecting heat from both its front and its back surfaces.

Performing a thermal balance on this cycle results in the conclusion that, with the solar collector, rejecting heat directly absorbed from the sunlight, heat reflected and emitted from the earth, and waste heat from the cycle, the equilibrium temperature is about 150°F, when the upper cycle temperature is established at 1250°F. Since the system continues to operate, while in the earth's shadow, using heat stored in lithium hydride, the cycle waste heat rejection will maintain the collector temperature at approximately 130°F during this period, and will actually assist in reducing the collector thermal cycling and distortion.

Operating between the temperature limits of 1250°F and 150°F, the binary Rankine cycle can achieve thermal conversion efficiencies in excess of 30% using many different low temperature cycle working fluids. Extensive analysis has shown that this system is superior to high temperature solar power systems, incorporating alkali metals as the working fluid, on both a size and a weight basis. The low temperature systems are also considered to be much more reliable, since they do not require high temperature technology advances and since they can be based upon the proven concepts of the SNAP, the SPUD and the SUNFLOWER programs.

It is therefore appropriate to consider the properties desired for the low temperature cycle working fluid. Obviously, for this fluid we desire capability for operating between the mercury condenser temperature, of approximately 600°F, and the heat rejection temperature of 150°F. We desire that the fluid be thermally stable for long durations in this temperature range, that it have suitable vapor pressure and suitable thermodynamic characteristics, for achievement of efficient turbine operation. Due to extensive stationary power plant experience with water, it would be expected that water would be chosen as the ideal fluid to fit these requirements. Detailed analysis of the water-steam cycle for these conditions, however, reveals that water is not well suited. The excessively high pressures, high velocities, and small flow volumes associated with the steam turbine produces the result that this component would have a low efficiency in the power range below 50 kilowatts and is, furthermore, difficult to integrate with a mercury turbine. Many other low temperature working fluids have, therefore, been considered. A working fluid having a very desirable combination of qualities is orthoxylene. The vapor pressure curve and the Mollier diagram for this substance are shown in Figures 61 and 62. It will be noted from the inclination of the saturated vapor line of the Mollier diagram, that this working fluid has the advantage of superheating slightly in an isentropic expansion. This characteristic provides dry turbine operation and also allows regeneratively preheating the boiler inlet flow. These factors produce very attractive efficiencies for a Rankine cycle using this fluid.

In view of the attraction of this cycle, an experimental program was initiated by TRW, and has been subsequently supported by the Air Force, to show the feasibility of the integrated collector radiator and the hydrocarbon type working fluids. Under these programs, fabrication feasibility of the integrated collector radiator has been demonstrated as shown in Figure 63. This figure shows a stretch-formed aluminum collector with tubing attached for circulation of the heat rejecting fluid. Present indications are that collectors having very good optical precision can be fabricated at a total weight of less than .25 lbs. per square foot. A large number of low temperature cycle working fluids have also been tested in capsules, as shown in Figure 64, at temperatures of up to 700°F and for periods of one month. These test conditions simulate operation for one year at 600°F and have shown excellent thermal stability for several different fluids. For example, Figure 65 shows the appearance of the capsules containing orthoxylene. Orthoxylene was exposed to stainless steel, carbon steel and aluminum and did not appreciably decompose or cause corrosion on any of these metals. For comparison, decomposition capsule results for other commonly accepted high temperature hydrocarbon fluids is shown in Figure 66.

As previously stated, the simplest techniques for operating such a binary Rankine cycle would be to utilize two separate turboalternators, each one

being similar to the present SUNFLOWER or SPUD units. A system schematic of such a power system is shown in Figure 67. This system is designed to deliver 6 kilowatts, using two 3 kilowatt SPUD units as previously described. This system can achieve 28.2% overall thermal conversion efficiency. The turbine pitch speed and volumetric flow rate for orthoxylene are so closely similar to mercury vapor that nearly the same turboalternator, operating at the same speed, can be used for both units. Using components designed on the same basis as the mercury units previously described, it is estimated that the total weight of this 6 kilowatt solar power system would be only 462 pounds, or a specific weight of 77 pounds per kilowatt. It is also significant to note that the deployed collector diameter for this 6 kilowatt system designed for operation in a 90 minute orbit, with 36 minute shade time operating capability, would only be 21.4 ft. The orthoxylene working fluid, being quite similar to kerosene in its characteristics, is expected to be a good lubricant. Orthoxylene vapor also provides a good non-corrosive low temperature environment for a reliable alternator operation period. The performance improvements previously noted are, therefore, expected to be readily attainable with an overall system reliability comparable to the single fluid systems. By suitable use of auxiliary pumps, it is also possible that each turboalternator may be made to operate independently of the other unit. Such an arrangement may, therefore, provide improved reliability for part power operation.

A further very interesting conversion unit design which is being analized and investigated is shown in Figure 68. In this unit the mercury turbine is cantilevered on the shaft of the hydrocarbon unit, with the two fluids separated by a shaft seal. The good lubricity and compatibility characteristics of the hydrocarbon can thereby be utilized and the system complexity can be reduced. The shaft seal required could potentially be merely a centrifugal shaft seal and separator, as has been previously tested at TRW and proven capable of sealing mercury. Component testing of this centrifugal shaft seal, and also of other seals, based upon rubbing contact and capillarity sealing principles, are being tested under the present Air Force sponsored program.

A schematic of a 15 kilowatt, single shaft, binary power conversion system is shown in Figure 69. In the 15 kilowatt size, this system is estimated to achieve a thermal conversion efficiency of 33.8%, at a total system weight of approximately 760 pounds, or 51 pounds per kilowatt. Furthermore, such a 15 kilowatt power system, designed for the 90/36 minute orbit-shade time requirement, would have a collector diameter of only approximately 31 ft.

Similar binary Rankine power systems are applicable to larger power requirements. System specific weight may be expected to further decrease as the power is increased to the 30 to 50 kilowatt range. Since the system uses separate pumps to circulate coolant to the radiator, it is particularly well suited to the use of multiple (or redundant) cooling circuits to prevent the meteoroid shielding weight from becoming excessive in the larger sizes.

The foregoing discussion has provided a very brief summary of the performance potential of advanced solar power systems, based upon binary Rankine system technology. It is believed that such systems are capable of providing an unexcelled performance and reliability which, for example, could be utilized by manned space stations in the 30-50 kilowatt electrical power range. It is considered extremely important that the NASA should include plans for developing the components needed to realize this potential as an important part of an extended SUNFLOWER program.

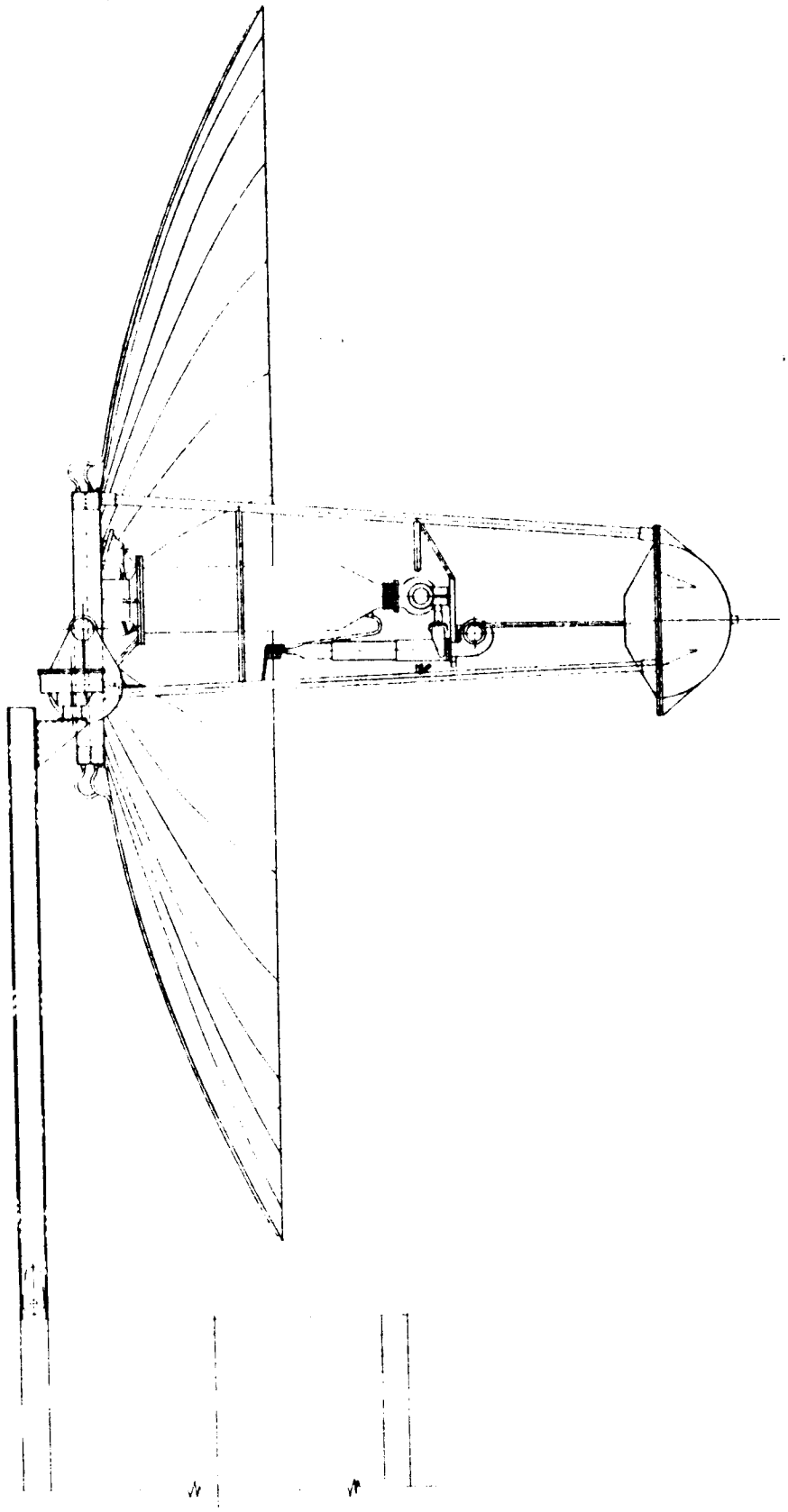


FIGURE 60

SYSTEM ARRANGEMENT SOLAR BINARY POWER PLANT

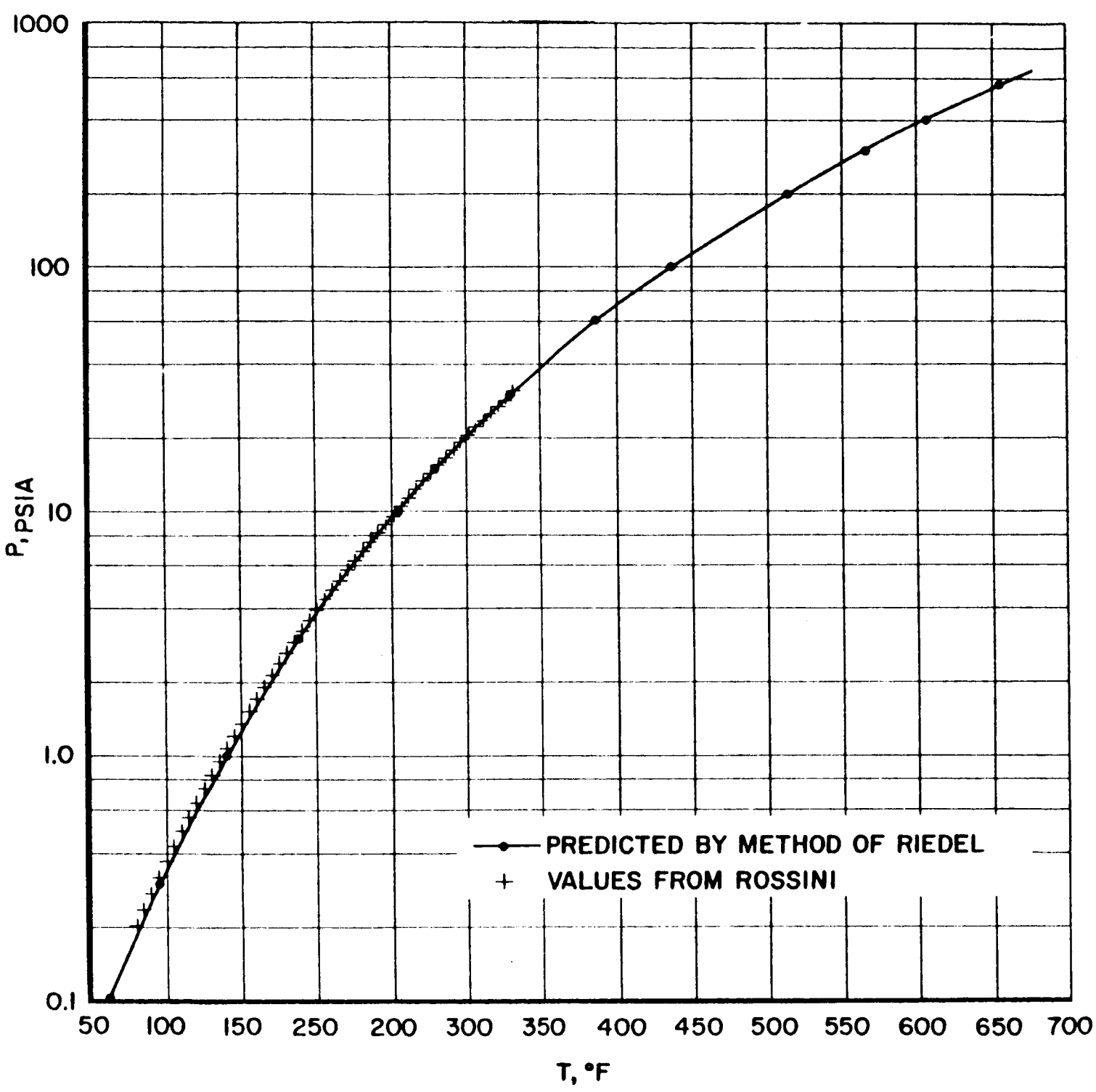

VAPOR PRESSURE OF O-XYLENE
1000
100
10
1.0
0.1
P, PSIA
50
100
150
250
200
300
350
400
450
500
550
600
650
700
T, °F
PREDICTED BY METHOD OF RIEDEL
VALUES FROM ROSSINI

FIGURE 61

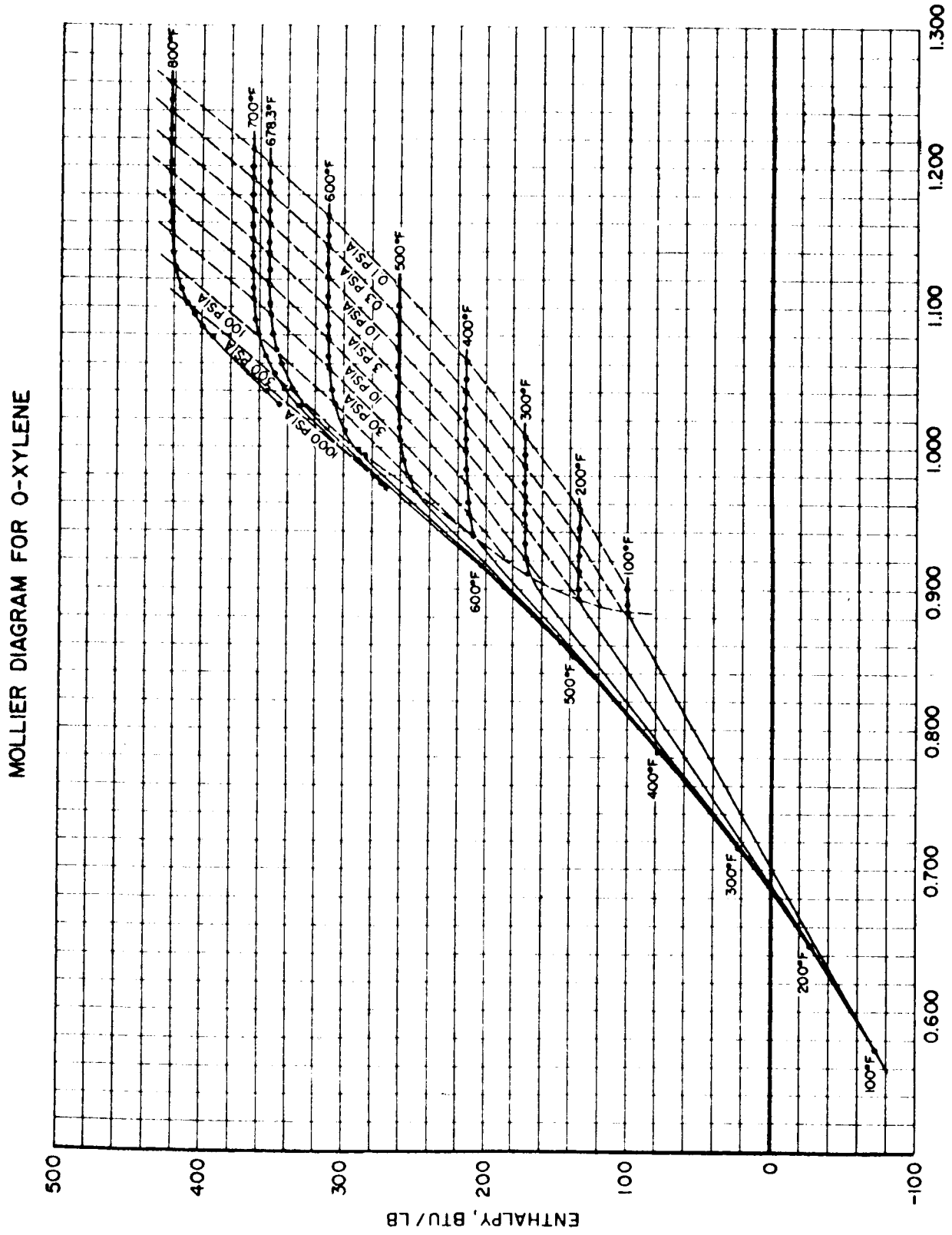
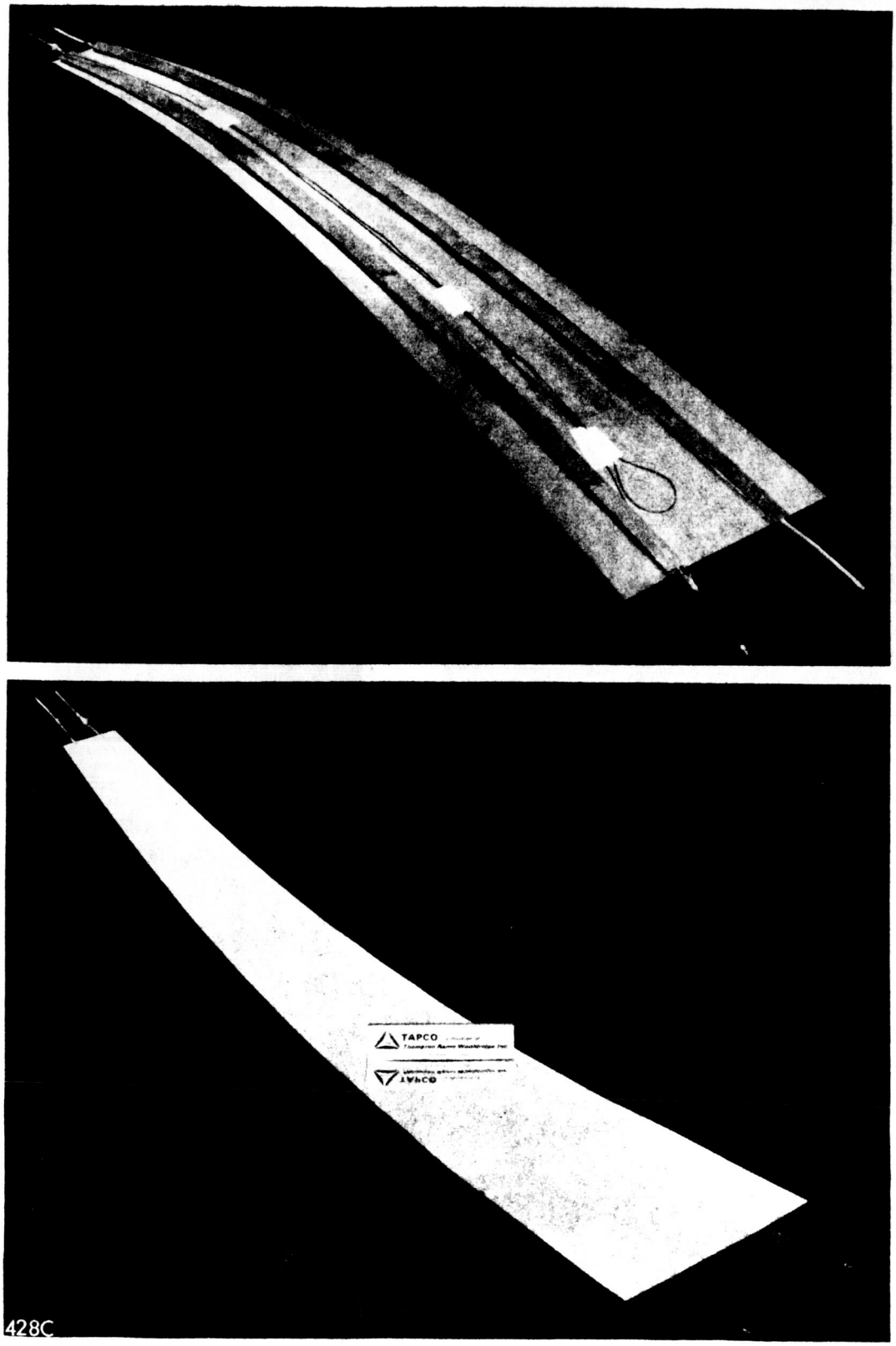
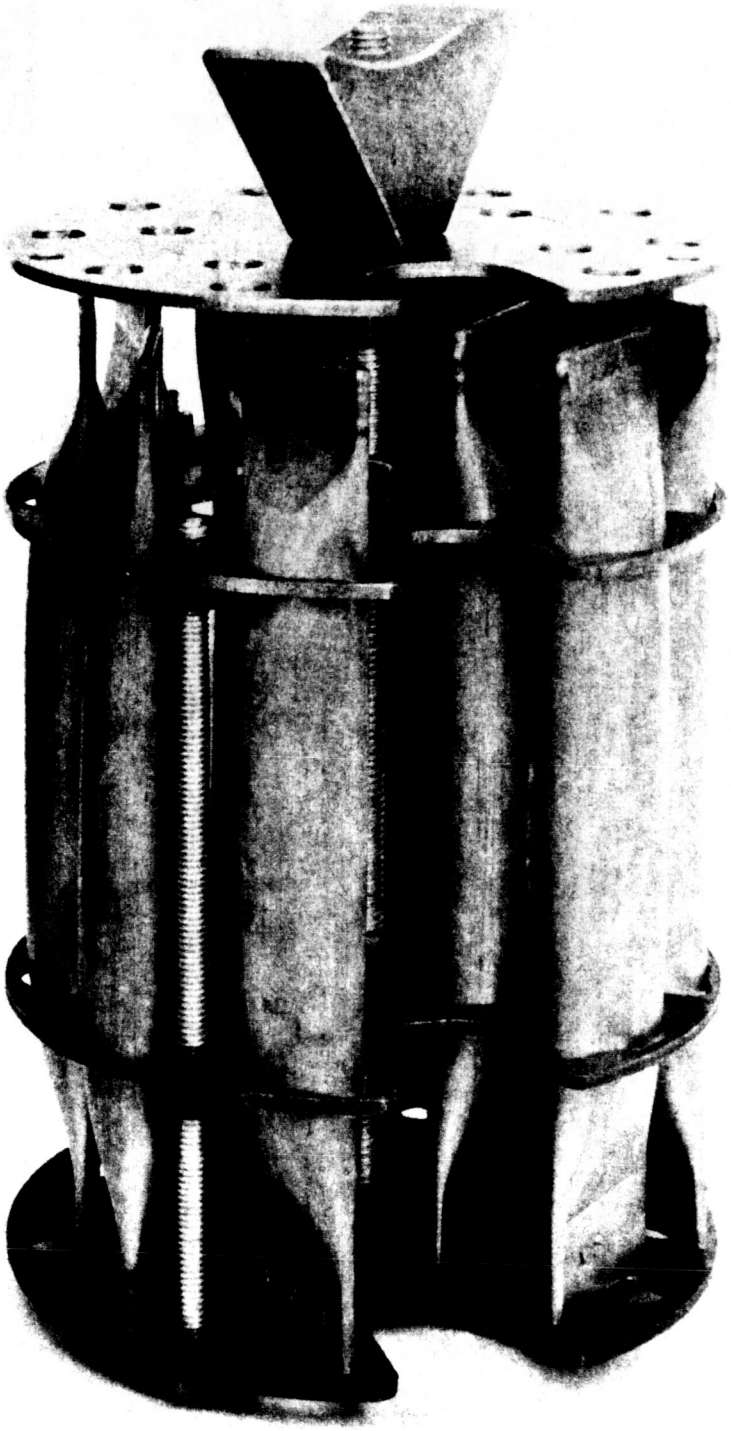

MOLLIER DIAGRAM FOR O-XYLENE
ENTHALPY, BTU/LB
ENTROPY, BTU/LB °R
500
400
300
200
100
0
-100
0.600
0.700
0.800
0.900
1.000
1.100
1.200
1.300
800°F
700°F
678.3°F
600°F
500°F
400°F
300°F
200°F
100°F
60.0°F
1000 PSIA
300 PSIA
100 PSIA
30 PSIA
10 PSIA
3 PSIA
1.0 PSIA
0.3 PSIA
0.1 PSIA

FIGURE 62

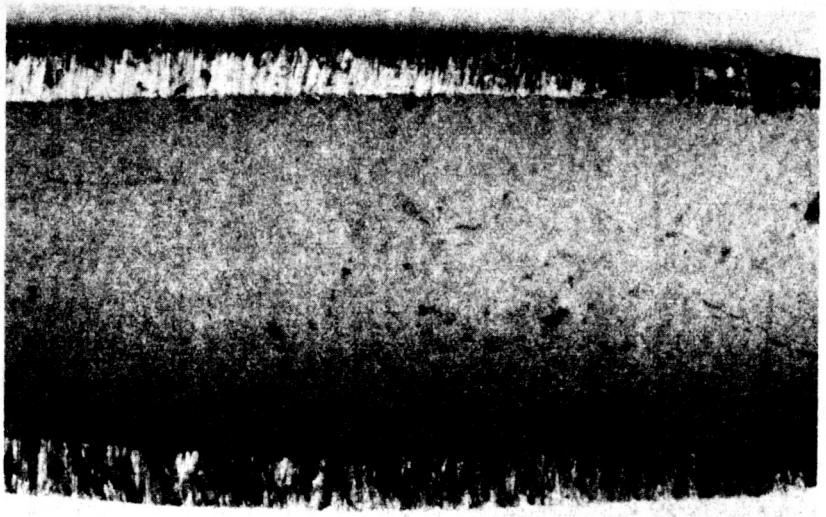


INTEGRATED COLLECTOR
RADIATOR PANEL FIGURE 63

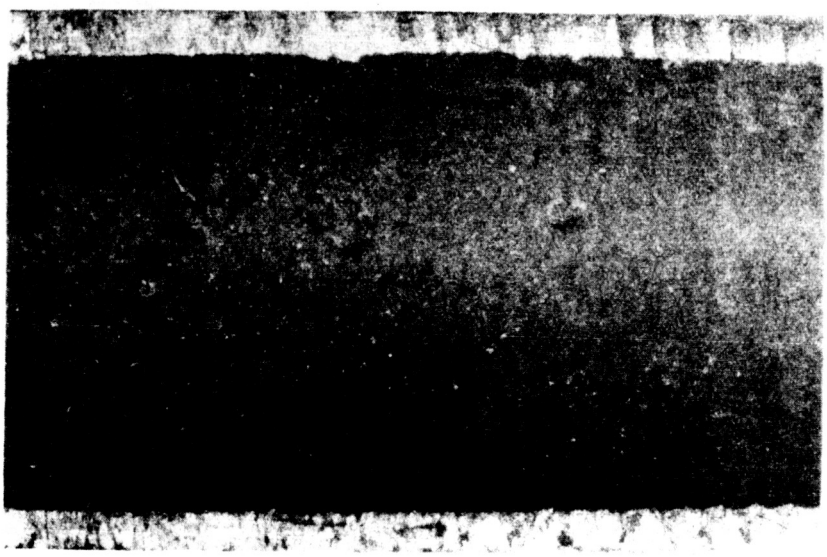


RACK WITH 10 CAPSULES.

FIGURE 64



A-1
TYPE 304 SS
ORTHOXYLENE
3X



A-2
AISI 1010
ORTHOXYLENE
3X



A-3
TYPE 304 SS
ORTHOXYLENE
3X

INSIDE SURFACES OF SERIES "A" CAPSULES THAT CONTAINED ORTHOXYLENE

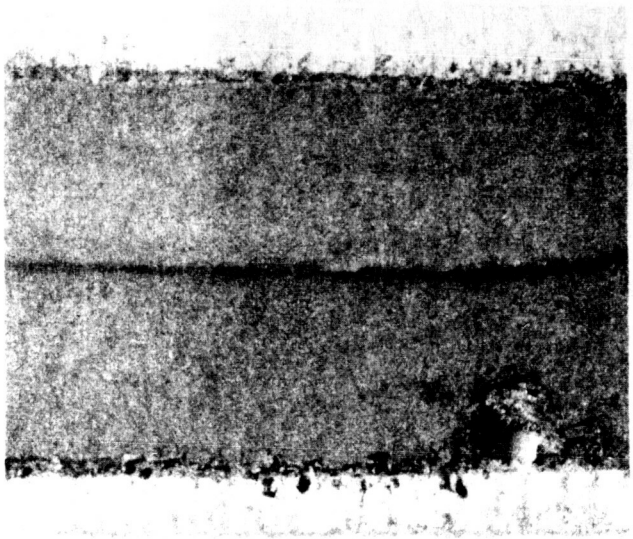
FIGURE 65



TYPE 304 SS 3X
A-6 CHLOROBENZENE



AISI 1010 3X
A-7 CHLOROBENZENE



TYPE 304 SS 3X
A-9 O-DICHLOROBENZENE



TYPE 304 SS 3X
A-11 METHOXYPROPANOL

INSIDE SURFACES OF SERIES "A" CAPSULES THAT CONTAINED CHLOROBENZENE.

FIGURE 66

6 KW, 2 SHAFT BINARY POWER CONVERSION SYSTEM

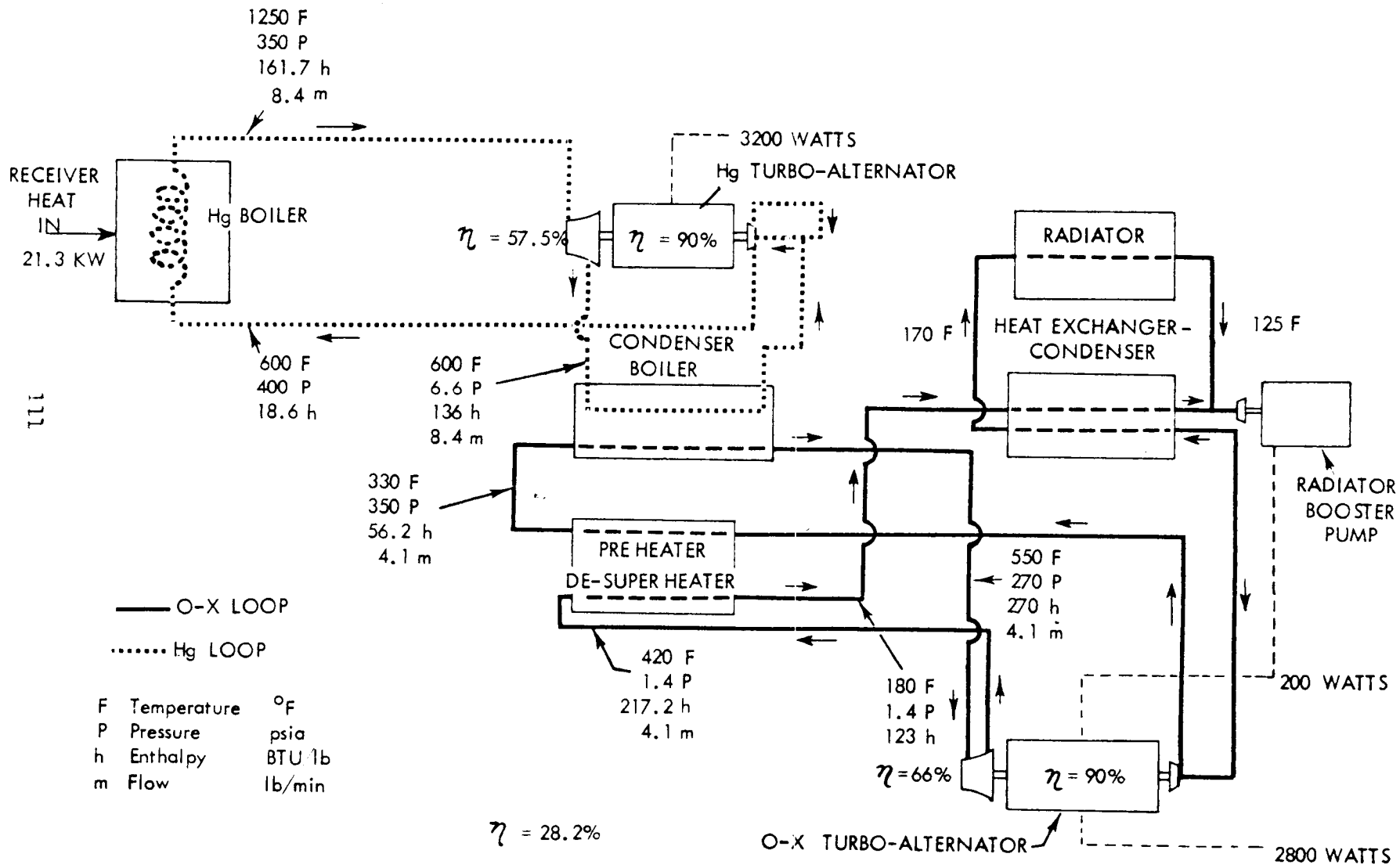
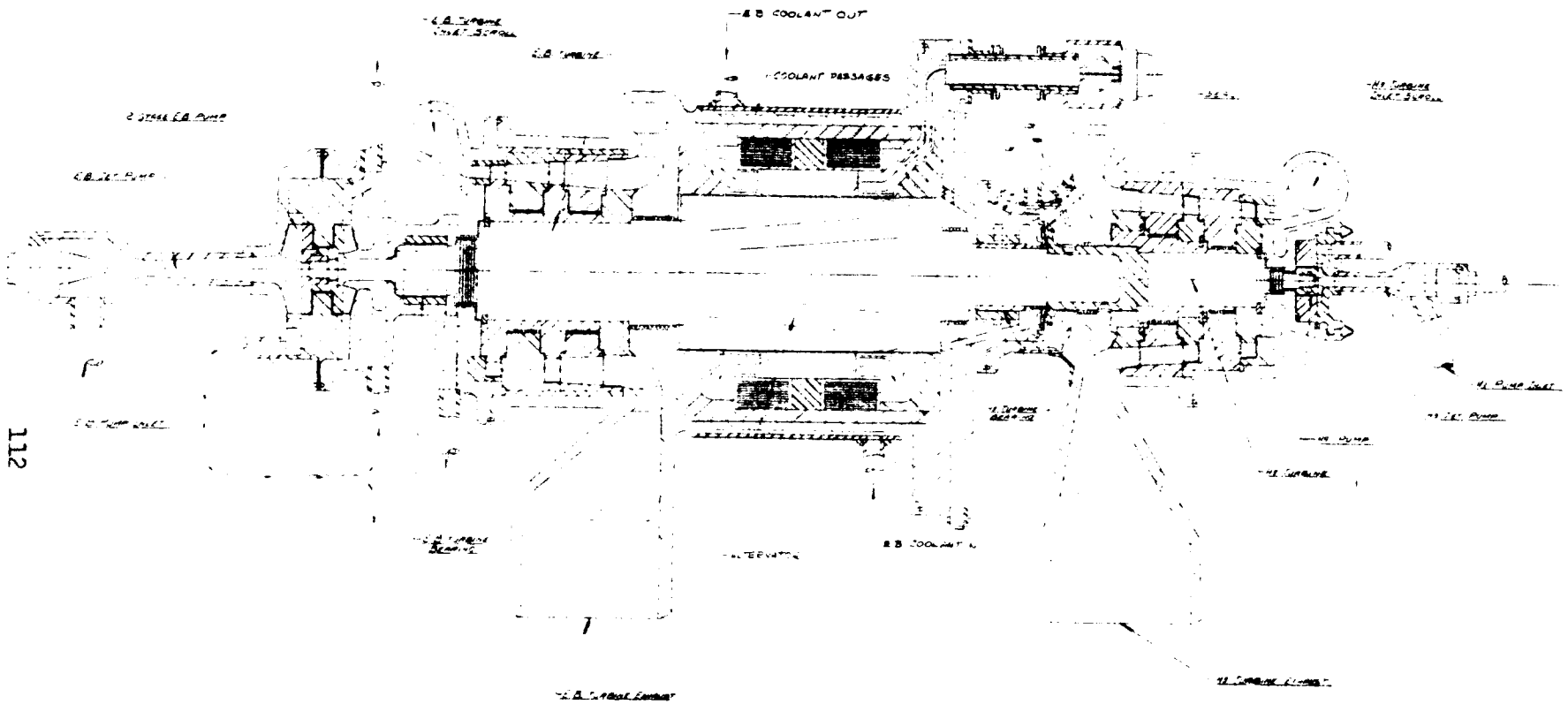


FIGURE 57



ADVANCED SINGLE SHAFT BINARY RANKINE CONVERSION UNIT

FIGURE 68

15 KW SINGLE SHAFT BINARY POWER CONVERSION SYSTEM

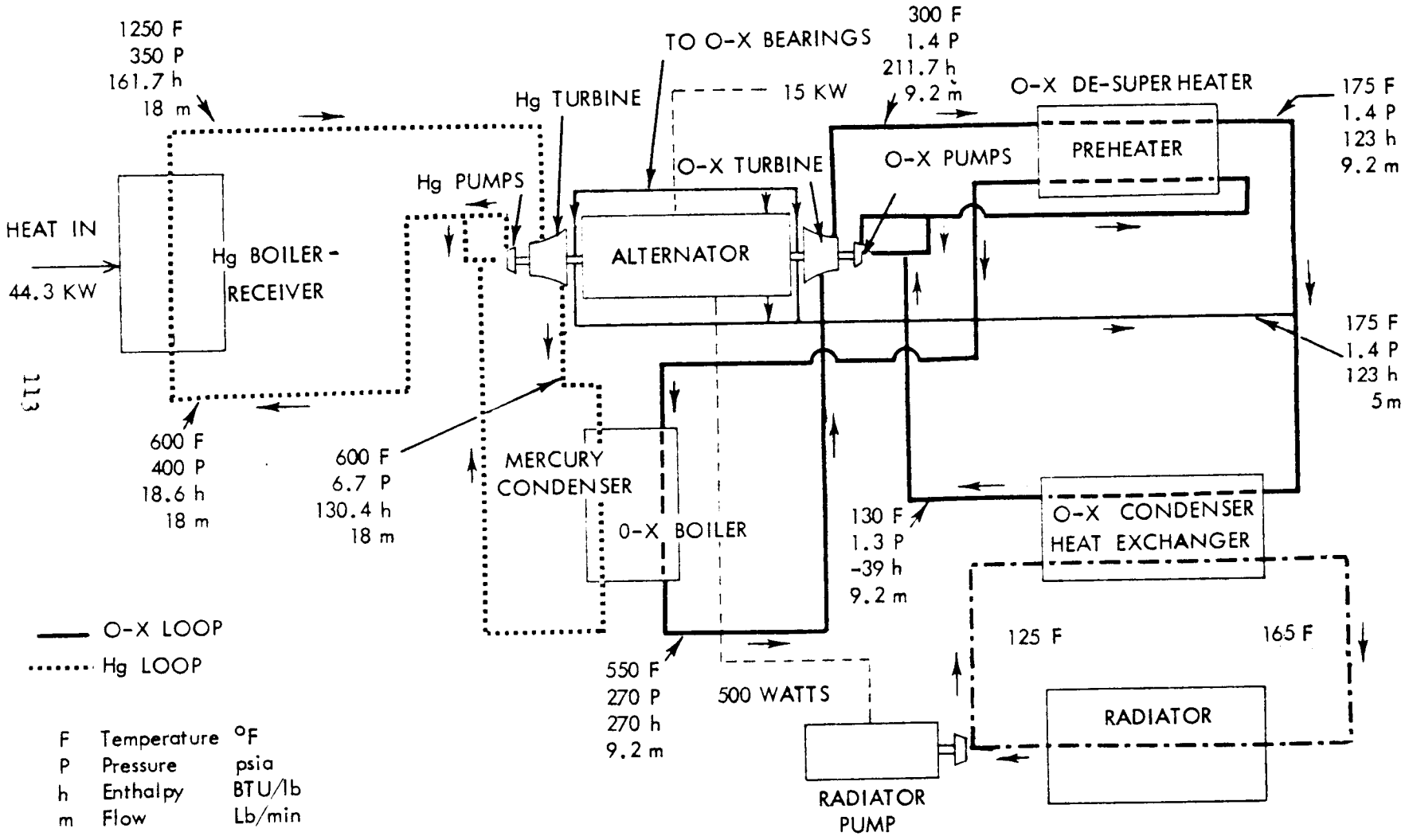


FIGURE 69

COMPETITIVE COMPARISONS

Electronic Power Conversion and Control

The purpose of this discussion is to establish the following points:

1. In considering power systems for space application, attention must be given not only to the power source but also to the electrical load requirements before any comparative analysis can be made of either system weight or efficiency.

2. No matter what the power source is, typical load requirements indicate the need for power conversion devices between the power source and the load.

3. A comparative advantage exists from both the standpoint of weight and efficiency of power conversion devices with AC inputs over those with DC inputs.

In order to discuss the above points, it is necessary to define a typical load requirement for a space power application. The usual requirements for these applications can be summarized as follows:

1. Low voltage DC for a variety of transistorized subcircuits performing such functions as: control, guidance computation and signal conditioning for telemetry purposes.

2. High voltage DC for such load requirements as telemetry transmitters and ion engine power.

3. Single phase or three phase AC, 400 cycles, to power such loads as gyros, miscellaneous motor actuators and source requirements from which higher DC voltages can be derived.

4. A combination of the above load requirements.

Next, the basic types of power sources which are available must be examined. These sources can be placed in either of two categories. The first source provides DC power from such units as solar cells, thermionic or thermoelectric devices, and batteries. The second category is AC power generated by rotating equipment. In incorporating power sources from either category, an important point is this: To meet the typical load requirements just described, it is mandatory that conversion devices be placed between the power source and the load.

Conversion devices are of the following basic types:

1. The inverter which converts DC to any required AC output.

2. The frequency changer which accepts AC input power and provides as an output a lower frequency AC output.

3. A DC to DC converter which accepts a DC input and converts it to either a lower or a higher DC output.

4. A rectifier which accepts an AC input and provides a DC output.

Of course, all of these devices must be tailored to meet the specific parameters of load requirements such as frequency stability, harmonic content, regulation, overload protection, etc.

The operation and comparison of subsystems involved in converters which produce AC outputs can be explained with reference to Figure 70 . In the case of a DC input, an inverter is required. The Reference and Firing Control portions of this unit provide the time base and control of the Power Switches which alternately switch the DC power input through an Output Transformer to provide an alternating voltage output of the required frequency. A filter is used to minimize harmonic content in the final AC output. In the case of an AC input, a frequency changer is employed to derive an AC output at the proper frequency. Here a comparatively high AC input frequency is converted to a lower AC output frequency. A minimum ratio of input frequency to output frequency for this device is about 4 to 1. As in the inverter, the Reference and Firing Control subsystems provide the gating control for the power switches. In the frequency changer, the function of these power switches is the gating of the high input frequency at appropriate times so that portions of the input power waveform are combined to produce the required output waveform. Filtering again is used to minimize output harmonics.

Three important differences exist between the inverter and the frequency changer circuitry.

1. In the case of the frequency changer, natural commutation of the power switches is achieved because of the AC rather than DC input. The result is a considerable reduction in circuitry and complexity in the frequency changer as compared to the inverter.

2. The output transformer required in the inverter to obtain the proper output voltage has completely eliminated the frequency changer.

3. Since in the frequency changer the output of its power switch stage more closely approximates the desired waveform of the AC output, a lesser filtering requirement exists in the case of the frequency changer.

The above differences result in both a higher efficiency and a lower weight for the frequency changer as compared to the inverter.

A comparison of DC producing converters can be seen by reference to Figure 71 . In the DC to DC converter, the Oscillator and Firing control operating in conjunction with the power switches invert the DC input to a square wave AC output which is subsequently transformed into an appropriately higher AC square wave output, rectified and filtered to produce the final DC output.

With an AC input, only a simple rectifier and filter are required to produce the final DC output. It is obvious that considerable circuitry and a transforming is eliminated utilizing AC power which is reflected in increased efficiency and weight reduction. The discussion of the basic types of converters and their associated subcircuitry gives a qualitative feel for weight and efficiency comparisons. To give a more quantitative type of comparison, it is necessary to choose a more

specific DC or AC source. Such a comparison has been made based on the following:

AC Source - Solar Cells

Output voltage - 40 ± 12 v DC
Storage battery - 28 v DC + 1.4 - 0

AC Source - Alternator

Output voltage - 120 v, 2000 c.p.s., 3 phase

These sources were used to provide output power through appropriate converters for either a 28 v ± 5% DC load of 3000 watts or an AC load at 110 v ± 5%, 400 c.p.s. ± 1%, 3 phase at 3000 watts.

The results of the weight efficiency comparison are tabulated in Figure 72 , both for the case of AC output and the DC output. A similar comparison is made for a combined load requirement, that is, the Lewis ion engine. In this case, the DC input, efficiency and pounds per kilowatt figure are those for actual hardware which has been developed at TRW. This device accepts a 56 v DC input and provides low and high voltage DC and AC outputs

In summary, power converters are required regardless of the prime input power source, both the basic technologies and existing hardware are available for all of these converters whether their inputs be AC or DC. Very distinct advantages from the standpoint of weight and efficiency, however, accompany those converters which have an AC input.

A.C. PRODUCING CONVERTERS

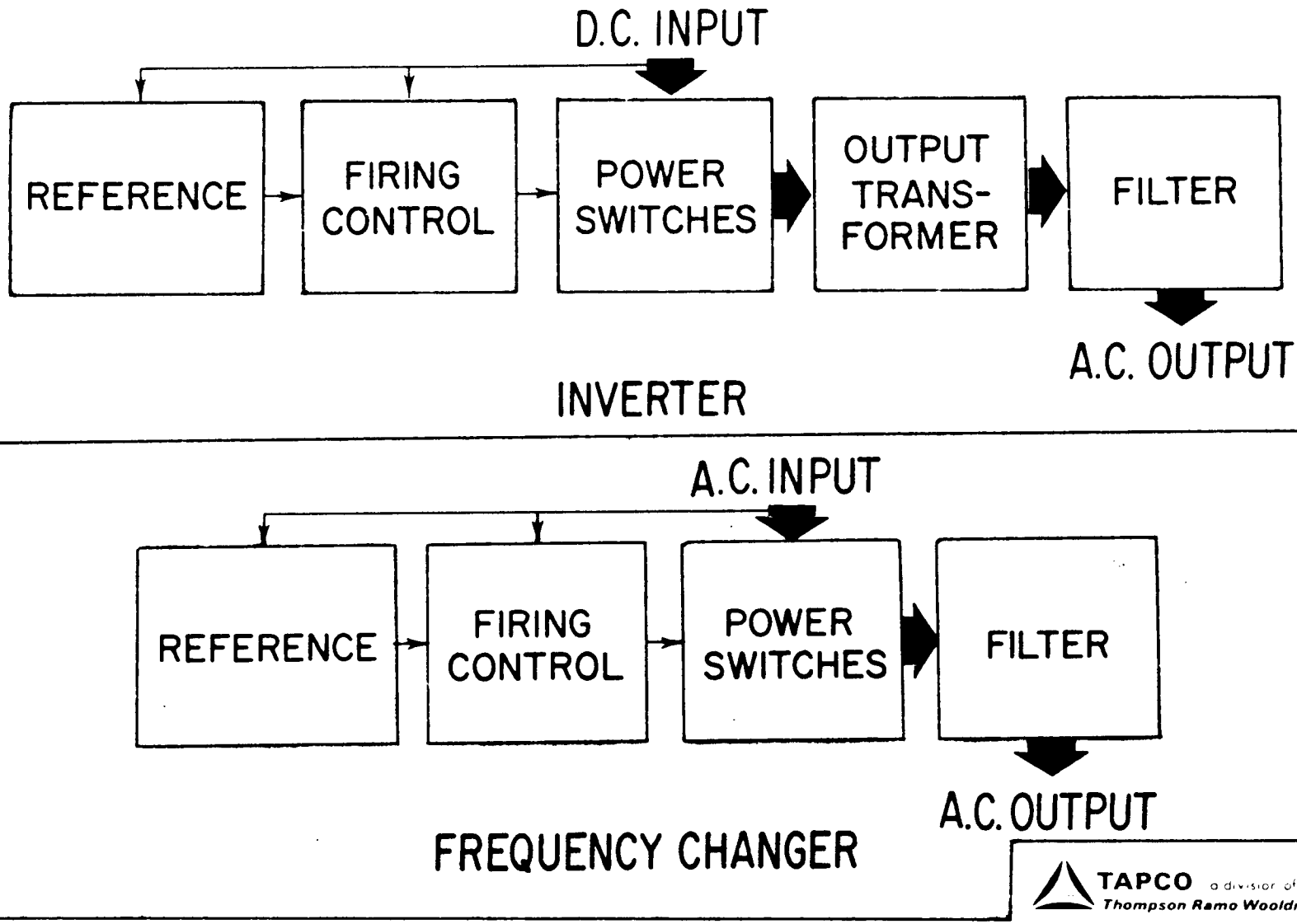
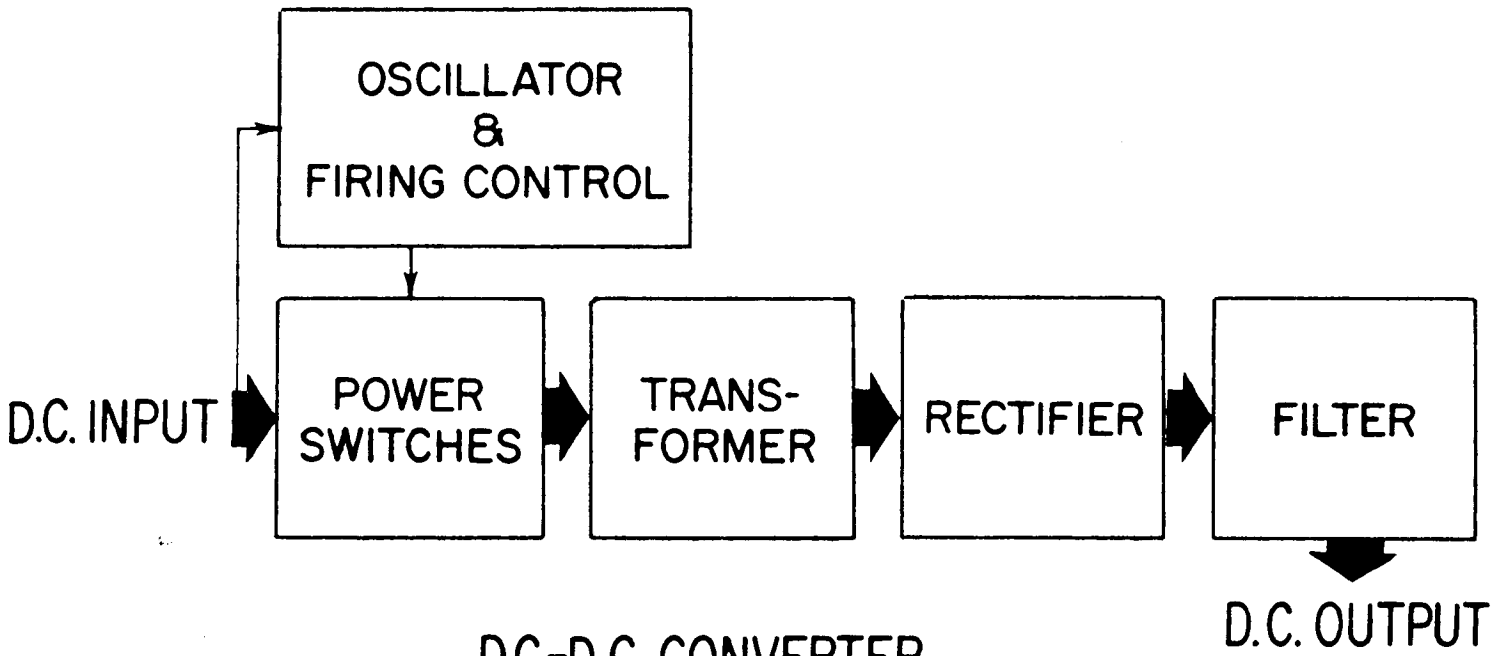
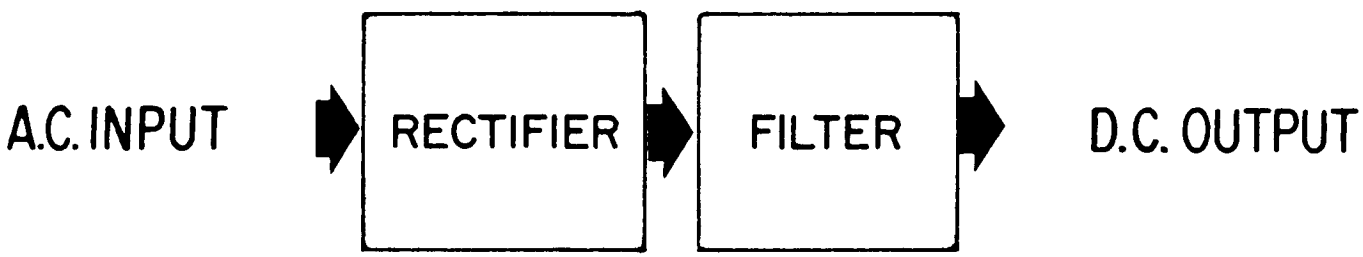


FIGURE 70

D.C. PRODUCING CONVERTERS



D.C.-D.C. CONVERTER



RECTIFIER

FIGURE 71

TAPCO a division of Thompson Ramo Wooldridge Inc.

WEIGHT-EFFICIENCY COMPARISON

		% EFFICIENCY	LBS PER KILOWATT
A.C. OUTPUT	D.C. INPUT INVERTER	80	27
	A.C. INPUT FREQUENCY CHANGER	85	13
D.C. OUTPUT	D.C. INPUT D.C.-D.C. CONVERTER	80	12
	A.C. INPUT RECTIFIER	90	8
ION ENGINE SUPPLY	D.C. INPUT	80	25
	A.C. INPUT	90	13

TAPCO a division of Thompson Ramo Wooldridge Inc.

FIGURE 72

System Comparisons

To evaluate the advantages of the solar dynamic system for space applications it is necessary to make a comparison with competitive power systems. The systems of primary interest fall into the static conversion category and include the following:

I. Solar Cells

II. Thermionic Generators

III. Fuel Cells.

The following pages include examples of these systems for a specific mission and power requirement. The conditions are:

1. 300 nautical mile orbit (ecliptic)

2. Continuous 3 KW power of

   a) $28^{V} \pm 5\%$ D.C., or

   b) $110^{V} \pm 5\%$; 3Ø; 400 cycle

3. 1 year life.

A complete set of calculations is included for the solar cell system while the thermionic and fuel cell systems are presented in a schematic and graphical form respectively.

Following the calculations is a list of several recent technical papers. These documents, plus conversations with recognized experts in the field, are the basis for the system synthesis presented.

I. Solar Cells

3 KW Photovoltaic Power System*

Design Parameters

A. Solar Cells		
1. Efficiency (η_{S/C_1}); uncorrected	12%(2)	Solar Space Spectrum @ 28°C
2. Degradation factors		
a) adhesives, wiring, .006" cover glass	13%(2)	
b) temperature - .5%/°C above standard @ 70°C	21%(3)	
c) radiation degradation after 1 year	25%(3)	
d) stacking factor, concentrator	10%(4)	
e) manufacturing error	5%(1)	
3. a) concentration ratio	2.0(1&5)	
∴ incident flux	260 $\frac{\text{Watts}}{\text{Ft}^2}$	
b) efficiency increase at higher solar intensity	5%(1)	
4. Specific weight, structure	.35(1)	lbs/ft^2
5. Specific weight, solar cell	.6(1)	lbs/ft^2
6. Misc. hardware, antenna, brackets, deployment	.2(6)	lbs/ft^2
B. Batteries		
1. Capacity	20(7)	Watt-Hrs/Lb
2. Discharge depth	25%(7)	
3. Charging efficiency (η_{ch})	80%(8)	
C. Power Conditioning Equipment**		
1. DC-DC converter - 28^V ± 5% output		
a) efficiency (η_{vr})	80%	
b) weight	36 lbs	

* A Boeing Company concentrating panel concept has been used for this comparison since this yields the most competitive results.

** See Preceding Section of this report.

2. Inverter - $110^V \pm 5\%$; 3Ø; 400 cycle output

a) efficiency (η_I)	80%
b) weight	81 lbs

3. Battery charger

a) efficiency ($\eta_{B/C}$)	80%
b) weight	30 lbs

Calculations:

For a 3 KW $28^V \pm 5\%$ DC useful power output system, the primary conversion device must generate enough power to account for the inefficiency losses of the necessary accessory equipment. The powerout of the solar panel is:

$$P_{S/C} = P_{useful} \times \frac{1}{\eta_{VR}} \left(1 + \frac{T_{Shade}}{T_{Sun}} \times \frac{1}{\eta_{CH}} \times \frac{1}{\eta_{BC}}\right)$$

$$= 3.0 \times \frac{1}{.80} \left(1 + \frac{36 \text{ min}}{60 \text{ min}} \times \frac{1}{.80} \times \frac{1}{.80}\right)$$

$$= 3.75 \ (1 + .938)$$

$$= 3.75 + 3.52$$

$$\underline{P_{S/C} = 7.27 \text{ KW}}$$

Solar cell efficiency must be degraded by the applicable factors (Par. A-2) to establish the corrected space efficiency.

$$\eta_{S/C} = \eta_{S/C_1} \times .87 \times .79 \times .75$$

$$= 12.0 \times .515$$

$$\underline{\eta_{S/C} = 6.18\%}$$

Applying increase in efficiency due to higher intensity (Par. 3-b)

$$\eta_{S/C} = 6.18 \times 1.05 = 6.5\%$$

Therefore, the power density of the solar cells is,

$$\frac{P_{S/C}}{A_{S/C}} = \text{solar constant} \times \text{concentration ratio} \times \eta_{S/C}$$

$$= 130 \text{ Watt/Ft}^2 \times 2.0 \times 6.5\%$$

$$= 16.9 \text{ Watt/Ft}^2$$

Therefore, since the solar cells require only 50% of the total concentrator array[145], the required array area

$$= \frac{P_{S/C}}{P_{S/C}/A_{S/C} \times .50}$$

$$A_{a'} = \frac{7.27 \text{ KW} \times 1000 \text{ Watts/KW}}{16.9 \text{ Watts/Ft}^2 \times .50}$$

$$= 880 \text{ Ft}^2$$

Applying the 5% manufacturing error penalty and the 10% stacking factor

$$= \frac{A_{a'}}{.95 \times .9} = 1028 \text{ Ft}^2$$

and since approximately 50% of the array is covered with solar cells, array weight is

$$W_a = A_{a'} \times .50 \times \text{Sp. Wt. of S/C} + A_{a'} \times (\text{Sp. Wt. of Struct.} + \text{Misc. Hdwe.})$$

$$= 1028 \text{ Ft}^2 \times .50 \times .6 \frac{\text{lb}}{\text{Ft}^2} + 1028 \text{ Ft}^2 \times (.35 \frac{\text{Lb}}{\text{Ft}^2} + .2 \text{ Lb/Ft}^2)$$

$$= 308 \text{ Lbs} + 565 \text{ Lbs}$$

$$W_a = 873 \text{ Lbs}$$

The battery weight is calculated as follows

$$W_{Battery} = \frac{P \times T_{Shade} \times 1/\eta_{VR}}{\text{Capacity} \times \text{Disch. Depth}}$$

$$= \frac{3.0 \text{ KW} \times .6 \text{ Hr} \times 1000 \text{ Watts/KW} \times 1/0.80}{20.0 \frac{\text{Watt-Hrs}}{\text{Lb}} \times .25}$$

$$W_b = 450 \text{ Lbs}$$

Therefore, total system weight will be:

$$W_{Syst.} = W_{Array} + W_{Batteries} + W_{Accessories}:$$

Since for the $28^V \pm 5\%$ DC System

$$W_{Access.} = W_{Batt.Ch.} + W_{Converter}$$

$$= 30.0 + 36.0$$

$$= 66.0 \text{ Lbs}$$

$$W_{Syst.} = 873 \text{ Lbs} + 450 \text{ Lbs} + 66.0$$

$$\underline{W_{S(DC)} = 1389 \text{ Lbs}}$$

Since the efficiencies of the power conditioning equipment are the same for an AC or DC system, the only weight difference will be in the accessory weight.

Therefore, a comparable $110^{V} \pm 5\%$, 3Ø, 400 cycle AC system would weigh

$$W_{System} = 873 + 450 + W_{Inverter} + W_{Batt.\ Chg.}$$

$$= 1323 + 81 + 30$$

$$\underline{W_{S(AC)} = 1434 \text{ Lbs}}$$

Schematics for both the AC and DC systems are shown in Figures 73 and 74. It is interesting to note that the area-to-power ratio for full sun operation is

$$\frac{A_a}{P_{S/C}} = \frac{1028}{7.27} = 141 \frac{Ft^2}{KW}$$

and the weight-to-power ratio is

$$\frac{W_{Syst.}}{P_{S/C}} = \frac{873}{7.27} \text{ Lbs/Kw} = 120 \text{ Lbs/KW}$$

These numbers compare with the values presented by R. J. Tallent of the Boeing Company[1] of area-to-power ratio, APR = 83 Ft^2/KW and
weight-to-power ratio, WPR = 54 Lbs/kW
for continuous sun operation.

The discrepancy in these numbers is due to the assumed solar cell efficiency at the mission orbit environment.

A telephone conversation with Mr. Tallent of the Boeing Company on 7/20/62 revealed the basis for his numbers. He has assumed the availability of 12½% efficient solar cells (space efficiency, i.e. 28°C and 140 mw/cm^2) and a conservative degradation factor of only 12%. This factor is a result of a more optimistic effect of elevated cell temperature and complete disregard for radiation damage.

If Boeing's APR is corrected to include the degradation effects assumed in the above calculations,

$$APR' = 83 \frac{Ft^2}{KW} \times \frac{.88}{.515 \times 1.05}$$

$$= 135 \frac{Ft^2}{KW}$$

Likewise, if the WPR is corrected

$$WPR' = 54 \text{ Lbs/KW} \times \frac{.88}{.515 \times 1.05}$$

$$= 88 \text{ Lbs/KW}$$

It is now seen that the APR value compares favorably with that obtained in the above calculations, but there is still a difference in the WPR. This is due to the lower array density assumed by Boeing.

$$\sigma_a = \frac{WPR}{APR} = \frac{54 \text{ Lbs/KW}}{83 \text{ Ft}^2/\text{KW}}$$

$$= .65 \text{ Lbs/Ft}^2$$

Compared to $\sigma_a = .85 \text{ Lbs/Ft}^2$ assumed in the above analyses. Correcting for this ratio

$$WPR' = 88 \text{ Lbs/KW} \times \frac{.85}{.65} = 115 \frac{\text{Lbs.}}{\text{KW}}$$

Which again compares favorably with the above analyses.

If the possibility that the density of the array can be reduced to a .65 Lbs/Ft^2 is accepted, the 3 KW DC system weight would be

$$W_{S/DC} = A_{a'} \times \sigma_a + W_{Batt.} + W_{Accessories}$$

$$= 1028 \text{ Ft}^2 \times .65 \text{ Lbs/Ft}^2 + 450 \text{ Lbs} + 66 \text{ Lbs}$$

$$= 668 + 450 + 66$$

$$= 1184 \text{ Lbs}$$

and the AC system weight would be

$$W_{S/AC} = 668 + 450 + 30 + 81$$

$$= 1229 \text{ Lbs.}$$

It should also be noted that perfect orientation of the panels has been assumed. A misorientation error will naturally increase the weight-to-power ratio. For example, Reference No. 5 states that a reduction in output power of 10% will result if a misorientation of 8° occurs about an axis parallel to the concentrator troughs.

References

(1) AIEE Conference Paper No. 62-1213*, "Optical Electrical Design Considerations for Concentrating Solar Cell Panels", R. J. Tallent, The Boeing Company, Aerospace Division, Seattle, Washington.

(2) AIEE Conference Paper No. 62-1202*, "Design Parameters for Photovoltaic Power Conversion in Space", K. A. Ray, Hoffman Electronics Corp., El Monte, California.

(3) Ibid (2), operating temperature was confirmed as typical of concentrating panel by J. P. Wise (ASRMFP-2), Static Energy Conversion Section, ASD, WADD.

(4) AIEE Conference Paper No. 62-1143*, "Design Considerations in the Use of Photovoltaic Systems", P. S. DuPont, Martin Marietta, Corp., Denver, Colorado.

(5) "Photovoltaic Power for Space Vehicles", Alfred Klammer, Jr., The Boeing Company, Seattle, Wash., presented at the Seventh Regional Meeting of the IRE, Seattle, Wash., May 23-25, 1962.

(6) Based on conversations with Jet Propulsion Laboratory personnel regarding design parameters for earth orbiting missions.

(7) a.) AIEE Conference Paper No. 62-470, "Sealed Secondary Batteries: Nickel-Cadmium and Silver-Cadmium for Space Power", R. C. Shair, Gulton Industries, Inc., Metuchen, N. J., presented at the AIEE Winter General Meeting, New York, N. Y., January 31, 1962.

b.) AIEE Conference Paper No. 62-1143*, "Sealed Alkaline Batteries for Space Applications", J. E. Cooper (ASRMFP-2), USAF, Static Energy Conversion Section, ASD, WADD.

The selection of this parameter was based on a reasonable extension of the art of silver cadmium batteries, since the only long cycle life tests that have been successful thus far have been on low watt-hr per pound batteries at room temperature. J. E. Cooper has ratified the use of 20.0 watt-hrs per pound as a reasonable design parameter for this type of mission.

(8) Confirmed as a valid assumption for this mission by J. E. Cooper, (ASRMFP-2), USAF, Static Energy Conversion Section, ASD, WADD.

* These papers were presented at the AIEE Summer General Meeting, Denver, Colorado, June 17-22, 1962.

II. Thermionic Generators

Schematics and weight summaries for typical thermionic systems are presented as Figures 75 and 76. The weight of 45 Lbs/KW for the thermionic conversion portion of the system is consistent with both the industry and TRW research program estimates.

The thermionic power conversion system is similar to the solar cell system in that it requires the same type of energy storage for sun-shade missions. Therefore, the design criteria utilized in this weight estimate is the same as Section I.

The thermionic generator type system appears to enjoy a distinct weight advantage over solar cells. However, there are several other factors which must be included in a discussion of this type of system. Major developmental consideration must be directed to the material problems associated with the extreme temperature cycling of the components and the exacting orientation requirements. To achieve the stated specific power density of 45 Lbs/KW, the thermionic modules must be oriented to a greater degree of accuracy than other solar power conversion devices or additional weight penalties must be paid. A secondary consideration which is not inconsequential is the precision manufacturing processes required to obtain the high quality solar concentrators which are employed in this type of system.

III. Fuel Cells

In some applications the fuel cell enjoys several advantages over competing power conversion systems. The major desirable characteristics inherent in this system are the independence of sun-shade operation and solar orientation requirements. However, these advantages quickly disappear as soon as mission durations exceed more than a few days. This is primarily due to the fact that the specific fuel consumption (SFC) of a fuel cell system is about 1.0 Lbs/KW Hr.

A fuel cell specific weight of 50-60 Lbs/KW and the above mentioned SFC are supported by TRW research programs and those of other power system suppliers.

A curve of specific system weight vs. electrical power output is presented as Figure 77.

Summary

A summary of solar dynamic Rankine system specific weights vs. power output at a 300 nautical mile orbit is shown in Figure 78. These curves are representative of the systems discussed in earlier sections of this report. The specific weight has been corrected to account for the weight penalty associated with appropriate power conditioning equipment.

For comparison, the specific weight for both the solar cell and thermionic systems are shown. The specific weight of these systems remains essentially constant throughout the range of power discussed.

SOLAR CELL
3 KW STATIC SOLAR POWER SYSTEM-DC SCHEMATIC & WEIGHT SUMMARY

SOLAR CELL PANEL

a) SPACE EFF. @ 28°C = 12%

b.) INCIDENT SOLAR FLUX = 260 $\frac{\text{WATTS}}{\text{FT}^2}$

c.) STRUCTURE DENSITY = .55 LB/FT^2

d.) SOLAR CELL DENSITY = .6 LB/FT^2

e.) TOTAL DEGRADATION = 46.0%

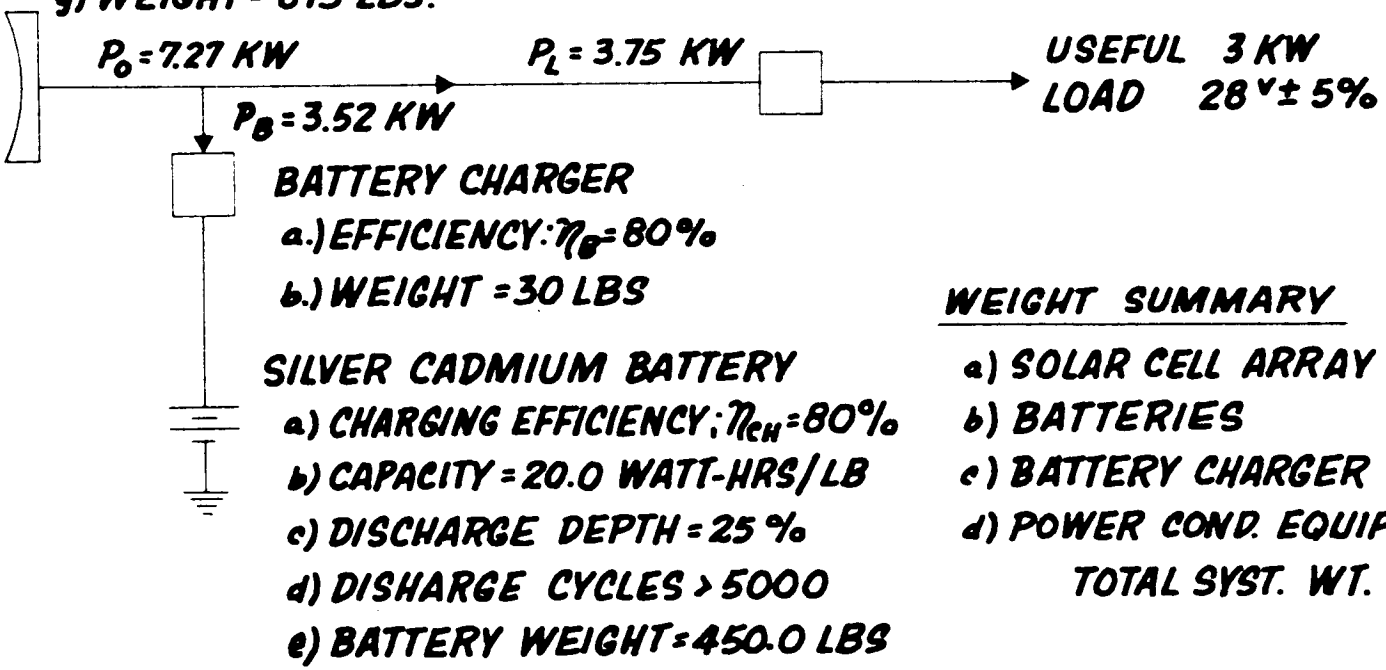
f.) ARRAY AREA = 1028 FT^2

g) WEIGHT = 873 LBS.

DC-DC CONVERTER

a.) EFFICIENCY: η_v = 80%

b.) WEIGHT = 36 LBS



WEIGHT SUMMARY

a) SOLAR CELL ARRAY	873 LBS
b) BATTERIES	450 LBS
c) BATTERY CHARGER	30 LBS
d) POWER COND. EQUIP.	36 LBS
TOTAL SYST. WT.	1389 LBS

FIGURE 73

TAPCO a division of Thompson Ramo Wooldridge Inc.

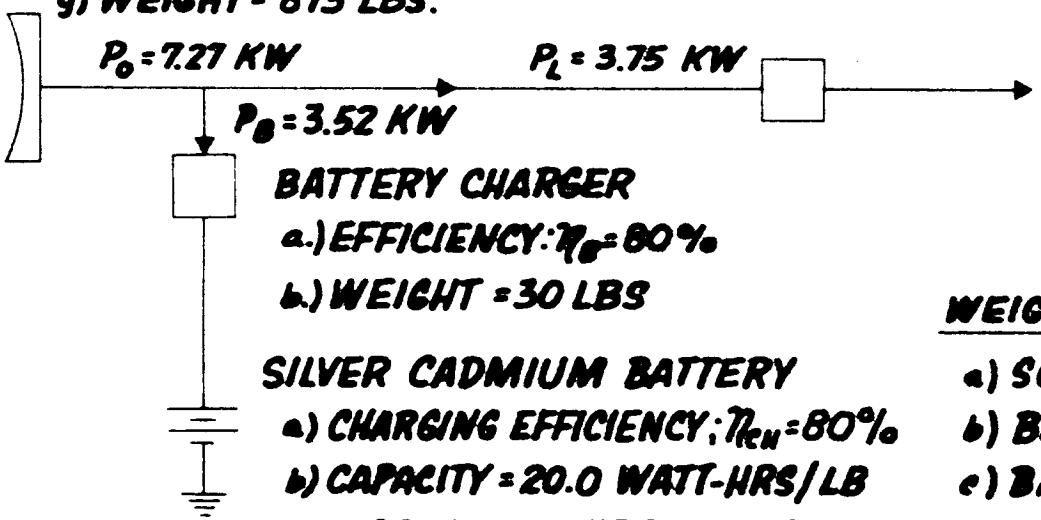
SOLAR CELL
3 KW STATIC SOLAR POWER SYSTEM - AC
SCHEMATIC & WEIGHT SUMMARY

SOLAR CELL PANEL

a.) SPACE EFF. @ 28°C = 12%
b.) INCIDENT SOLAR FLUX = 260 $\frac{\text{WATTS}}{\text{FT}^2}$
c.) STRUCTURE DENSITY = .55 LB/FT^2
d.) SOLAR CELL DENSITY = .6 LB/FT^2
e.) TOTAL DEGRADATION = 46.0%
f.) ARRAY AREA = 1028 FT^2
g.) WEIGHT = 873 LBS.

INVERTER

a.) EFFICIENCY: η_v = 80%
b.) WEIGHT = 81.0



BATTERY CHARGER

a.) EFFICIENCY: η_B = 80%
b.) WEIGHT = 30 LBS

SILVER CADMIUM BATTERY

a) CHARGING EFFICIENCY; η_{CH} = 80%
b) CAPACITY = 20.0 WATT-HRS/LB
c) DISCHARGE DEPTH = 25%
d) DISHARGE CYCLES > 5000
e) BATTERY WEIGHT = 450.0 LBS

WEIGHT SUMMARY

a) SOLAR CELL ARRAY	873 LBS
b) BATTERIES	450 LBS
c) BATTERY CHARGER	30 LBS
d) POWER CONR. EQUIP.	81 LBS
TOTAL SYST. WT.	1434 LBS

FIGURE 74

TAPCO a division of Thompson Ramo Wooldridge Inc.

THERMIONIC

3 KW STATIC SOLAR POWER SYSTEM - DC SCHEMATIC & WEIGHT SUMMARY

THERMIONIC GENERATOR

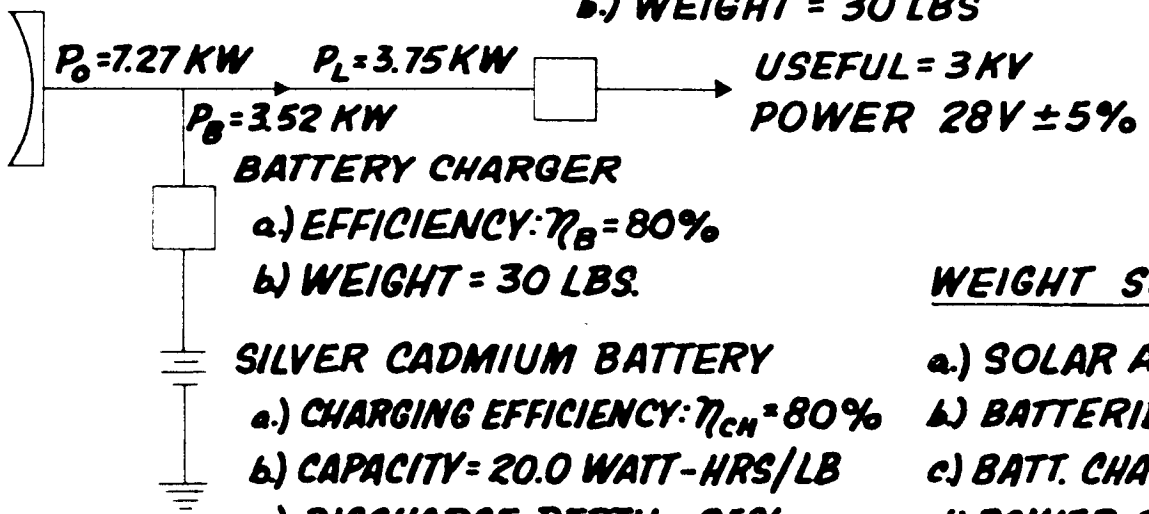
a.) SPECIFIC WEIGHT = 45 LBS/KW

b.) ARRAY WEIGHT = 327 LBS.

DC-DC CONVERTER

a.) EFFICIENCY: $\eta_v = 80\%$

b.) WEIGHT = 30 LBS



WEIGHT SUMMARY

a.) SOLAR ARRAY	327 LBS.
b) BATTERIES	450 LBS.
c) BATT. CHARGER	30 LBS.
d) POWER COND. EQUIPMENT	30 LBS.
TOTAL SYST. WT.	837 LBS.

FIGURE 75

TAPCO a division of Thompson Ramo Wooldridge Inc.

THERMIONIC

3 KW STATIC SOLAR POWER SYSTEM - AC SCHEMATIC & WEIGHT SUMMARY

THERMIONIC GENERATOR

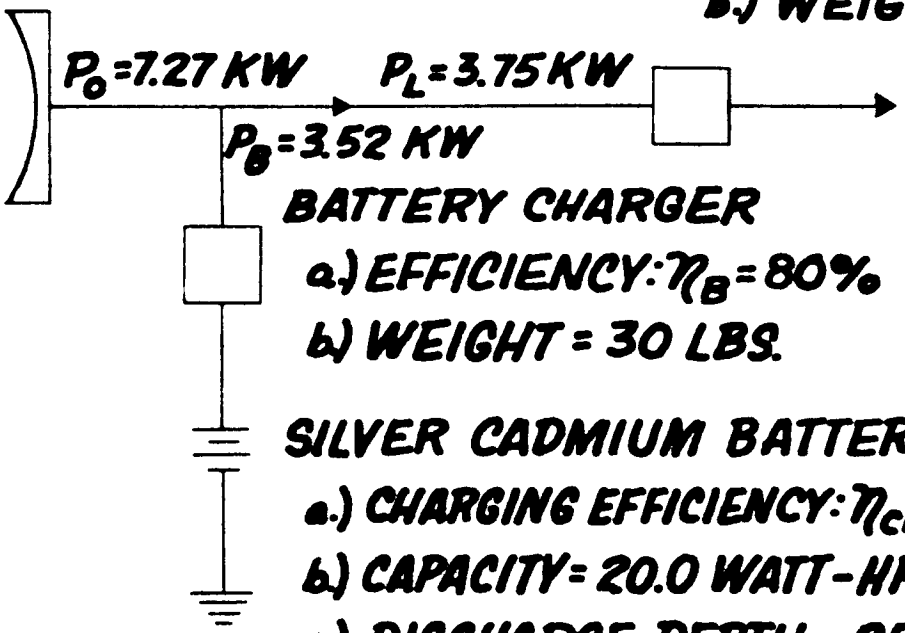
a.) SPECIFIC WEIGHT = 45 LBS/KW

b.) ARRAY WEIGHT = 327 LBS.

INVERTER

a.) EFFICIENCY: $\eta_v = 80\%$

b.) WEIGHT = 81 LBS.



WEIGHT SUMMARY

a.) SOLAR ARRAY	327 LBS.
b.) BATTERIES	450 LBS.
c.) BATT. CHARGER	30 LBS.
d.) POWER COND. EQUIPMENT	81 LBS.
TOTAL SYST. WT.	888 LBS

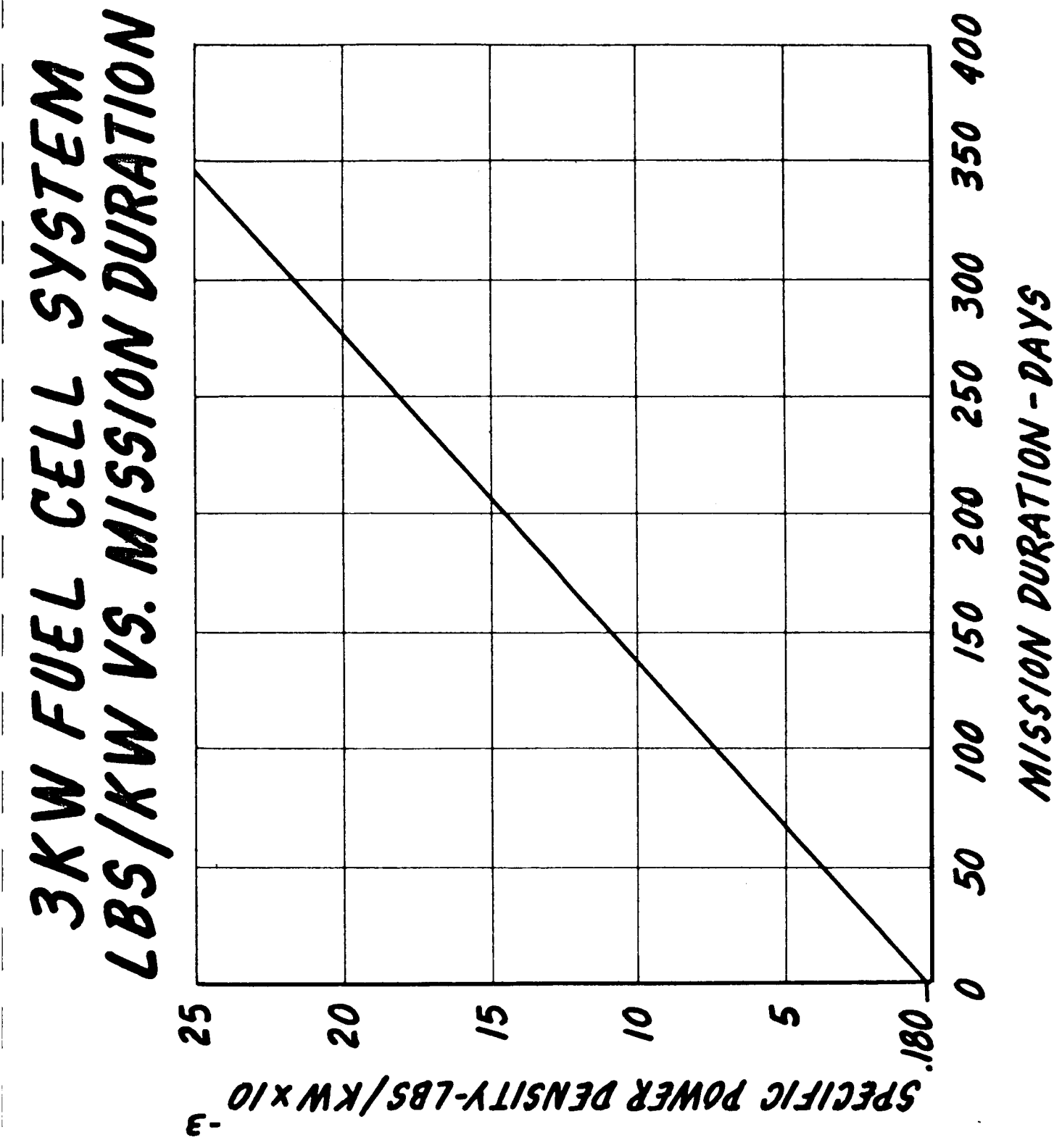

3KW FUEL CELL SYSTEM
LBS/KW VS. MISSION DURATION
SPECIFIC POWER DENSITY-LBS/KW x 10 -3
25
20
15
10
5
.180
0
50
100
150
200
250
300
350
400
MISSION DURATION-DAYS

FIGURE 77

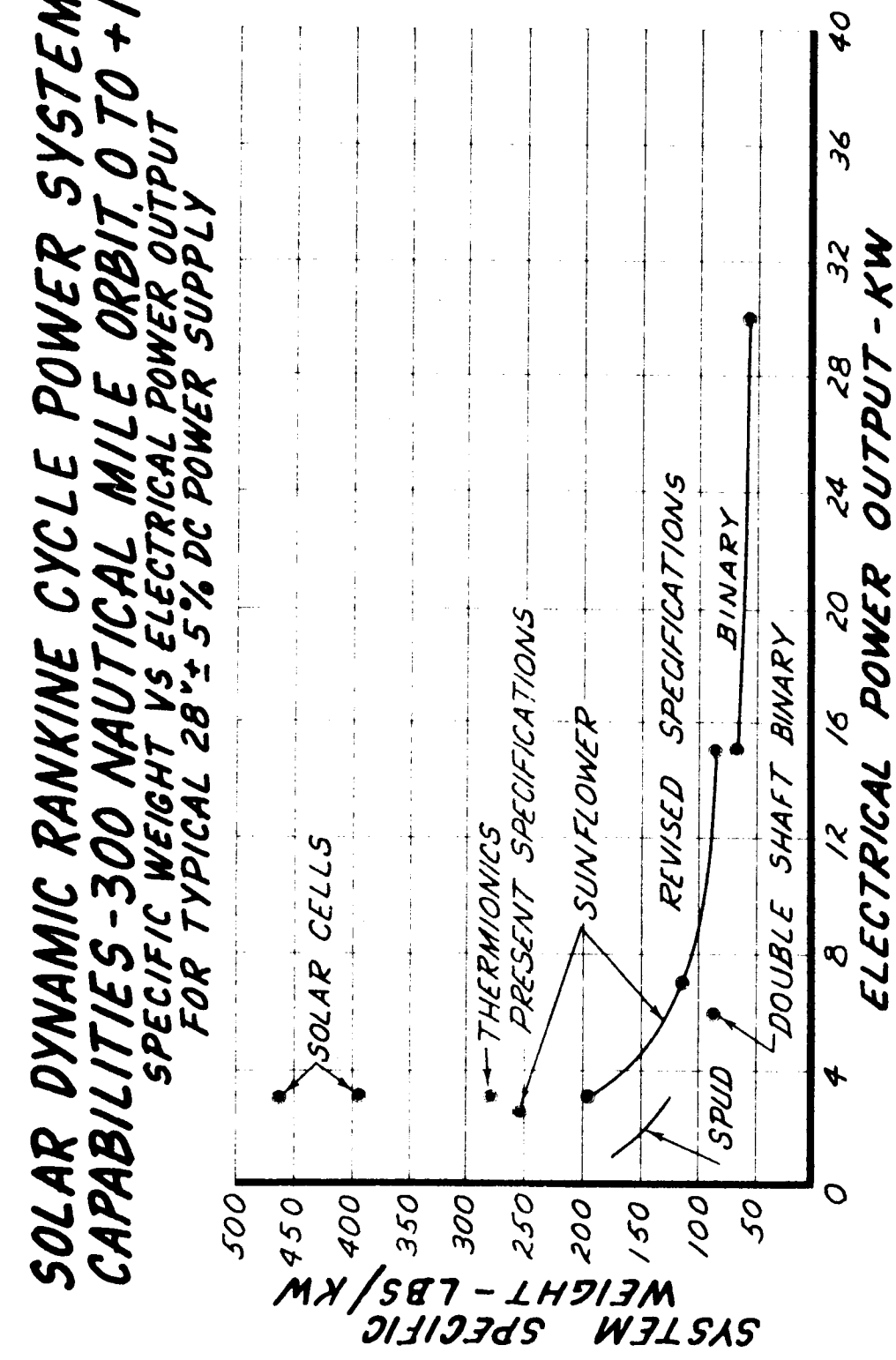

SOLAR DYNAMIC RANKINE CYCLE POWER SYSTEMS
CAPABILITIES - 300 NAUTICAL MILE ORBIT, 0 TO +1g
SPECIFIC WEIGHT VS ELECTRICAL POWER OUTPUT
FOR TYPICAL 28 V ± 5% DC POWER SUPPLY
SYSTEM SPECIFIC WEIGHT - LBS/KW
500
450
400
350
300
250
200
150
100
50
0
4
8
12
16
20
24
28
32
36
40
ELECTRICAL POWER OUTPUT - KW
SOLAR CELLS
THERMIONICS
PRESENT SPECIFICATIONS
SUNFLOWER
REVISED SPECIFICATIONS
BINARY
SPUD
DOUBLE SHAFT BINARY

FIGURE 78